CHARACTERISATION OF THE PHOTOSYSTEM-I REACTION CENTRE COMPLEX

A thesis submitted by

JONATHAN ANTONY HANLEY

For the degree of Doctor of Philosophy

Department of Biology
University College London
May 1993

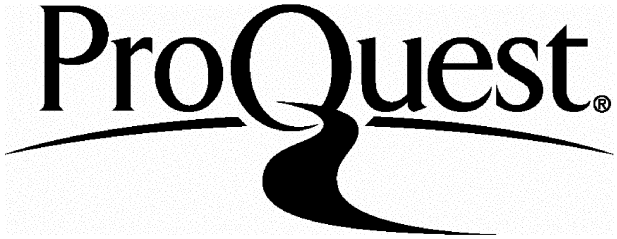

ABSTRACT

This thesis reports studies of the structure and function of higher plant photosystem-I electron transfer components. The function of stromal side polypeptides has also been investigated with particular reference to the transfer of electrons through the bound iron-sulphur centres ($Fe\text{-}S_{A/B}$) to $NADP^+$. The principle techniques used have been low temperature electron paramagnetic resonance spectroscopy (EPR), room temperature kinetic spectroscopy and column chromatography.

First reported is the isolation of a photosystem-I core complex devoid of its terminal bound iron-sulphur centres and other peripheral polypeptides. The core complex was prepared by incubation of either Triton or Digitonin photosystem-I in 6.8M urea. EPR analysis reveals it to contain P700, A_0 and A_1 and room temperature $P700^+$ re-reduction kinetics indicate the presence of $Fe\text{-}S_X$.

The respective role of PSI-C, the $Fe\text{-}S_{A/B}$ holoprotein, PSI-D and PSI-E was investigated by carrying out a series of reconstitution experiments utilising the PS-I core complex and stromal polypeptides isolated from photosystem-I by *n*-butanol extraction. Room temperature kinetic experiments demonstrated that reconstitution of the core complex with the PSI-C holoprotein resulted in the recovery of 20 ms kinetics observed in control PS-I. EPR analysis showed that PSI-D, and possibly PSI-E, was also required in order stabilise the rebound PSI-C holoprotein. Measurement of the rate of $NADP^+$ photoreduction, by monitoring change in OD 340 nm following 30 second periods of illumination with saturating

white light, demonstrated that redox centres Fe-$S_{A/B}$ were essential for forward electron transfer to $NADP^+$ at room temperature. The reconstitution experiments also showed that components PSI-D and PSI-E were essential for interaction with the soluble intermediates ferredoxin and ferredoxin NADP oxidoreductase.

Illumination of photosystem-I at 4^0C in the presence of sodium dithionite has been shown to result in the double reduction of the quinone species A_1 thereby rendering it EPR silent. This thesis reports that gradual quinone double reduction also results in a concomitant disappearance of the photo-accumulated EPR signal previously attributed to A_1^-. The assignment of the g = 2.0048 and 0.95 mT linewidth EPR signal, photo-accumulated by 205K illumination, to the reduction of the quinone component A_1^- was thus confirmed.

Photo-accumulation of A_1^- and A_0^- by illumination of photosystem-I at 230K in the presence of sodium dithionite at pH 10.0 resulted in the rise of approximately 4 spins per $P700^+$ reaction centre. This forms the first direct evidence that the photosystem-I reaction centre complex may exhibit the same C_2 symmetry observed in other types of photosynthetic reaction centre complex.

DEDICATION

This Thesis is dedicated to Emma and Puska

for patiently listening to me drivel on about

photosynthesis for the last seven months.

ACKNOWLEDGEMENTS

Firstly I would like to thank Prof. Mike Evans for giving me the opportunity to carry out this work and for his advise and patience during its execution. I would also like to thank Dr. Pete Heathcote for his invaluable guidance and Dr. Jonathan Nugent for useful discussions.

I acknowledge Dr. D.A. Bryant for supplying antibodies raised against PSI-C and PSI-D and Brian Pickerell for keeping the kinetic spectrophotometer alive.

I am also grateful to the friends I have made at UCL, in particular Simon Bowden, Andrew Corrie and Fenton Beed, for their support both in and out of work.

This work was funded by a grant from the Science and Engineering Research Council (UK).

Table of Contents **Page**

List of Tables and Figures

Figure

Abbreviations

A_0	Photosystem-I primary acceptor
A_1	Photosystem-I secondary acceptor
A_0'	Proposed branch 2 chlorophyll
A_1'	Proposed branch 2 quinone
ADP	Adenosine diphosphate
ATP	Adenosine triphosphate
Chl	Chlorophyll
Da	Dalton
DC	Direct current
DCPIP	2,6-Dichlorophenolindophenol
DTT	1,4-Dithio$_{-L-}$threitol
EDC	N-ethyl-3-[3-9Dimethylamino)propyl] carbomide
EDTA	Ethylenediaminetetraacetic acid
ENDOR	Electron nuclear double resonance
EPR	Electron paramagnetic resonance
ESEEM	Electron spin echo envelope modulation
ESP	Electron spin polarised
EXAFS	Extended X-ray absorption fine structure
Fd	Ferredoxin
Fe-S	Iron-sulphur centre
FMN	Flavin mononucleotide
FNR	Ferredoxin NADP oxidoreductase
fs	Femtosecond

FTIR	Fourier transform infrared
GHz	Gigahertz
Hz	Hertz
H	Magnetic field
HA	Hydroxyapatite
K	Kelvin
kDa	Kilodalton
kHz	Kilohertz
LHC-I	Light harvesting complex 1
LHC-II	Light harvesting complex 2
M	Molar
MHz	Megahertz
mol	Mole
mT	Millitesla
mV	Millivolt
mW	Milliwatt
MW	Molecular weight
$NADP^+$	Oxidised Nicotinamide adenine dinucleotide phosphate
NADPH	Reduced Nicotinamide adenine dinucleotide phosphate
NC	Nitrocellulose
OD	Optical density
P	Primary electron donor
P700	Photosystem-I primary donor
PAGE	Polyacrylamide gel electrophoresis

Pc	Plastocyanin
PNR	Pyridine nucleotide reductase
ps	Picosecond
PS-I	Photosystem-I
PS-II	Photosystem-II
rRNA	Ribosomal Ribonucleic acid
SDS	Sodium dodecyl sulphate
TEMED	Tetramethylenediamine
Tfr	Transfer
Tricine	N-tris[Hydroxymethyl]-methylglycine
Tris	Tris-(hydroxymethyl)-aminomethane
Triton X-100	Octyl phenoxy poly(oxyethanol)

1.0 INTRODUCTION

1.1 General Introduction

All organisms require energy and organic molecules for maintenance and growth. One of the most intriguing systems of energy acquisition and storage is that of photosynthesis; the conversion of light energy into chemical energy by the light driven oxidation of an inorganic molecule yielding protons and electrons:

$2H_2A + Light \text{ -----> } A_2 + 4H^+ + 4e^-$

Where H_2A represents the universal electron donor.

Evolutionary refinements have conferred the ability to utilise the protons and electrons during light independent reactions for the fixation of carbon dioxide thus removing the organisms requirement for external sources of organic carbon:

$CO_2 + 4e^+ + 4H^+ \text{ -------> } CH_2O + H_2O$

Photosynthetic organisms are subdivided into two groups:

1.) Oxygenic, which use light to oxidise water thereby evolving oxygen.

2.) Anoxygenic organisms, which oxidise alternative inorganic compounds and do not evolve oxygen.

This thesis is concerned with the mechanisms involved in eukaryotic

oxygenic photosynthesis, however anoxygenic prokaryotic systems will be discussed during this introduction because of their importance in the understanding of higher plant photosynthetic systems.

1.2 Historical Summary of Photosynthesis Research

Probably the earliest breakthrough in photosynthesis research came in the 17th century when Van Helmont (1577-1644) carried out a five year experiment to demonstrate that "plants do not feed on soil". In 1727 Stephen Hales suggested that a plant's nourishment came from the atmosphere in a process which probably involved light. By 1771 Joseph Priestley had demonstrated the evolution of what we now know as oxygen and later Jan Ingenhousen (1779) showed oxygen evolution to be a light dependent process. During 1782 Jean Senebier carried out a series of experiments to show that the rate of oxygen evolution was stimulated by the presence of carbon dioxide although at this time CO_2 and O_2 were still being referred to as noxious gas and purified air.

The work of Lavoisier and others made it clear that it was indeed the gases oxygen and carbon dioxide involved in plant processes. In 1804 N.T. de Saussure made the first quantitative measurements and suggested that water also played a central role in photosynthesis. Sachs (1864) observed that starch particles only formed in areas of the leaf exposed to the light and suggested that organic matter was the end product of photosynthesis.

The overall reaction of photosynthesis was therefore proposed to be:

$$_nCO_2 + _nH_2O + \text{Light} \text{ ------> } _n(CH_2O) + _nO_2$$

It was still assumed at this point that the molecular oxygen was derived from carbon dioxide, probably by binding carbonic acid to chlorophyll which would undergo molecular transformation on absorption of light:

$$CO_2 + H_2O \text{ ----> } H_2CO_3 + \text{Light} \text{ ------> } CH_2O + O_2$$

As early as 1922 Warburg dismissed this theory concluding that the high quantum requirement for oxygen evolution indicated a much more complex and probably multi-step process.

Van Niel (1931) pointed out the similarity between green plant and anaerobic bacterial photosystems, particularly the green and purple sulphur bacteria. He noted that these bacteria utilised light and H_2S to fix carbon dioxide depositing sulphur, and not oxygen, as a by-product giving an overall reaction:

$$CO_2 + 2H_2S + \text{Light} \text{ -----> } CH_2O + H_2O + 2S$$

By comparisons between the two systems he suggested that molecular oxygen, evolved by green plants, is derived from the oxidation of water and

not from carbon dioxide.

Further evidence of water oxidation came from Hill and Scarisbrick (1940) who found that oxygen evolution could be obtained from illuminated chloroplasts or chloroplast fragments in the presence of an artificial electron acceptor. Light driven splitting of water in the absence of carbon dioxide fixation became known as the "Hill Reaction". More convincing evidence was offered by the ^{18}O labelling experiments of Samuel Ruben and his co workers who demonstrated the release of ^{18}O from labelled water in *Chlorella* (Ruben *et al.*, 1941). These experiments did not provide conclusive proof but a repeat of his work under more controlled conditions showed conclusively that water formed the initial electron donor in oxygenic photosynthesis (Stemler and Radner, 1975).

The discovery by Hill that additions of acetone-extracted water–soluble leaf proteins would stimulate the Hill reaction prompted a search for naturally occurring photosynthetic electron acceptors. San Pietro and Lang (1958) purified a reddish-brown protein that they called pyridine nucleotide reductase, or PNR. This was shown to have similar properties to the met factor isolated by Davenport (1960) which catalysed the photoreduction of $NADP^+$ by chloroplasts; ferredoxin became the established name for this type of iron-sulphur protein. Tagawa and Arnon (1962) isolated the flavoprotein (FNR) required to mediate electron transfer from ferredoxin to $NADP^+$.

Photophosphorylation of ADP by chloroplasts was first described by Arnon *et al.* (1954) who noted that ATP production was stimulated by the

presence of flavinmononucleotide (FMN) and vitamin K_3 (Arnon *et al.*, 1955), this was termed "cyclic photophosphorylation". Non-cyclic photophosphorylation was also enhanced in the presence of $NADP^+$ and ferredoxin with a concomitant evolution of oxygen. Bassham and Calvin (1957) demonstrated the necessity for both ATP and NADPH for the fixation of carbon dioxide during the light independent carbon reduction cycle. It was assumed, by analogy with mitochondria, that phosphorylation of ATP and reduction of $NADP^+$ was brought about by electron transfer and that the role of light was to drive these redox events.

In 1960 Hill and Bendallsummarised these findings in the Z-scheme of electron transport which suggested two photosystems working in series linked by cytochromes b_6 and f: photosystem-2 oxidises water and reduces cytochrome b_6, photosystem-I reduces $NADP^+$ and is itself re-reduced by the cytochrome b_6f complex.

Direct evidence of the Z-scheme's two photosystems came from the work of Duysens *et al.* (1961) working with the red alga *Porphyridium*. Duysens followed the redox state of a cytochrome, analogous to the b_6f complex, by measurement of absorbance change at 420 nm. He noted that illumination at 680 nm brought about the oxidation of the cytochrome whilst illumination at 680 nm and 562 nm resulted in its re-reduction. In the presence of DCMU, 680 nm excitation still resulted in oxidation of the cytochrome, however, the system had lost the ability to re-reduce the cytochrome on illumination at 562 nm. The two wavelength dependent reactions were termed reactions 1 and 2.

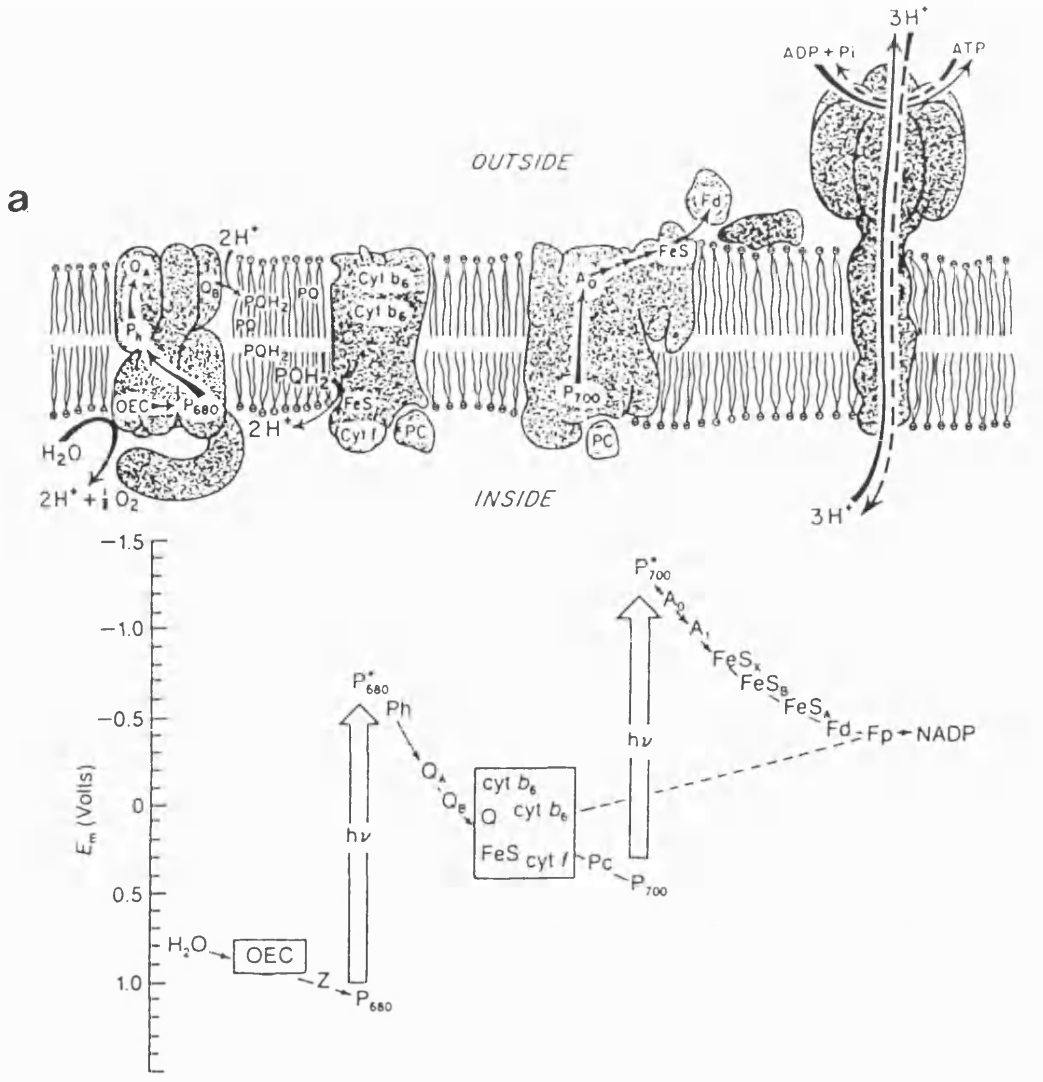

Figure 1.1

a.) The Z-Scheme:

A useful model for describing both the movement of electrons through the thylakoid protein complexes involved in electron transfer and the redox potential relationship between the cofactors. Electrons are made available through water oxidation at the thylakoid lumen side of PS-II and are then moved across the membrane by a series of electron transfer events. The mobile electron carrier PQH_2 leaves PS-II and moves within the membrane to the cytochrome b_6f complex, where it is oxidised. The electrons are then transferred to the soluble e^- carrier plastocyanin (PC). PC donates an electron to $P700^+$, in PS-I, that is subsequently transferred across the thylakoid and eventually used to reduce $NADP^+$. This diagram also shows where contributions are made to the proton gradient and the ATP-synthetase complex. The lower diagram shows the cofactors involved in each electron transfer event with their respective approximate mid-point redox potentials. OEC, oxygen evolving complex; Z, tyrosine residue; P680, PS-II reaction centre special chlorophyll; Ph, pheophytin; Q_A and Q_B, primary and secondary quinones; cyt, cytochrome; FeS, Rieske iron-sulphur protein; Pc, plastocyanin; P700, PS-I reaction centre special chlorophyll; A_0 and A_1, early acceptors of PS-I; FeS_X, FeS_B and FeS_A, are PS-I iron-sulphur centres; Fd, ferredoxin; FNR, ferredoxin-NADP reductase. [Diagrams from Ort and Good, 1988]

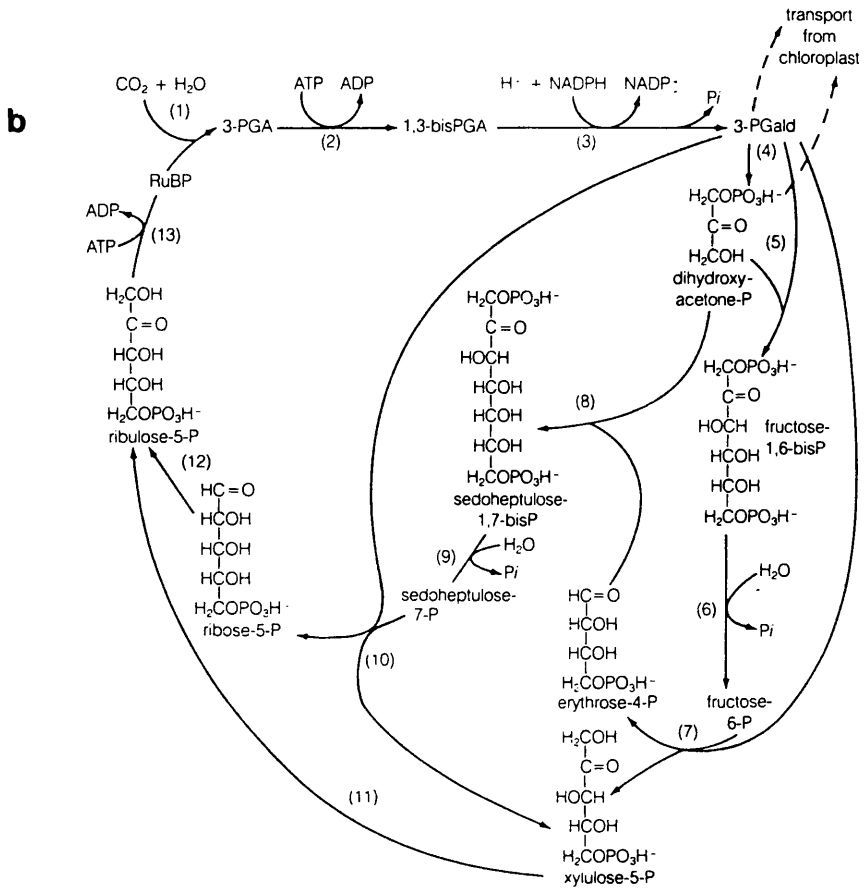

Figure 1.1

b.) Reactions of the Carbon Reduction Cycle

Carbon dioxide is reduced in the chloroplast by enzymes localised in the stroma. ATP and NADPH utilised during these reactions is renewed during the light reactions by the mechanisms outlined in sections 1.2 and 1.4. [Diagram from Salisbury and Ross: Plant Physiology, Third Edition, Wadsworth Publishing]

The existence of two wavelength specific photosystems also explained the findings of Emerson *et al.* (1957). Emerson and his co-workers observed that the rate of photosynthesis in chloroplasts illuminated at wavelengths above 680 nm was negligible as compared to the rates seen during illumination at wavelengths below 680 nm, although, the rate of photosynthesis was enhanced by simultaneous illumination with both wavelengths.

The process of photophosphorylation and electron transfer is now understood in terms of the chemiosmotic theory proposed by Mitchell (Reviewed in Mitchell 1966). The chemiosmotic theory suggested that electron transport creates a proton gradient across the thylakoid membrane via vectorially arranged redox components which, during oxidation and reduction reactions, serve to carry protons into the thylakoid lumen. The proton gradient thus formed drives the phosphorylation of ATP by flow through the membrane bound CF_1-CF_0 ATPase complex. Direct evidence of the chemiosmotic theory in the chloroplast was obtained by Jagendorf and Uribe (1966) who demonstrated that chloroplasts could synthesise ATP in the dark when an artificial proton gradient is created across the thylakoid membrane.

Oxidation of water, reduction of $NADP^+$ and phosphorylation of ADP, together with the utilisation of these intermediates, is given as a diagram atic representation of the Z-scheme and the light independent reactions in figure 1.1_{ab}.

1.3 Prokaryotic Photosynthetic Organisms

It has become obvious that there are similarities between prokaryotic and eukaryotic photosynthetic reaction centre complexes and membrane organisation. Studies of these systems may enable the elucidation of the function and structure of higher plant photosynthesis and possibly indicate the evolutionary pathway involved.

Prokaryotic photosynthetic organisms are classified into three groups:

1) *Rhodospirillales*

2) *Cyanobacteriales*

3) *Prochlorophyta*

Classification is dependent on their pigment type and whether or not they evolve oxygen. All photosynthetic prokaryotes are gram-negative with the exception of *Heliobacterium chlorum*.

1) *Rhodospirillales*. *Rhodospirillales* are divided into *Rhodospirillineae* (purple bacteria) and *Chlorobiineae* (green bacteria).

The purple bacteria are further divided into the purple sulphur bacteria (*Chromatiaceae*) and the purple non-sulphur bacteria (*Rhodospirillaceae*). Purple sulphur bacteria are obligate anaerobes, they grow photoautotrophically utilising the oxidation of hydrogen sulphide to provide reducing power for the fixation of carbon dioxide in the reductive pentose cycle. In contrast most purple non-sulphur bacteria are heterotrophic and are unable to tolerate hydrogen sulphide, they require an external source of organic material which is metabolised utilising ATP

generated during light driven cyclic electron transfer.

The green bacteria contain bacteriochlorophyll a in the reaction centre and bacteriochlorophylls c, d, or e in their light-harvesting chlorosomes. They are also divided into two families: the green sulphur bacteria (*Chlorobiaceae*) and the green non-sulphur bacteria (*Chloroflexaceae*).

Green non-sulphur bacteria are facultative aerobes, however their photosynthetic apparatus is only activated under anaerobic conditions. Generally these organisms are photoheterotrophic, although, under certain circumstances, they will grow photolithotrophically. The green sulphur bacteria are all obligate anaerobes and require sulphur compounds to provide reducing power for the fixation of carbon dioxide.

2) *Cyanobacteriales*. Cyanobacteria are generally aerobic photoautotrophs, although there are exceptions. Their photosynthetic apparatus can be compared to that seen in the eukaryotes, a thylakoid membrane housing two pigment protein photosystems with reaction centres P700 (PS-I) and P680 (PS-II). The light-harvesting complex, bound to the cytoplasmic face of the thylakoid membrane, contains phycobilins (linear tetrapyrroles) and chlorophyll a giving a blue-green appearance. The major differences in the photosynthetic apparatus of cyanobacteria as compared to eukaryotes is the lack of thylakoid differentiation and the reaction centre complexes contain no chlorophyll b.

3) *Prochlorophyta*. This phylum contains the most advanced examples of prokaryote oxygenic photosynthesis. An example of the

species is *Prochloron didemni*, an endosymbiont of ascidians, which contains: a differentiated thylakoid, two types of thylakoid membrane bound photosystem, both chlorophylls a and b, and does not use phycobil ins. The evolutionary origins of chlorophyll in higher plant light-harvesting systems is as yet undetermined but the discovery of this new group of bacteria may lead the way in the search for the precursor of the chloroplast.

1.3.1 Evolutionary Relationships

Studies into the origin of the two photosystem organisation seen in cyanobacteria and higher plants often cite the purple bacteria as a probable ancestor of the photosystem-II reaction centre complex. It was originally thought that in evolutionary terms the green sulphur bacteria most closely resembled photosystem-I and as such formed a likely candidate for common ancestry. However, Mathis (1990) suggested that the cyanobacteria originated by the fusion of a purple sulphur bacteria and a gram positive bacteria thereby discounting the green sulphur bacteria as the forerunner of photosystem-I. Mathis' work was adapted from the evolutionary tree presented by Woese (1987) which was based primarily on sequence analysis of rRNA but Mathis expanded these ideas by incorporating additional structural and functional information of various reaction centre complexes (Nitschke *et al.*, 1990_a; Sétif and Bottin, 1989).

Nitschke and Rutherford (1991) also suggested both photosystem-I and photosystem-II type reaction centres had evolved from a common

ancestor. They base their scheme on the structural and functional similarity of reaction centres from widely diverse organisms.

Photosystem-I, green sulphur and heliobacteria all appear to have a chlorin-type primary acceptor molecule (Nuijs *et al.*, 1985_{ab}), magnetically interacting iron sulphur centres Fe-$S_{A/B}$ (Nitschke *et al.*, 1990_{ab}) and display properties reminiscent of quinone double reduction (Nitschke *et al.*, 1990_{ab}). The green sulphur bacteria have also been shown to contain iron-sulphur centre X. However, in accordance with the common ancestor theory, the donor side of the reaction centre of green sulphur bacteria, and to an extent the heliobacteria, is comparable to that observed in the purple bacteria. Both green sulphur and heliobacteria photosystems have a primary donor with EPR characteristics of a chlorin dimer similar to those observed in purple bacteria. Purple and green sulphur bacteria also utilise cytochrome c to reduce the photo-oxidised reaction centre. Comparisons can also be drawn between higher plant photosystem-I and the purple bacteria. The photosystem-I core complex, depleted of its peripheral polypeptides, contains two quinone molecules, a proposed two primary chlorophyll molecules (one of which acts as the primary acceptor) and a reaction centre which is probably dimeric in the ground state (although in the cation state the electron is localised primarily over one chlorophyll molecule). This situation is similar to the purple bacteria reaction centre complex which contains two quinones that accept electrons from a chlorin molecule (bacteriopheophytin) and has a bacteriochlorophyll special pair reaction centre. Photosystem-I also appears to have the same C_2 symmetry

observed in purple bacteria with a photo-active electron transport chain and a second set of analogous redox components which, although photo-active, are far less efficient (Heathcote *et al.*, 1993). The major difference between photosystem-I and the purple bacteria is the existence of Fe-S A, B and X. However the position of Fe-$S_{A/B}$ on a peripheral 9 kDa polypeptide indicates that it could be a later addition.

In reality, the origin of higher plant photosynthesis remains undetermined and until both the sequence studies and a crystal structure is complete for all of the relevant organisms, it will probably remain so.

1.4 Introduction to Oxygenic Photosynthesis

Eukaryotic photosynthetic organisms are organised so that the capture of light energy and its conversion into biochemical intermediates occurs within chloroplasts (fig. 1.2_a). The chloroplast is an organelle comprising a double outer mer brane enclosing a matrix known as the stroma. Embedded throughout the stroma is a specialized system of internal membranes called the thylakoid. The thylakoid forms a selectively permeable barrier which maintains the internal thylakoid environment, the lumen, at a different chemical composition to that of the stroma. In certain regions (termed grana) the thylakoid membranes take on a stacked or appressed appearance. Appressed regions of granal lamellae are inter-connected by unappressed inter-granal thylakoid membranes which extend through the stroma and are termed the stromal lamellae (fig. 1.2_b).

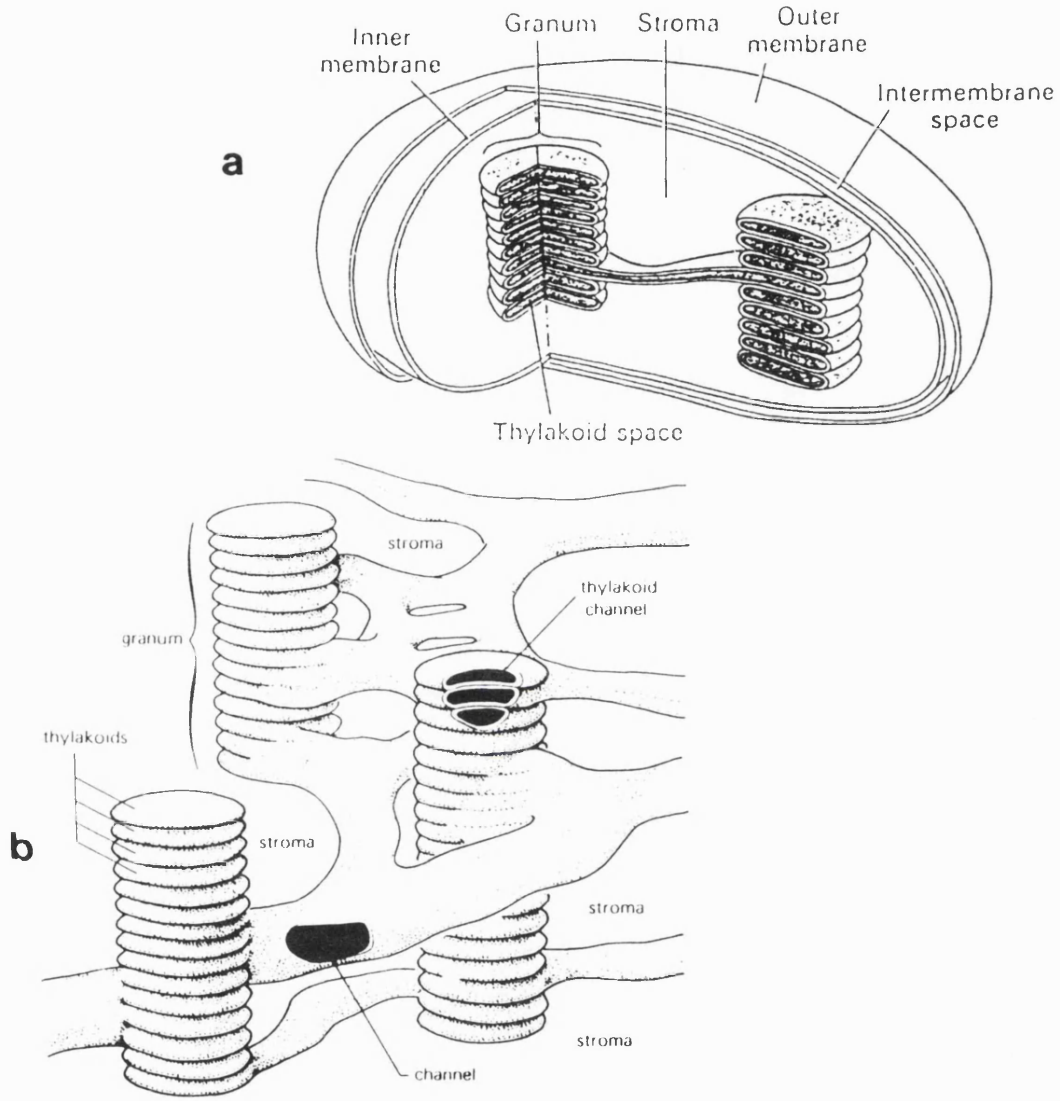

Figure 1.2

a. The Chloroplast Structure.

These organelles have three separate membranes: the inner and outer envelope membranes and the thylakoid. [Diagram from Wolfe: Biology of the Cell, 1972]

b. A Three Dimensional Interpretation of the Arrangement of the Thylakoid Membrane.

The thylakoid membrane forms the energy transducing region of the chloroplast and is divided into two distinct regions, the stromal lamellae and the granal stacks. It is the thylakoid, surrounded by the aqueous stroma, that binds the protein complexes involved in electron transport. [Diagram a. from Wolfe: Biology Of The Cell, 1972., Diagram b. from Salisbury and Ross: Plant Physiology]

Fixation of CO_2 is carried out by enzymes situated in the stroma; this process requires NADPH and ATP manufactured during the "light reactions" in a series of redox reactions which involves the oxidation of water, see section 1.2 and fig. 1.1_{ab}.

The conversion of light energy into biochemical intermediates occurs in integral thylakoid membrane pigment protein complexes. The difference in potential between O_2/H_2O and $NADP^+/NADPH$ is about 1.1V; the mechanism of photosynthetic energy transfer is not 100% efficient and thus a single visible photon cannot lower the potential by this amount. The problem of energetics is solved by coupling two protein-pigment complexes, termed photosystem-I and photosystem-II, in series. Each photosystem operates over a different range of redox potentials. Photosystem-I complex (PS-I) is localised mainly in the stromal lamellae and Photosystem-II complex (PS-II) is found mainly in the grana (fig. 1.2_b).

Both photosystem-I and photosystem-II contain two functionally distinct regions: an antenna complex, forming the light-harvesting region, and a core complex which binds the reaction centre and other redox components and is involved primarily with charge separation.

The absorption of light and the transfer of energy by pigment molecules is the fundamental event of photosynthesis. The majority of these pigments are bound to the antenna proteins, although the core complex is also involved in antenna pigment binding. The most important pigments in higher plant energy absorption and transfer are the cyclic tetrapyrrole chlorophylls but there are other pigments, such as carotenoid,

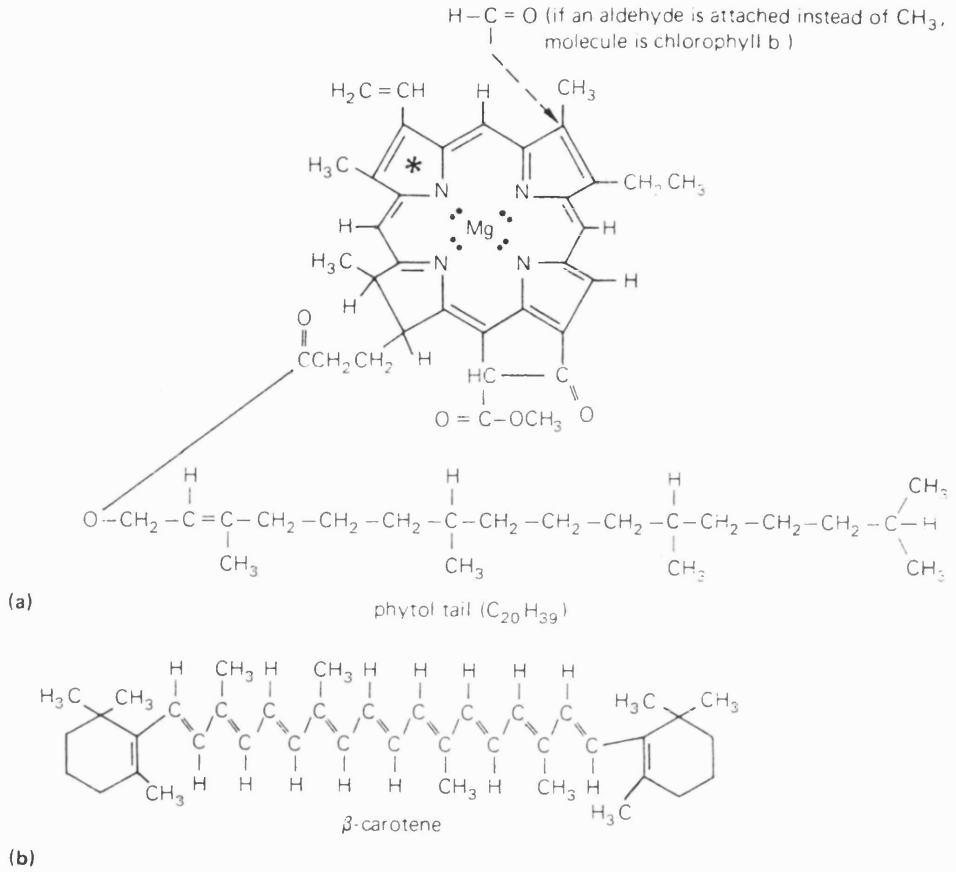

Figure 1.3

Photosynthetic Pigments.

a. The Cyclic Tetrapyrrole Structure of Chlorophyll a. The four nitrogen atoms of the pyrroles are co-ordinated to a magnesium atom making chlorophyll a magnesium porphyrin. These molecules are very efficient photoreceptors because of their polyene structure of alternating single and double bonds. There are other related molecules such as chlorophyll b which has an aldehyde (-CHO) in the place of the methyl (-CH_3) on ring II.

b. Carotene which plays a role in both light harvesting and photo-protection. [Diagram from Salisbury and Ross: Plant Physiology, Third Edition, Wadsworth Publishing]

which absorbs light in the spectrum unavailable to the chlorophylls (fig. 1.3_{ab}).

Absorption of a photon by the antenna pigment causes an electron transition from a low energy ground state to a higher energy excited singlet state. This absorption is extremely rapid, the first excited singlet state is formed in a time inversely proportional to the frequency of the incident wavelength, for red light this would be around 2.3×10^{-15} s. The excited singlet electron is paired with the spin of an electron in the ground state and tends to drop into the stable ground state with a concomitant release of energy. The fate of the energy, as the singlet relaxes, may proceed in several ways: radiationless transition (thermal relaxation), fluorescence, delayed light emission (luminescence), phosphorescence or energy transfer to the reaction centre complex. *In vivo* the most important mechanism is energy migration to the reaction centre. The rate of energy transfer from one molecule to the next depends on an overlap between the fluorescence spectrum of the donor and the absorption spectrum of the acceptor; it is also inversely proportional to $r \times 10^6$, where r is the distance between molecules. Time resolved kinetic experiments indicate an average time of exciton transfer between pigments of 0.21 ps with an average 2.4 visits to the reaction centre before photochemical energy trapping.

The essential feature for trapping the energy corresponds to the step containing photoinduced charge separation between the primary donor (P) and the primary acceptor (A). In both photosystem-I and photosystem-II the reaction centre chlorophyll (P) most likely takes the form of a dimer of

chlorophyll molecules. On excitation P becomes a powerful reducing agent (P^*) and interacts with a cofactor (A) forming the primary light induced electron transfer event:

$$P + A + \text{Energy} \text{ ------> } P^* + A \text{ ------> } P^+ + A^-$$

The ability of a chemical species to transfer electrons is measured in terms of its redox potential. The redox potential of a component is measured by comparison to a standard hydrogen electrode which has a voltage (E^o) under standard conditions and a pH of 0.

The relationship between measurable redox potential and relative concentrations of oxidised and reduced component is given by:

$$E = E^0 + \frac{RT}{nF} \ln \frac{[Ox]}{[Red]}$$

Where:

R = the gas constant.

T = the absolute temperature.

n = the number of electrons transferred.

F = the Faraday's constant.

Redox potentials are therefore concentration dependent and the potential of a given component (E_m) is the midpoint where the concentrations of oxidised and reduced forms are equal. Substances with a more negative redox potential are energetically able to reduce those of a more positive potential.

The reaction centre special pair chlorophyll of photosystem-II, called P680 due to its bleaching at 680 nm, is photo-oxidised by the mechanisms outlined above and the electron passes to a plastoquinone via a number of redox components associated with the photosystem-II pigment protein complex. P680 is re-reduced by the oxygen evolving complex with a concomitant splitting of water (fig. 1.1_a). Analogous redox events are observed in photosystem-I with the net result the reduction of $NADP^+$ and oxidation of plastocyanin (a diffusible copper protein) by the reaction centre P700. Electron transfer events in photosystem-I and photosystem-II are linked by the cytochrome b_6f complex which is a membrane bound protein complex containing two cytochromes and two iron-sulphur centres. The b_6f complex can be considered as a membrane bound enzyme catalysing the oxidation of plastoquinol and the reduction of plastocyanin.

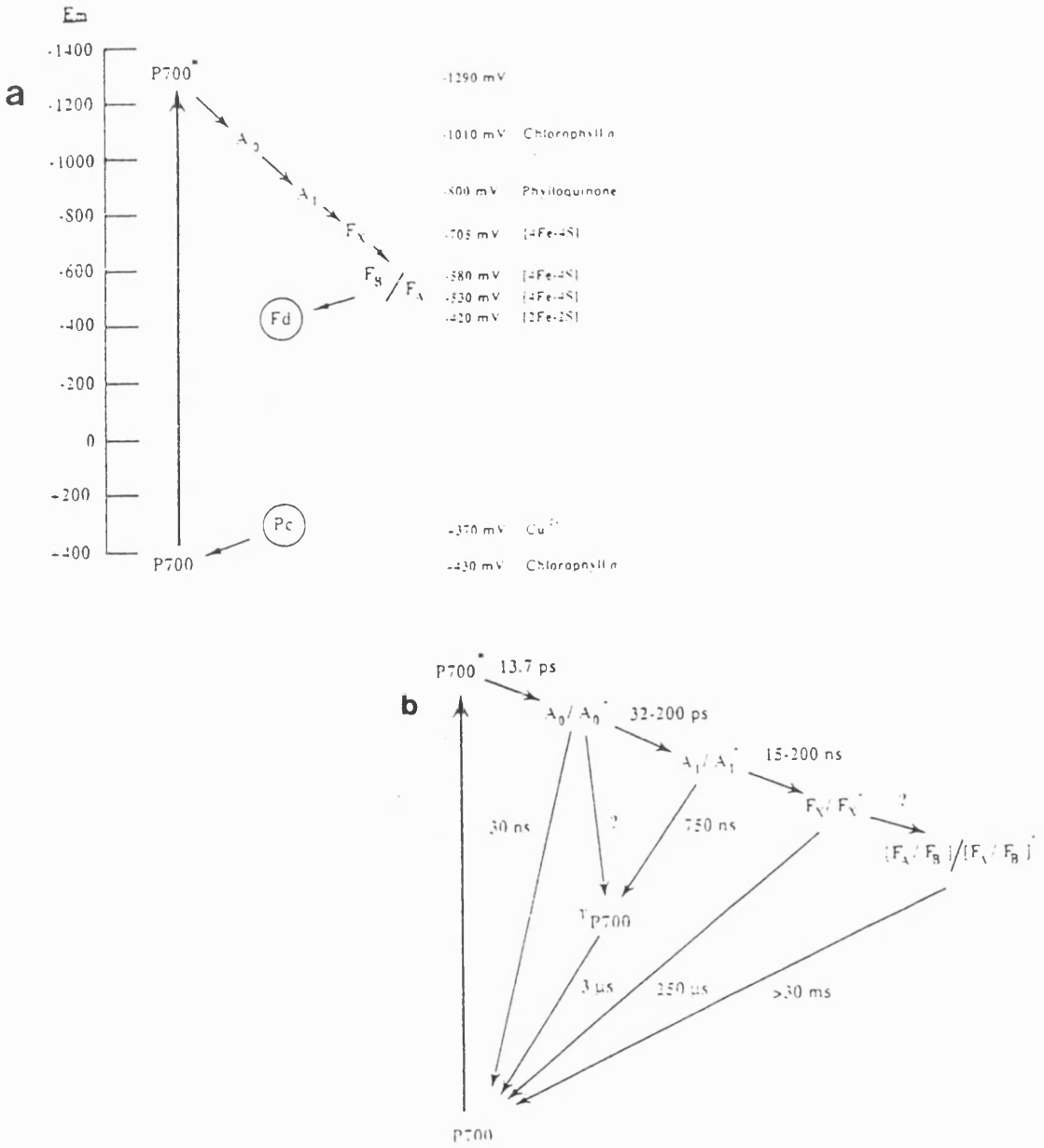

Figure 1.4

a. Redox Components of Photosystem-I with Respective Midpoint Potentials.

P700, the primary donor; A_0, the primary acceptor chlorophyll molecule; A_1 the phylloquinone secondary acceptor; and three iron-sulphur centres Fe-S_X, Fe-S_B and Fe-S_A. The E_m of A_0 and A_1 has not been directly measured, the order of these components in this scheme is based primarily on kinetic and photo-accumulation data. The flow of electrons through the iron-sulphur centres is also uncertain and their order here is based on photo-accumulation experiments and measured redox potential. [Diagram from Golbeck and Bryant, (1991)].

b. Room Temperature Kinetics of Electron Flow in Photosystem-I.

There are discrepancies in the published data and variations in time constants depending on the type of preparation used, however, figure 1.4_b gives an indication of the time scales involved in photosystem-I redox interactions. [Diagram from Golbeck and Bryant, (1991)].

1.5 Electron Transfer Components of Photosystem-I

Some of the properties of the photosystem-I reaction centre complex have been summarised in the earlier part of this thesis, however, the redox components involved in energy trapping and electron transfer in photosystem-I will now be discussed in more detail. Figure 1.4_{ab} outlines the redox components together with their redox potentials and time scale of redox events.

1.5.1 The Primary Donor P700

The photochemical energy trap and primary electron donor P700 derives its name from the observation of a bleaching at 700 nm induced in illuminated chloroplasts (Kok, 1956). The identification of this bleaching as a one electron oxidation of a chlorophyll molecule came from both optical (Kok, 1957) and EPR studies (Kok and Beinert, 1962). The midpoint potential of P700 was initially measured at +430 mV, since then, a number of values have been reported. A value of +490 mV was determined for the redox potential for most intact photosystem-I particles (Sétif and Mathis, 1980), although Evans and his co-workers have demonstrated that cryogenic EPR measurements of redox titrations of Triton X-100 photosystem-I particles indicate an E_m of +375 mV Evans *et al.* (1977) and room temperature titrations give a value of +420 mV (unpublished). The variation in observed midpoint potentials has been attributed to different experimental procedures during the preparation of photosystem-I particles and the decrease of apparent redox potential at

lower temperatures.

The ratio of P700 to bulk chlorophyll varies widely depending on the organism. Cyanobacterial thylakoids have the lowest ratio at 130-160 Chl/P700 (Melis and Brown, 1980; Takahashi *et al.*, 1982) with ratios of 500 (±100) being found in C_3 chloroplasts (Melis and Brown, 1980; Whitmarsh and Ort, 1984).

The EPR line width of $P700^+$ (0.70-0.71 mT) is narrowed by a factor of $\sqrt{2}$ as compared to a monomeric chlorophyll cation (0.9 mT). This was interpreted as the delocalisation of an unpaired electron over two chlorophyll molecules indicating that P700 is a chlorophyll dimer (Norris *et al.*, 1971). The dimer theory gained support from circular dichroism spectroscopy (Philipson *et al.*, 1972; Karapetyan *et al.*, 1984), optical absorption (Ikegami and Itoh, 1986; Ikegami and Itoh, 1988) and resonance Raman studies (Möenne-Loccoz, 1990). Comparison of P700 to the bacterial reaction centre also led to the conclusion that the higher plant reaction centre is probably a dimer but alternative viewpoints have been advanced. Analysis of ENDOR data shows that not all of the proton hyperfine interactions are halved as would be expected if the electron were delocalised over a symmetric dimer (O'Malley and Babcock, 1984). Wasielewski *et al.* (1981) suggested that the hyperfine interactions are more easily attributable to the chlorophyll $\underline{a}^+$ monomer with an enolisation in ring V but this view has been challenged by FTIR spectra which indicates the presence of a keto and not an enol (Nabedryk *et al.*, 1989). EPR analysis of triplet state P700 has also shown parameters similar to

those of a monomeric triplet state chlorophyll (Frank *et al.*, 1979; Rutherford and Mullet, 1981) indicating that the electron is located on a single chlorophyll molecule. Such disparate data is difficult to reconcile although interpretation of more recent information may go some way towards an explanation of the observed results. It has been suggested that the two chlorophyll a molecules forming the proposed chlorophyll dimer P700 reaction centre are oriented such that there is a small electronic overlap. This results in a resonance interaction between their singlet excited states giving rise to two new transitions (excitonic coupling). One of these transitions was initially assigned to the major bleaching at 700 nm and the other at 680 nm. Analysis of more recent absorption and CD spectra suggests that there is no resolution of the transitions and the excitonic couple gives rise to a broad band at 694-696 nm for neutral P700. The oxidation of P700 leads to the appearance of a further absorption band at 687-690 nm with a band width and area corresponding to the ratio $P700:P700^{+}$ of 2:1, (Ikegami and Itoh, 1988). Electron spin echo envelope modulation (ESEEM) data also indicates that the unpaired electron of $P700^{+}$ is extensively localised over one of the chlorophyll molecules but gives a ratio of 3-4:1 (Davis *et al.*, 1993).

Although it is impossible to draw any final conclusions as to the exact structure of the P700 reaction centre much of the recent spectroscopic data suggests that in the ground state P700 exists as a dimer but in the cationic state the electron is distributed asymmetrically but involves both chlorophyll molecules.

Picosecond measurements of the initial events involved in the rise of $P700^*$ and primary charge separation have proven difficult due to interference from energy transfer events occurring in the antenna complex. However, taking an oxidised-minus-reduced difference spectrum of pump/probe kinetic data has made it possible to investigate the kinetics of early redox dependent events in photosystem-I. These experiments assume that the mode of energy transfer in the antenna complex is independent of the redox state of P700.

In practice it is impossible to differentiate between the rise of $P700^*$ and $P700^+$ by measuring the reaction centre directly, the formation of both excited state and oxidised reaction centre are exhibited as a bleach arising within the resolution of the spectrophotometer. However, Wasielewski *et al.* (1987) reported the formation of the $P700^+/A_0^-$ radical pair with a time constant of 14 ps (fig. 1.5). This was based on the rise of a redox dependent bleaching at 690 nm, the proposed absorbance peak of the primary chlorophyll electron acceptor A_0. Kim *et al.* (1989) confirmed these findings using photosystem-I particles depleted of the majority of their light-harvesting pigment by ether extraction.

It has been suggested that P700 is chemically distinct from chlorophyll a. A chlorinated chlorophyll species was isolated in a ratio of 1:1 with P700 (Scheer *et al.*, 1986), but this was dismissed as an artefact of preparation (Senger *et al.*, 1988). Other suggested chemical types have also been put forward such as; 13^2-Hydroxy-20-chlorophyll a (Dörnemann and Senger, 1986), a C-10 epimer of chlorophyll a (Watanabe *et al.*, 1985)

and a chlorophyll a enol (Wasielewski *et al.*, 1981). However, there is no conclusive evidence of any of these and most probably reflect either the isolation procedure or the protein environment.

1.5.2 The Primary Acceptor A_0

The midpoint potential of the primary acceptor A_0^-/A_0 is suggested to be -1000 mV. Indirect measurements obtained from kinetics of chlorophyll luminescence, induced by applied electrical field, imply an A_0 midpoint potential of -1010 mV (Vos and Van Gorkom, 1988). Comparison to bacterial reaction centres would indicate that a chlorin probably forms the primary acceptor molecule. It was also suggested that the rapid rate of primary electron transfer in bacterial systems is enhanced by the similar nature of the primary acceptor and the primary donor molecules, by analogy a chlorophyll a molecule would therefore form the likely primary acceptor molecule.

A_0 has been studied primarily by two methods: photo-accumulation and time resolved optical spectroscopy. Photo-accumulation of A_0^- is achieved by steady state illumination under reducing conditions; optical difference spectra obtained under such conditions indicate A_0 to be an anionic chlorophyll a molecule occurring in a ratio of 0.94 with P700 (Mansfield and Evans, 1985). Illumination at 200K in the presence of dithionite initially gives rise to an asymmetric EPR spectra centred at g = 2.0058 with a line width of 1.03 mT compatible with the reduction of the secondary electron acceptor A_1. The presence of dithionite serves to reduce

P700 at 200K and also to maintain the iron-sulphur centres in a reduced state. Further illumination at 200 K broadens the spectra to 1.35 mT centred at 2.0025 and is consistent with the identification of the photo-accumulated primary acceptor as a chlorophyll a anion (Mansfield and Evans, 1988; Smith *et al.*, 1987). Confirmation of identification of the primary acceptor initially came from optical absorbance measurements of photo-accumulated photosystem-I samples which indicated an absorbance peak at 670 nm (Mansfield and Evans, 1985). More recent picosecond time resolved studies also indicate the presence of a redox dependent chlorophyll species acting as the first electron acceptor from P700.

Time resolved optical absorption studies of primary charge separation are dependent on identifying absorption changes characteristic of the reduction of A_0. This technique therefore requires the calculation of an oxidised-minus-reduced difference spectrum to remove the large absorption changes due to exciton transfer within the antenna complex of photosystem-I. This assumes that the characteristics of the excited state antenna complex are identical in both redox states of P700. The flash induced $P700^+/A_0^-$ absorption spectrum show a bleach centred at 690 nm consistent with the proposal of the primary acceptor chlorophyll (Mathis *et al.*, 1988). Picosecond measurements also indicate the presence of a redox dependant bleaching at 690 nm rising with a time constant of 14 ps (Wasielewski *et al.*, 1987). Experiments which excite P700 directly, thereby removing the majority of antenna effects, also show a chlorophyll a acceptor bleaching at 693-695 nm but the time scale of reduction was not

resolved during these experiments (Shuvalov *et al.*, 1979_{ab}, 1986).

The 15-20 nm discrepancy in the observed wavelength of A_0 determined by photo-accumulation, as compared to picosecond spectroscopy, is of a magnitude which might indicate the formation of two different components. It has been suggested that the true primary acceptor chlorophyll molecule (A_0) is seen at 690 nm. The bleach observed at 670 nm is possibly an artefact generated by the reduction of a near-by chlorophyll molecule which photo-accumulates during the time period of the experiment (Mathis *et al.*, 1988). Recent data indicates the existence of a second chlorophyll acceptor (and Quinone secondary acceptor) reduced by prolonged illumination at 230K in the presence of dithionite. It is possible that this species forms the 670 nm absorption observed in photo-accumulation experiments (Heathcote *et al.*, 1993).

Not all workers support the identity of the primary acceptor molecule as a chlorophyll. Klug *et al.* (1989), working with intact photosystem-I, found no evidence of a chlorophyll molecule with a 690 nm optical transient acting as a primary charge acceptor.

Although the evidence strongly supports the model of a chlorophyll dimer reaction centre interacting with a monomeric chlorophyll primary electron acceptor the results obtained to date are not conclusive and further work is required in this field.

1.5.3 The Secondary Acceptor A_1

The chemical identity and function of the photosystem-I redox

component designated A_1 still remains a controversial subject. Although A_1 is believed to be a quinone molecule mediating redox interactions between A_0 and iron-sulphur centre Fe-S_X, an exact model of the electron transfer pathway has yet to be established.

Illumination at 200K under reducing conditions gives rise to an asymmetric EPR signal 1.03 mT wide centred at g = 2.0040 consistent with a reduced quinone species (Bonnerjea and Evans, 1982). UV absorbance spectra and low temperature flash induced absorption changes indicate that this species is probably a phylloquinone (Vitamin K-1) radical (Mansfield and Evans, 1985; Brettel *et al.*, 1986.).

The presence of quinone molecules is confirmed by solvent extraction which indicate that native photosystem-I reaction centre preparations contain two molecules of phylloquinone per P700 (Malkin, 1986). Removal of one of these by relatively mild solvent extraction of freeze dried photosystem-I does not affect electron transfer (Malkin, 1986; Sétif *et al.*, 1987) but hexane-methanol extraction of both quinones results in the blockage of electron transport past A_0 (Itoh *et al.*, 1987; Sétif *et al.*, 1987; Mansfield *et al.*, 1987_a). Under these conditions the EPR signal assigned to A_1 cannot be photo-accumulated and only the A_0^- signal is present (Mansfield *et al.*, 1987_a), although, photoreduction of iron-sulphur centres still occurs at low temperature (Sétif *et al.*, 1987). EPR experiments indicate Fe-S_X is closer to A_0 than A_1 and it has been suggested that this may provide a route for low temperature photoreduction of iron-sulphur centres (Ikegami and Itoh, 1987; Mansfield and Evans, 1988). In A_1

depleted cyanobacterial preparations, forward electron transfer can be reconstituted by the addition of phylloquinone, this restores both the millisecond kinetics and the ability to reduce $NADP^+$ (Biggins and Mathis, 1988). However, a range of quinones have been reported to reconstitute to the reaction centre complex (Iwaki and Itoh, 1989) and there has been questions over the specificity of reconstitution.

Photosystem-I samples illuminated under high light conditions, in the presence of dithionite, at 4^0C show $P700^+$ re-reduction kinetics of $t_{½}$ 30 ns indicative of redox centres being blocked beyond A_0. This has been interpreted as the double reduction of quinone to quinol thereby altering its midpoint potential to a value which prevents forward electron transfer to Fe-S_X and confirming the identity of A_1 (Sétif and Bottin, 1989,1990). Photosystem-I also exhibits an electron spin polarised (ESP) EPR signal thought to arise from the $P700^+/A_1^-$ radical pair (Thurnauer and Gast, 1985). This signal is lost on both solvent extraction (Rustandi *et al.*, 1990) and double reduction (Snyder *et al.*, 1991) but it is reconstituted by re-addition of the solvent extracted quinone (Rustandi *et al.*, 1990) or re-oxidation of the quinol (Snyder *et al.*, 1991).

All the evidence thus far clearly indicates A_1 to be a molecule of phylloquinone involved in mediation of electron transfer from the primary acceptor to Fe-S_X, however, there is contradictory data which renders the situation much less clear cut.

Mansfield *et al.* (1987_b) found a narrowing of the photo-accumulated A_1 EPR signal after photosystem-I particles had been exchanged with D_2O.

In contrast, cyanobacteria grown in deuterated methionine, which deuterates most of the phylloquinone, showed no sign of narrowing in the EPR signal attributable to A_1 (Barry *et al.*, 1988). Ziegler *et al.* (1987) and Biggins *et al.* (1989) found that total destruction of both molecules of phylloquinone by irradiation with UV light at 354 nm did not affect either the photo-accumulated A_1 EPR spectra or the room temperature photoreduction of benzyl viologen although inactivation of $NADP^+$ photoreduction has been reported (Biggins and Mathis, 1988). Low temperature photoreduction of iron-sulphur centres was also unimpeded by photo-inactivation of phylloquinone, although this may be a result of the formation of the $A_0^+/Fe\text{-}S_X^-$ couple at cryogenic temperatures (Mansfield and Evans, 1988).

Techniques of phylloquinone removal or inactivation are extremely harsh and the results gained from such treatments may bear little relevance to the *in vivo* situation. Cryogenic measurements may also be misleading causing anomalies in low temperature redox events which are irrelevant at room temperature.

Although the majority of evidence suggests that phylloquinone plays a role in mediation of forward electron transfer recent experimental data suggests that the situation is not as straight forward as was originally thought and further work is required before its role can be fully defined.

1.5.4 The Bound Iron-Sulphur Centres

There are three iron-sulphur centres bound to the photosystem-I

reaction centre complex; Fe-S_X, bound to the core complex proteins PSI-A and PSI-B, and Fe-S_A and Fe-S_B housed on a peripherally bound polypeptide, PSI-C. The structure and function of these centres has been extensively researched and is discussed below.

Iron-Sulphur Centre Fe-S_X

Chemical reduction of Fe-S centres A and B followed by low temperature illumination gives rise to another photoreduced EPR signal coupled to the photo-oxidation of P700. This component has g values of 2.04, 1.88, and 1.78 and an EPR line shape consistent with identification as a modified iron-sulphur centre (Evans *et al.*, 1975). The EPR spectrum of Fe-S_X^- is broader than would be expected of an iron-sulphur centre and it has an unusual temperature dependence but there is no evidence to suggest that it is liganded by anything other than cysteine residues (see section 1.6.1). Flash induced difference spectra, achieved under similar conditions to EPR experiments, confirm the identification of this component as an iron-sulphur centre (Koike and Katoh, 1982; Parrett *et al.*, 1989).

Determination of the precise chemical nature of Fe-S_X has proven difficult with experimental evidence indicative of both [2Fe-2S] and [4Fe-4S] clusters. These anomalies are due largely to the close proximity of Fe-S_X to iron-sulphur centres A and B which results in inconsistencies of data interpretation. However, early Mossbauer experiments identified Fe-S_X to be a 4Fe-4S iron-sulphur centre (E. H. Evans *et al.*, 1981). Further

Mossbauer studies, using core complex photosystem-I devoid of its two terminal iron-sulphur centres, confirmed the findings of E. H. Evans *et al.* (1981) demonstrating that both oxidised and reduced spectra showed isomer shifts typical of those expected in a 4Fe-4S centre (Petrouleas *et al.*, 1989).

EXAFS studies on photosystem-I particles containing Fe-$S_{A\backslash B}$ and Fe-S_X proved ambiguous indicating Fe-S_X to be either 2 X [2Fe-2S] clusters or a distorted 4Fe-4S cluster (McDermott *et al.*, 1988). However, experiments on Fe-$S_{A\backslash B}$ depleted particles had simulated spectra most characteristic of a 4Fe-4S cluster (McDermott *et al.*, 1989) and it is now generally agreed that Fe-S_X is a four iron centre.

$P700^+$/Fe-S_X^- back reaction kinetics (Sauer *et al.*, 1979; Golbeck and Cornelius, 1986), midpoint potential (Chamorovsky and Cammack, 1982; Parrett *et al.*, 1989), photo-accumulation (Evans *et al.*, 1975) and position on the core complex all suggest that it is an intermediate redox component situated between A_1 and Fe-$S_{A\backslash B}$ in a system of linear electron transport from P700 to the terminal iron-sulphur centres. Two pathways of electron flow have been postulated: a linear path from X->B->A or a branched system of delivery to either Fe-S A or B (See section 1.6.6), but in reality the role of Fe-S_X in down stream reduction of iron-sulphur centres has not been directly demonstrated at physiologically relevant temperatures.

Iron-Sulphur Centres Fe-$S_{A\backslash B}$

Iron-Sulphur Centres Fe-$S_{A\backslash B}$ were first described by optical

spectroscopy as an oxidised-minus-reduced absorption band with a bleach centred at 430 nm. Kinetic measurements of the 430 nm optical transient showed that it back reacted with $P700^+$ with a $T_{½}$ of 30 ms and a midpoint potential of -520 mV was measured (Hiyama and Ke, 1971; Ke, 1972). These initial findings lead workers to believe that this redox component, labelled P430, was an iron-sulphur centre and the electron acceptor involved in primary charge separation with P700. At around the same time Malkin and Bearden (1971) demonstrated low temperature photoreduction of a bound redox component giving an EPR signal with g values of 2.05, 1.94, and 1.86 characteristic of an iron-sulphur centre. Subsequent EPR studies identified a further iron-sulphur centre with g values of 2.07, 1.92, and 1.89 (Bearden and Malkin, 1972; Evans *et al.*, 1972). It was proposed that these two sets of signals represented two magnetically interacting iron sulphur centres existing on a single polypeptide with an interactive EPR spectra at g = 2.05, 1.94, 1.92 and 1.89 (Evans *et al.*, 1974). Sauer *et al.* (1977) confirmed this showing that P430 could hold two electron equivalents on successive flashes. The iron-sulphur centres within the acceptor complex were labelled Fe-S_A and Fe-S_B. Redox measurement of Fe-S A and B placed the midpoint potentials at -530 mV and -580 mV respectively (Ke *et al.*, 1973; Evans *et al.*, 1974).

Identification of Fe-S_A and Fe-S_B as 4Fe-4S centres came from EPR (Cammack and Evans, 1975), EXAFS (McDermott *et al.*, 1988), and Mossbauer studies (Evans *et al.*, 1979). Furthermore, sequence studies on the 9 kDa gene product of *psa*C, the polypeptide most likely to house the

Fe-$S_{A/B}$ centre (ref. section 1.6.2), show a distribution of cysteine characteristic of those found in bacterial 2 X [4Fe-4S] ferredoxins (Oh-oka *et al.*, 1988_{ab}).

Fe-$S_{A\backslash B}$ plays an essential role in forward electron transfer to soluble ferredoxin but the exact pathway of transfer from Fe-S_X to ferredoxin through the Fe-$S_{A\backslash B}$ complex is uncertain.

1.5.5 Pathway of Electron Transport Through the Photosystem-I Reaction Centre Complex

Photo-accumulation experiments and assessment of redox potentials would suggest a linear electron transport chain;

P700 --> A_0 --> A_1 --> Fe-S_X --> Fe-S_B --> Fe-S_A --> Ferredoxin

However, electron transfer between each of the centres has not been directly demonstrated and the redox potentials of A_0 and A_1 have not been determined. Anomalies in the results obtained by different techniques has lead to alternative viewpoints as to the system of electron transport by which electrons flow to ferredoxin. One such system is a branched electron transport chain in which A_0 can interact with either A_1 or Fe-S_X in order to reduce Fe-$S_{A/B}$.

P700 --> A_0 --> Fe-S_X.....> / A_1 .....> --> Fe-$S_{A/B}$ --> Ferredoxin

EPR measurements indicate that Fe-S_X strongly interacts with A_0 and not A_1, this infers that A_0 is closer to the iron-sulphur centre than the quinone (Ikegami and Itoh, 1987; Mansfield and Evans, 1988). This is an unusual scenario if A_1 acts as an intermediate of electron transport between A_0 and Fe-S_X as suggested by photo-accumulation experiments. In samples depleted of A_1 by U.V. destruction or solvent extraction there is little difference in the ability to raise a photoinduced Fe-S_X^- EPR spectra at cryogenic temperatures (Biggins *et al.*, 1989; Ziegler *et al.*, 1987) indicating direct interaction between A_0 and Fe-S_X.

Measurements of the rise time kinetics of electron transfer to iron-sulphur centres Fe-S_X Fe-S_A and Fe-S_B is difficult because of their similar nature and the weakness of their optical absorption spectra. However, it has been suggested that when Fe-S A and B are reduced A_1 will not reduce Fe-S_X at room temperature (Brettel, 1989). Comparison of ESP decay and Fe-S_X rise time also indicates there to be no interaction between the two centres indicating that A_1 may interact directly with Fe-$S_{A/B}$. The inefficient electron transfer to Fe-S_X on single flash turnover has been interpreted as a reflecting competition between A_1 forward and back reaction but the 5-200 ns Fe-S_X reduction kinetics, as compared to the $P700^+/A_1^-$ back reaction kinetics of 120 µs, makes this unlikely. Such inefficiency of Fe-S_X photoreduction is more easily explained by competition between either the $P700^+/A_0^-$ back reaction and A_0^-/Fe-S_X forward electron transfer or by competition between A_1 and Fe-S_X for the electron from A_0^- in a system of parallel electron transport. This is difficult to reconcile with

the findings of Sétif and Bottin (1989,1990) who demonstrated the blocking of electron transport past A_0 at room temperature by quinone double reduction.

Such divergence in the available data makes a final conclusion as to the role of redox components in photosystem-I difficult to draw. There is evidence of a peripheral role for both Fe-S_X and A_1 but the weight of evidence falls in favour of direct involvement of Fe-S_X. The function of the quinone electron acceptor is less certain; it may be involved directly in a system of linear electron transfer or a parallel electron transport. Alternatively, it may play little role in forward electron transfer from A_0^- to Fe-$S_{A/B}$ but function primarily as a component of cyclic electron transport.

The path of electron flow through iron-sulphur centres A and B is also uncertain, although the presence of Fe-$S_{A/B}$ is essential for forward electron transfer to $NADP^+$ (Hanley *et al.*, 1992_a). Low temperature illumination of higher plant photosystem-I indicates that Fe-S_A is the terminal electron acceptor but centres A an B have similar redox potentials and show strong magnetic interaction indicating that they are close together. This would indicate that any definite path of electron transport through these centres is probably a result of the location of each component with respect to Fe-S_X.

1.6 The Polypeptide Composition of Photosystem-I

The photosystem-I multi-protein complex can be isolated from the

thylakoid by treatment with detergents such as Triton X-100 and then selectively depleted of its peripheral polypeptides by ion exchange chromatography and chaotrope extraction. The nature of the various polypeptides has been intensively studied using protein biochemical and molecular biology techniques. The structure and function of some is well understood but the functionality and location of others is less well defined.

Photosystem-I depleted of its light-harvesting complex (LHC-I) is believed to be composed of eleven subunits. This unit contains: the reaction centre P700, electron acceptors A_0, A_1, Fe-S_X and Fe-$S_{A\backslash B}$ and around 120 core antenna chlorophylls per P700. Further enrichment is achieved by additional detergent washes or diethyl ether extraction yielding a P700:chl ratio of 25-30 and 8-12 respectively, whilst preserving a normal complement of redox components. Chaotrope treatment followed by ultra filtration removes low molecular weight peripheral polypeptides and results in a photosystem-I core complex consisting primarily of two polypeptides with an apparent molecular weight of approximate 68 kDa housing redox centres P700, A_0, A_1, and Fe-S_X but devoid of terminal iron-sulphur centres A and B.

Figure 1.5 shows a proposed model for the arrangement of constituent photosystem-I polypeptides. Each of the polypeptides will be discussed with relation to their structure and role in binding electron transfer components or docking of soluble redox intermediates.

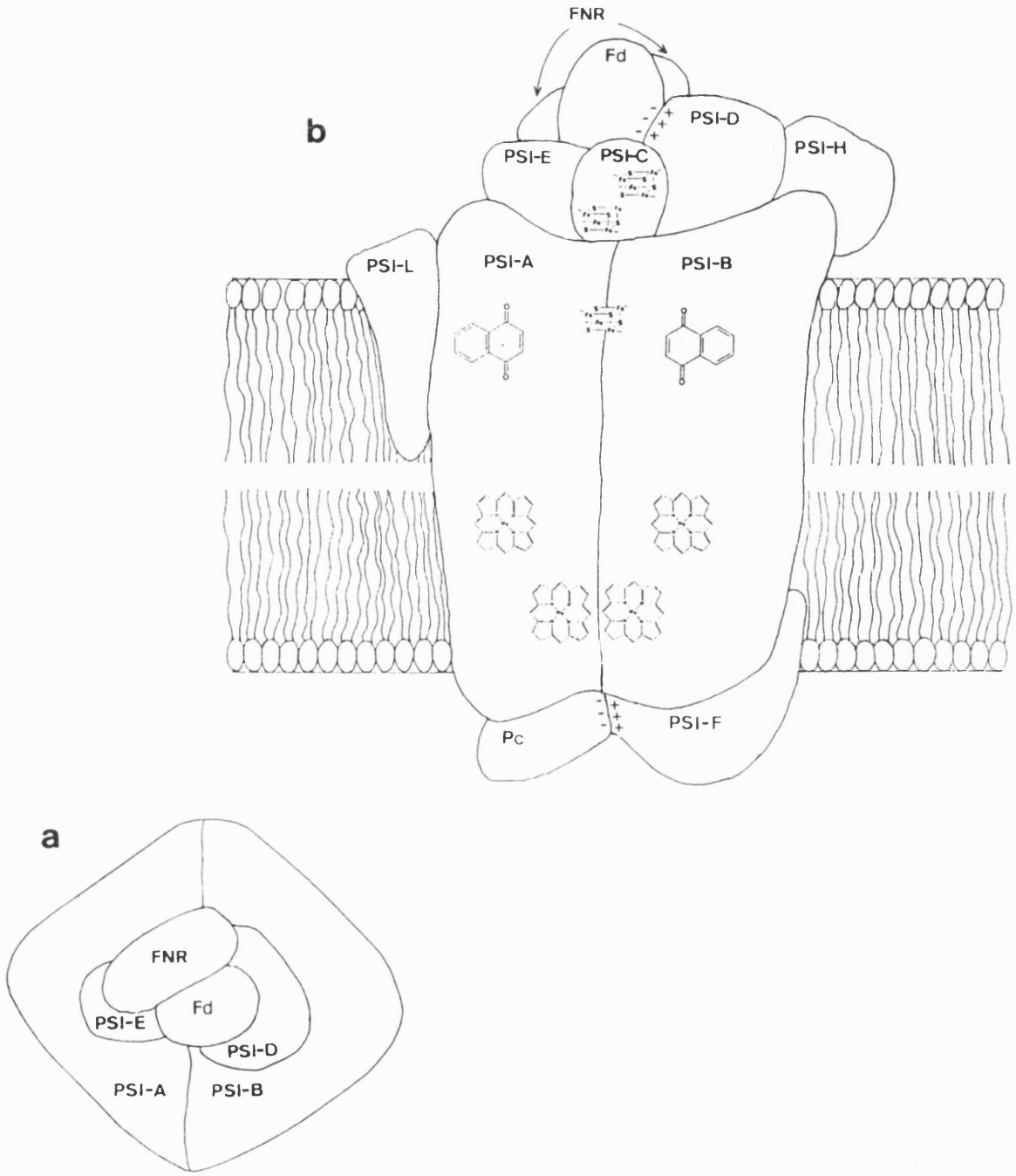

Figure 1.5

Model of Photosystem-I.

a.) Viewed from the stromal side of the complex.

b.) Viewed in the plane of the membrane

PSI-C to PSI-E are stromally oriented extrinsic polypeptides which have been shown to have a close interaction with each other and with the soluble intermediates ferredoxin and FNR. PSI-E has been cited as the FNR binding polypeptide and PSI-D the ferredoxin binding protein, although, both cross-linking and kinetic studies indicate some sharing of both roles. The text gives a possible role for the other peripheral polypeptides and gives the function of the redox components.

Component	Numeric Title	Gene * Title	Mass kDa	Cofactors	Function/ properties
PSI-A	Ia	*psa*A (C)	82-83	chla,P700,A_0,A_1, (A_0',A_1') and Fe-S_X binding	Light harvesting, Initial charge separation and e^- Tfr. from P700 to Fe-S_X.
PSI-B	Ib	*psa*B (C)	82-83		
PSI-C	VII	*psa*C (C)	9	2X[4Fe-4S]	Terminal e^- acceptors
PSI-D	II	*psa*D (N)	15-18	None	Fd./FNR docking PSI-C stabilisation
PSI-E	IV	*psa*E (N)	8-11	None	Fd./FNR docking
PSI-F	III	*psa*F (N)	17-18	None	Pc. docking
PSI-G	V	*psa*G (N)	10-11	None	Membrane Intrinsic?
PSI-H	VI	*psa*H (N)	10-11	None	LHC-I docking ?
PSI-I	X	*psa*I (C)	3-4	None	Trans-membrane α Helix. Quinone binding ?.
PSI-J	IX	*psa*J (C)	4-5	None	Trans-membrane α Helix
PSI-K	VIII	*psa*K (N)	8	None	Trans-membrane α Helix
PSI-L	V'	*psa*L (N)	18?	None	Trans-membrane α Helix
PSI-M		*psa*M (C)	3-4	None	Membrane Intrinsic
PSI-N		*psa*N (C)?	5?	None	Membrane Intrinsic
PSI-O		*psa*O (N)	9?	None	Membrane Intrinsic

Table 1.1

Nomenclature, structure and possible function of photosystem-I subunits

* C and N denote chloroplast and nuclear encoded respectively.

The nomenclature of photosystem-I subunits is often confusing, however, for the purpose of this work each subunit is labelled in a manner corresponding to its encoding gene.

Table 1.1 gives a comprehensive polypeptide description and gene location; table 1.1 also gives a comparison of terminology previously used to label each polypeptide subunit.

1.6.1 PSI-A and PSI-B

Fish *et al.* (1985) demonstrated that the chloroplast genome contains two light inducible genes, denoted *psa*A and *psa*B, which encoded for two high molecular weight polypeptides of 82 kDa, (PSI-A and PSI-B). These proteins have been subsequently identified as the two core complex proteins, stripped of peripheral polypeptides by chaotrope washes, which house redox components P700, A_0, A_1, and Fe-S_X. Both polypeptides are very hydrophobic and each has an estimated 12-14 transmembrane helices (Fish *et al.*, 1985; Kirsch *et al.*, 1986), although preliminary analysis of photosystem-I crystals to 6 Å resolution indicates there to be 9 per polypeptide (Krouss *et al.*, 1993). The apparent difference in molecular weight between that obtained by gene sequence studies and SDS-PAGE is explained by greater mobility of the hydrophobic proteins in SDS gel electrophoresis.

PSI-A and PSI-B contain three and two cysteine residues respectively, which are highly conserved between species and have been implicated as likely candidates for Fe-S_X ligands. The identification of Fe-

S_X as a 4Fe-4S iron sulphur centre, requiring a total of four cysteine ligands, indicates that it must be an inter polypeptide redox centre located between PSI-A and PSI-B. Correlation of EPR data and measurement of zero valence sulphur, created by the oxidative destruction of iron sulphur centres, in photosystem-I samples stripped of all low molecular weight polypeptides confirms this view (Evans *et al.*, 1975; Golbeck *et al.*, 1987; Warren *et al.*, 1990). Oxidative destruction of iron-sulphur centre X also demonstrates that it is not necessary for the structure of the basic photosystem-I core complex, complexes in which Fe-S_X has been destroyed still allow electron transfer to A_0 and A_1 (Warren *et al.*, 1990; Hanley *et al.*, 1992_b). However the presence of Fe-S_X is essential for rebinding the Fe-$S_{A/B}$ holoprotein to the core complex indicating that it may play a role in PSI-A and B acceptor side photosystem-I structure. Characterisation of a photosystem-I core complex stripped of its peripheral polypeptides provided the first direct evidence of Fe-S_X binding to PSI-A and PSI-B, a number of cysteines have been proposed as the likely binding sites (Golbeck and Cornelius, 1986; Golbeck and Bryant, 1991). Site directed mutagenesis has implicated cysteines 560 and 565 of PSI-B as two of the ligands binding Fe-S_X. Golbeck (1992) also pointed out the possible importance of the cysteine/proline motif found in most 4Fe-4S ferredoxins but mutation of proline 559 to either an alanine or a leucine made no difference to the resulting reaction centre (Webber *et al.*, 1992).

Removal of the photosystem-I low molecular weight polypeptides does not directly alter the P700:chl ratio. This has prompted workers to

suggest that most of the 75-100 antenna chlorophylls are associated directly to the two major core complex polypeptides. The large number of conserved histidines, asparagines and glutamines have been cited as likely ligands to the chlorophyll a molecules.

1.6.2 PSI-C

Lagoutte *et al.* (1984) first proposed a 9 kDa polypeptide as the probable holoprotein for binding Fe-S A and B based on the high cysteine content. Further evidence came from the *in vivo* incorporation of ^{35}S and the analysis of zero valence sulphur bound onto photosystem-I components which shows 65-70% associated with a polypeptide of approximately 9 kDa (Høj *et al.*, 1987; Sakurai and San Pietro, 1985). Wynn and Malkin (1988_a) isolated the 9 kDa protein from spinach and showed that it cross reacted with antibodies raised against the *psa*C gene product and gave a low temperature EPR spectra typical of a 2 X [4Fe-4S] ferredoxin, although broader than the observed photoreduced Fe-$S_{A\backslash B}$ signal. The amino acid sequence, deduced from the nucleotide sequence of *psa*C, also showed characteristics typical of known bacterial 2 X [4Fe-4S] ferredoxin (Oh-oka *et al.*, $1987,1988_{ab}$). Sequence studies predict a mature polypeptide with a molecular weight of 8.9 kDa containing nine cysteine residues eight of which are believed to be involved in iron sulphur centre binding. Site directed mutagenesis studies show that cysteines 14 and 51 are involved in ligation of Fe-S_B and Fe-S_A respectively. This work, and comparison of PSI-C with bacterial 2 X [4Fe-4S] ferredoxins, has led to the proposal that

cysteines 11, 14, 17 and 58 ligate Fe-S_B whilst cysteines 21, 48, 51 and 54 ligate Fe-S_A (Zhao *et al.*, 1992).

Absolute confirmation of the role of PSI-C as the bound terminal electron acceptor came from a series of experiments carried out by Golbeck and his co-workers in which charge separation between P700 and Fe-$S_{A\backslash B}$ observed by low temperature EPR was restored on incubation of the 9 kDa PSI-C holoprotein to the photosystem-I core complex. The reconstitution of PSI-C to the core complex also involved the rebinding of PSI-D and PSI-E in stoichiometric quantities and resulted narrowing of the reduced Fe-$S_{A\backslash B}$ EPR signal from the values obtained in the isolated apoprotein (Wynn and Malkin, 1988_a) to those expected in native PS-I samples (Golbeck *et al.*, 1988). Reconstitution of the Fe-$S_{A/B}$ holoprotein to the core complex also restored the 30 ms $P700^+$ back reaction kinetics observed in the wild type.

1.6.3 PSI-D

The 17 to 21 kDa polypeptide reported in various species corresponds to the gene product of *psa*D. Hydropathy studies indicate it to be a hydrophil.ic protein lacking in transmembrane helices and therefore likely to be a thylakoid extrinsic polypeptide. Consistent with this is the co-extraction of PSI-D with PSI-C and PSI-E by *n*-butanol treatment and its accessibility to protease (Oh-oka *et al.*, 1989; Zilber and Malkin, 1992). Reconstitution of stromal polypeptides onto a core complex stripped of its low molecular weight proteins indicates a structural role for

PSI-D (Parrett *et al.*, 1990; Li *et al.*, 1991_a). In the absence of PSI-D the reconstitution of PSI-C is reversible and has a photoinduced EPR signal indicative of an altered orientation of the iron sulphur centres. The addition of PSI-D to the reconstitution system results in the stabilisation of PSI-C rebinding and a normalisation of the photoinduced EPR signals (Li *et al.*, 1991_b).

PSI-D carries a positive charge which lead several workers to propose an additional role in the stabilization of redox interactions between ferredoxin and the 9 kDa Fe-$S_{A\backslash B}$ holoprotein. Zanetti and Merati (1987) confirmed this, demonstrating that the PSI-D/Ferredoxin interaction could be cross linked by EDC which stabilizes electrostatic interactions. Subsequent cross linking and antibody labelling studies have also indicated a close interaction between PSI-D, PSI-C, PSI-E, ferredoxin, and FNR (Wynn *et al.*, 1989; Andersen *et al.*, $1990,1992_{ab}$). This lead to the proposal that PSI-D and E play a role in mediation of electron flow from Fe-$S_{A\backslash B}$ to $NADP^+$, although the exact nature and location of ferredoxin and FNR binding has yet to be discovered.

1.6.4 PSI-E

The *psa*E gene of several species have been isolated and sequenced, they indicate a polypeptide which is positively charged and has a molecular weight of 7.7-10.8 kDa depending on species (Bryant, 1992). The apparent molecular weight determined by gel electrophoresis is considerably higher than that determined by DNA sequencing but this is probably attributable

to the strongly basic nature of the protein. The amino acid sequence does not indicate a definite function although the lack of a transit sequence in cyanobacteria and hydrophil ic nature indicate it to be a stromal polypeptide. Initial cross linking studies support this view demonstrating a close involvement with PSI-D and indicate a role in FNR binding and ferredoxin interactions (Oh-Oka *et al.*, 1989; Andersen *et al.*, 1992_b).

Synechococcus mutants deficient in PSI-E show autotrophic growth rates equal to the wild type (Chitnis *et al.*, 1989; Bryant *et al.*, 1990). However, they are unable to grow heterotrophically in the presence of DCMU (Bryant *et al.*, 1990; Bryant, 1992). This would indicate that PSI-E is not involved in forward electron transfer to $NADP^+$ but may have a role in cyclic electron transfer (Bryant, 1992). In contrast treatment of isolated PS-I with antibodies raised against PSI-E prevents electron transport to $NADP^+$ (Andersen *et al.*, 1992_a).

1.6.5 PSI-F

The gene encoding for PSI-F has been isolated and sequenced as has the N-terminal for the mature protein. The gene sequence indicates a protein of about 17.5 kDa rich in charged amino acids with some hydrophobic regions. PSI-F has long been considered to be an extrinsic lumenal polypeptide but its hydrophobic nature and resistance to *n*-butanol or chaotrope extraction indicates that it may be membrane intrinsic although the situation is far from clear.

The function of PSI-F in the photosystem-I reaction centre complex

is also unclear. Bengis and Nelson (1977) demonstrated that its removal with Triton X-100 resulted in a loss of plastocyanin donation to $P700^+$ and thus proposed it to be involved in plastocyanin docking. Chitinis *et al.* (1991) demonstrated that the addition of divalent cations to photosystem-I depleted of PSI-F by mutation resulted in normal electron transfer from plastocyanin to $P700^+$ indicating a role for PSI-F in facilitation of an interaction between plastocyanin and P700. Cross linking experiments supported this view demonstrating an electrostatic interaction between plastocyanin and PSI-F (Wynn and Malkin, 1988_b). A homologous protein has been identified in cyanobacteria which has been shown to cross link with cytochrome c553, thereby fulfilling a comparative role to that observed in higher plants (Wynn *et al.*, 1989). This evidence strongly suggests that PSI-F plays an important part in the reduction of $P700^+$ by plastocyanin but there has been conflicting data. Sheller *et al.* (1989) showed that the rate of $NADP^+$ reduction by PS-I was independent of the relative amount of PSI-F. Other workers have also suggested a role for PSI-F in both light-harvesting (Thornber *et al.*, 1991) and as a subunit within a ferredoxin-plastoquinone oxidoreductase (Bendall and Davies, 1989), although it has been suggested that these results are an artefact of Triton X-100 preparations.

1.6.6 PSI-G,H,I,J, K, and L

The discovery of these low molecular weight subunits is relatively recent. Structure for all of them have been predicted from sequence

analysis but functional proposals are at this time speculative and further work is required to assign a definite function.

PSI-G has a molecular weight of about 11 kDa (Steppuhn *et al.*, 1988) (16.6 kDa by SDS-PAGE, Staffan and Andersson, 1991) and it appears to be absent in cyanobacteria. Although it is difficult to deduce a function from the sequence it is an acidic protein. Hydropathy studies indicate that it is hydrophobic and the inability to extract it with chaotropes (Okkels *et al.*, 1991) and its resistance to proteolysis (Zilber and Malkin, 1992) suggest that it is membrane intrinsic.

PSI-H is estimated to be 11 kDa. The transit sequence suggests that it is stromally oriented (Steppuhn *et al.*, 1989) and hydropathy plots suggest it to be extrinsic (Okkels *et al.*, 1989). These views are confirmed by chaotrope extraction, Triton X-114 partitioning (Staffan and Andersson, 1991), and proteolytic cleavage (Zilber and Malkin, 1992). Anderson *et al.* (1992_a) demonstrated cross linkage to PSI-D although treatment of isolated PS-I with antibodies raised against PSI-H did not prevent electron transport to $NADP^+$ (Andersen *et al.*, 1992_b). The function of PSI-H remains undetermined although the photoperiodicity of the *psa*H mRNA and the lack of this protein in cyanobacteria has prompted suggestion that it is linked in some way to photosystem-I light-harvesting, possibly the docking of LHC-I (Steppuhn *et al.*, 1989).

The genes encoding for PSI-I, J and K have been sequenced and indicate polypeptides of 4, 5, and 8 kDa respectively which are very hydrophobic and predicted to form one alpha transmembrane helix.

Consistent with this view they cannot be extracted from the PS-I complex by *n*-butanol but are released on treatment with chloroform/methanol, although protease treatment indicates the presence of a stromally exposed loop in PSI-K (Zilber and Malkin, 1992). Workers have suggested a role for these proteins in cofactor binding, however, at this point there is no biochemical evidence to indicate this.

The sequence of PSI-L shows a protein of 18 kDa which is hydrophobic and is predicted to contain two transmembrane alpha helices. Consistent with this, PSI-L cannot be chaotrope extracted (Okkels *et al.*, 1991). Assessment of its properties have lead workers to postulate a role in cyclic electron transport (Bryant, 1992), but at present no direct evidence has been provided to support this.

1.7 Aims of this Thesis

The aims of this thesis were as follows:

1.) To demonstrate the role of iron-sulphur centres A and B in forward electron transfer to $NADP^+$ involving soluble ferredoxin and ferredoxin NADP oxidoreductase (FNR).

2.) To investigate the role of stromally oriented peripheral polypeptides in ferredoxin and FNR binding and stabilisation of the PSI-C holoprotein.

3.) An examination of the effect of quinone double reduction on the 200K photo-accumulated EPR spectrum attributed to the secondary acceptor phylloquinone A_1.

Investigations into the structure and function of secondary acceptor molecule yielded results which indicated that higher plant photosystem-I displayed C_2 symmetry. These findings were investigated further.

2.0 MATERIALS AND METHODS

2.1 Preparations of Photosystem-I

2.1.1 Isolation of the Thylakoid Membrane

Photosystem-I particles were prepared from market spinach (*Spinacea oleracea*). The spinach leaves were washed and the large leaf stems and ribs removed. The plant material was then ground in a Waring blender for 15 seconds in ice-cold 0.33 M sorbitol, 20mM Mes-NaOH, 0.2mM $MgCl_2$ pH 6.5 (grinding medium) with additional sodium ascorbate (5mM). This mixture was filtered through 8 layers of muslin and the filtrate centrifuged at 3,000 g for 5 minutes to obtain a chloroplast pellet. The pellet was resuspended in a hypotonic solution of 5mM $MgCl_2$ for 60 seconds to osmotically shock the chloroplasts. This was immediately followed by the addition of an equal volume of double concentration grinding medium. A thylakoid pellet was obtained by a further centrifugation at 3,000 g for 20 minutes. This was resuspended in 20mM Mes-NaOH, 25mM NaCl, 5mM $MgCl_2$ pH 6.3 (resuspending medium) and left on ice, in the dark, for a period of 2 hours to promote thylakoid stacking.

2.1.2 Preparation of Triton X-100 Photosystem-I Particles

The method of Berthold, Babcock and Yocum (1981) with modifications by Ford and Evans (1983) was initially used in order to separate the photosystem-I from the photosystem-II.

Triton X-100 (20% (w/v) stock) and resuspending medium were added to the stacked thylakoids so that the final detergent and chlorophyll concentrations were 5% (w/v) and 2 mg/ml respectively. The mixture was inverted twice, left to digest for 25 minutes then centrifuged at 40,000 g for 30 minutes to pellet the bulk of photosystem-II. The resulting supernatant was centrifuged at 145,000 g for 2 hours thereby removing any remaining photosystem-II.

The photosystem-I (TSF-I) supernatant was raised to 20mM Tris-HCl pH 8.0 and 100mM NaCl then dialysed overnight in the dark at 4^0C against 100mM NaCl and 20mM Tris-HCl pH 8.0 in preparation for further purification by column chromatography.

2.1.3 Purification of Photosystem-I by Hydroxyapatite Chromatography

Removal of the light harvesting complex, free pigments and some low molecular weight polypeptides was achieved by application of the TSF-I to a column packed with hydroxyapatite.

The column was pre-equilibrated with 20mM Tris-HCl pH 8 and 100mM NaCl, after application the sample was washed with 20mM Tris-HCl pH 8, 100mM NaCl and 0.5% Triton X-100 until the eluate ran clear. It was then washed with 3 column volumes of 0.1% Triton X-100, 20mM Tris-HCl and 100mM NaCl to remove excess detergent. The photosystem-I, which appeared as a dark green band towards the top of the column, was eluted from the column by slowly washing with 5-15mM KH_2PO_4 pH 6.8,

100mM NaCl and 0.1% Triton X-100.

The eluted sample was raised to 20mM Tris-HCl pH 8.0 and then dialysed for 12 hours in the dark at 4^0C against 20mM Tris-HCl pH 8 and 100mM NaCl to remove the phosphate buffer. Finally it was concentrated in an Amicon ultra filtration cell over a YM100 membrane and stored under liquid nitrogen.

All of the steps during the purification procedure were carried out at 4^0C in the dark.

2.1.4 Preparation of Digitonin Photosystem-I Particles

Thylakoids were prepared by the method in section 2.1.1. Digitonin isolation was carried out largely by the method of Boardman (1971). Digitonin (2% w/v stock) and 50mM Tris-HCl, 5mM $MgCl_2$ and 2mM EDTA (TEM) buffer were added to the chloroplasts to a final concentration of 1.0 mg/ml chlorophyll and 0.5% Digitonin. The mixture was well stirred and left to digest for 30 minutes on ice in the dark. It was then centrifuged at 15,800 g for 30 minutes to pellet photosystem-II and the pellet discarded. The supernatant was further centrifuged at 144,000 g for 90 minutes and the pellet containing the photosystem-I was resuspended in TEM buffer and stored under liquid nitrogen until required.

2.1.5 Preparation of the Photosystem-I Core Complex

The Fe-$S_{A/B}$ protein and other low molecular weight peripheral polypeptides were removed from photosystem-I by treatment with 6.8M

urea. 9M urea in 0.1M Tris-HCl pH 8.0 was added dropwise with rapid stirring to a suspension of photosystem-I particles, initial concentration 1.5 mg chlorophyll/ml. The suspension was diluted with oxygen-free Tris-HCl pH 8.0 to 250 µg chlorophyll/ml, 0.1% 2-mercaptoethanol and 6.8M urea and stirred under argon at room temperature in the dark. The removal of the Fe-$S_{A/B}$ protein was monitored by measuring the re-reduction kinetics of $P700^+$ by back reaction from electron acceptors following laser flash excitation. Kinetic measurements were made using the kinetic spectrophotometer outlined in section 2.5. When the $t_{½}$ for $P700^+$ re-reduction had changed from 20 ms and stabilised at 1 ms (25-30 minutes incubation) the treatment was stopped by diluting the reaction mixture 10X with oxygen-free 20mM Tris-HCl pH 8.0. and 5mM dithiothreitol. Urea was removed by washing the preparation over an ultrafiltration membrane (Amicon YM100) or by centrifugation for 2 hours at 150,000 g and resuspension of the resulting pellet in 20mM Tris-HCl pH 8.3 and 0.1% 2-mercaptoethanol. The preparation was finally concentrated to approximately 1 mg chlorophyll /ml and stored in liquid nitrogen until required.

2.2 Determination of Chlorophyll Concentration

The concentrations of chlorophyll a and b in a sample were calculated by the method described by Arnon (1949) using the extinction coefficients given by MacKinney (1941) for chlorophyll extracted in 80% (v/v) acetone (pathlength 1 cm). The contributions to absorbance by each

chlorophyll at 663 and 645 nm is given by:

$$A_{663} = 82.04 \text{ Chl } \underline{a} + 9.27 \text{ Chl } \underline{b}$$

$$A_{645} = 16.75 \text{ Chl } \underline{a} + 45.6 \text{ Chl } \underline{b}$$

where:

A = Absorbance

Chl = chlorophyll concentration in mg/ml

When the above simultaneous equations are solved:

$$\text{Chl } \underline{a} = 0.0127 \, A_{663} - 0.00259 \, A_{645}$$

$$\text{Chl } \underline{b} = 0.0229 \, A_{645} - 0.00467 \, A_{663}$$

A value for the total chlorophyll, both a and b, can be calculated using the absorbance at 652 nm:

$$\text{Chl} = 0.029 \, A_{652}$$

In practice the chlorophyll from either 25 or 50 µl of sample was extracted in a total volume of 10 ml 80% acetone (v/v). It was well mixed then filtered through Whatman No.1. The absorbance was measured in a 1 cm path length quartz cuvette against an 80% acetone blank at 663, 652 and 645 nm. It was necessary to use a dilution correction factor of either 400 or 200 to give a final chlorophyll concentration. Absorbance

measurements were carried out using a Phillips PU 8740 UV/VIS scanning spectrophotometer.

The amount of P700 was determined from an ascorbate reduced minus ferricyanide oxidised difference spectrum using an extinction coefficient of $64mM^{-1}.cm^{-1}$ at 697 nm (Hiyama and Ke, 1972) and assuming a molecular weight of 893.5 Da for chlorophyll a. Difference spectra measurements were carried out using an Aminco DW 2000 dual beam scanning spectrophotometer.

2.3 Preparation of the Fe-$S_{A/B}$ Holoprotein

The Fe-$S_{A/B}$ holoprotein was extracted from purified Triton X-100 photosystem-I particles by *n*-butanol treatment. Triton isolated photosystem-I at a concentration of 2 mg/ml chlorophyll in 50mM Tris-HCl, 1mM EDTA and 30mM NaCl was flushed with ultra pure argon for 3 hours followed by the addition of dithiothreitol to 5mM. Ice-cold *n*-butanol was then carefully layered over the photosystem-I to an equal volume and both phases thoroughly degassed. The mixture was vortexed until it appeared to be homogeneous and then immediately centrifuged for 10 minutes at 30,000 g. The Fe-$S_{A/B}$ protein, contained in the lower straw coloured aqueous phase, was concentrated and freed of *n*-butanol by washing with oxygen-free Tris-HCl pH 8.1 and 0.1% 2-mercaptoethanol over an Amicon YM5 ultrafiltration membrane for use in redox titrations.

Further purification of the extracted polypeptides was achieved by one of three methods:

1) Application to a DEAE fractogel column pre-equilibrated with oxygen-free 20mM NaCl in 20mM Tris-HCl buffer pH 8.0, washing with oxygen-free 20mM NaCl in 20mM Tris-HCl buffer pH 8.0 and elution with 0.3 M NaCl in 20mM Tris-HCl buffer pH 8.0.

2) Passage of the butanol extract through a 2.6 cm X 40 cm Sephacryl S-200 HR column in oxygen-free 20mM Tris-HCl pH 8.0, 100mM NaCl and 5mM dithiothreitol. The sample was eluted over a 1-2 hour time period.

3) Application of the butanol extract to a 2.2 cm X 90 cm Sephadex G 50 gel filtration column. The sample was eluted over a 24-48 hour time period with oxygen-free 20mM Tris-HCl pH 8.0, 100mM NaCl and 5mM dithiothreitol.

All of the columns were run at 4^0C and column materials were thoroughly degassed prior to packing. The packed columns were then equilibrated with the appropriate running buffer which had been thoroughly degassed. Each of the buffers contained 5mM dithiothreitol to maintain the structural integrity of the iron-sulphur centres.

The eluent was monitored with a U.V. single path monitor (Pharmacia) and collected in 0.2 ml fractions. Each set of 0.2 ml fractions corresponding to a 280 nm elution peak was pooled and stored under liquid nitrogen. Each peak was assayed by SDS-PAGE electrophoresis, low

temperature EPR, Western blot and oxidised-minus-reduced optical difference spectra. The protein concentration was estimated by Bradford assay (Bradford, 1976).

2.4 Photosystem-I Reconstitution Assay

The ability of each iron sulphur protein preparation to replace the 1 ms optical kinetics of the core particle with the 20 ms kinetics observed in native photosystem-I was measured. A three fold excess by volume of the preparation was then used in the experiments to reconstitute $NADP^+$ photoreduction and for preparation of EPR samples.

Reconstitution was carried out with a core photosystem-I concentration of 12µg chlorophyll/ml in 25mM Tricine-KOH pH 7.8, 0.1% 2-mercaptoethanol and 0.07% Triton X-100. This was incubated with excess Fe-$S_{A/B}$ protein for 10 min in the dark at room temperature under argon. Increasing the incubation time did not improve the level of reconstitution. The reconstituted preparation was then washed over an ultra filtration membrane (Amicon YM100) to remove unbound protein and concentrated to 0.5 mg chlorophyll/ml for EPR measurements.

Reconstitution for $NADP^+$ reduction was carried out *in situ* as above. The recovery of $NADP^+$ reduction was followed by measuring the change in OD 340 following 30 second periods of illumination of the reaction mixture in a 1 cm path length cuvette by saturating white light. Before illumination 6.7mM Sodium Ascorbate, 68 µM dichlorophenol indophenol, 1.5 µM plastocyanin, 5 µM ferredoxin, 0.5mM NADP+ and ferredoxin-

NADP+ reductase were added to the reconstituted sample.

The rate of $NADP^+$ reduction is given by:

$$\text{Rate in } \mu\text{mol.mg chl}^{-1}\text{hr}^{-1} = \frac{A340 \times 3600 \times 1000}{5.85 \times [\text{chl}] \times \text{time(s)}}$$

Ferredoxin, FNR and plastocyanin were prepared by methods based on those of Buchanan and Arnon, (1973), Shin, (1973) and Katoh, (1973) respectively with some modifications.

Washed and de-veined spinach was ground in ice cold 400mM sucrose, 50mM NaCl, 10mM Tris-HCl pH 8.0 and 2% (w/v) polyvinylpyrrolidone. It was then filtered through 8 layers muslin and the filtrate centrifuged at 5000 g for 5 minutes. The pellet was resuspended to about 4 mg chl/ml in 0.5 M Tris-HCl pH 8.0, and cold acetone added to 35% (v/v). The mixture was sonicated on ice for about 3 X 30 second bursts and then centrifuged at 10000g for 5 minutes. Cold acetone was added to the supernatant to a final concentration of 80% (v/v) and the mixture allowed to stand for about 1 hr on ice/salt. Excess acetone was decanted off and the precipitate centrifuged for 5 minutes at 10000g, resuspended in 2-300 ml 50mM K_2HPO_4 pH 7.5 and dialysed overnight against 20mM K_2HPO_4 pH 7.5. The dialysed material was centrifuged for 10 minutes at 10000g to remove precipitates, loaded onto a 3 X 15 cm DEAE cellulose column (pre-equilibrated with 20mM K_2HPO_4 pH 7.5) and washed with 3 column volumes of the same buffer.

The fraction containing plastocyanin and FNR eluted with 20mM K_2HPO_4 pH 7.5 and 200mM NaCl, the ferredoxin containing fraction eluted with 20mM K_2HPO_4 pH 7.5 and 800mM NaCl. Both fractions were dialysed overnight against 20mM K_2HPO_4 pH 7.5. The ferredoxin was further purified on a Sephadex G-50 column.

The plastocyanin/FNR fraction was applied to a Bio-Rad affi-gel blue column (3 X 10 cm) which had been prewashed with 1M NaCl and equilibrated with 3 column volumes of 50mM Tris-HCl pH 8.0. The plastocyanin eluted in the loading buffer; it was collected and loaded onto a DEAE-Sephadex A-50 column (1.5 X 10 cm) equilibrated with 20mM K_2HPO_4 pH 7.0), washed with equilibration buffer, then eluted with 1M K_2HPO_4 pH 7.0. The reductase eluted from the affi-gel blue column with 400mM NaCl in 50mM Tris-HCl pH 8.0. Both plastocyanin and reductase were finally purified by passage down a 3 X 60 cm Sephadex G-50 column equilibrated with 50mM K_2HPO_4 pH 7.0.

2.5 Kinetic Optical Spectroscopy

The lay-out of apparatus used to measure time-resolved absorbance changes at 820 nm is shown in figure 2.1. The single beam spectrophotometer measures the kinetics of absorption changes in P700 induced by a laser flash.

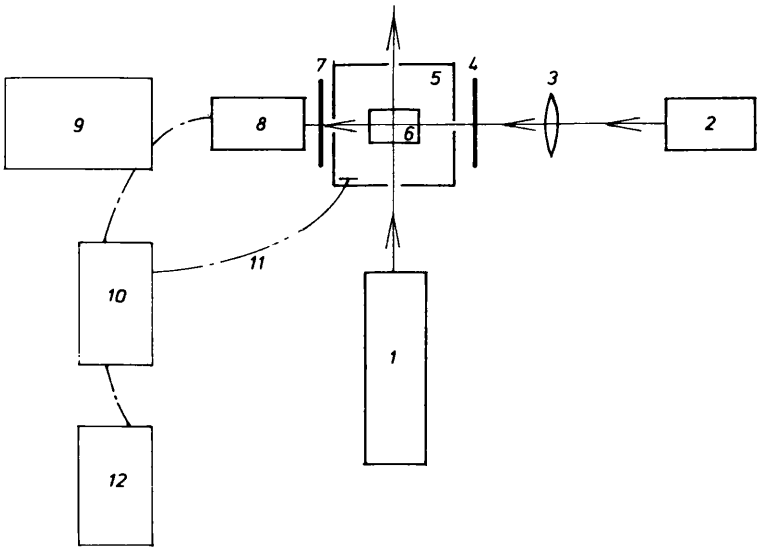

Figure 2.1

Schematic Diagram of the Kinetic Spectrophotometer

The diagram represents the apparatus used to measure absorbance changes at 820 nm due to excitation of P700. Excitation of the sample is provided by an 800 ps 337 nm pulse from a nitrogen laser (1). The measuring beam is provided by an infrared LED emitting maximally at 820 nm (2) which is focused (3), passed through an 820 nm interference filter (4), into the 'dark box' (5) and through the sample (6). A large-area silicon photodiode, protected from the laser flash by an 820 nm cut-off filter (7), detected the 820 nm measuring beam (8), which is amplified (9). The transients were recorded on the digital storage scope (10) which is simultaneously triggered by the laser flash by means of a photodiode (11). Data manipulation was carried out using wavesaver software on a Dell PC (12).

Samples were excited at 0.5 Hz at 337 nm with an 800 ps flash from a nitrogen laser (Photochemical Research Associates Inc. LN1000). The measuring beam was provided by an infrared LED emitting maximally at 820 nm which was filtered by an 820 nm interference filter to ensure an incident beam of 820 nm. The measuring beam was detected by a large-area silicon photodiode type PIN 102.1 kinetic spec-D (United Detector Technology, Optilas, U.K.) coupled to an amplifier (EG/G Princeton Applied Research, Model 113). An 820 nm cut-off filter was used to protect the detector diode from the U.V. laser flash. Spectra were averaged and stored by a 100 MHz digital storage scope (Tektronix 2232, Tektronix, Inc, Beaverton. U.S.A.) and manipulated using Tektronix wavesaver software. Each kinetic trace was taken as an average of 30 excitations at a repetition rate of 0.5 Hz. All kinetics were measured at 10-20 μg/ml chlorophyll, 25mM Tricine-KOH pH 7.8, 6.7mM Sodium Ascorbate, 68 μM dichlorophenol indophenol, 0.07% Triton X-100. Final manipulation was carried out on ASYST software written by M.C.W. Evans.

2.6 Redox Potentiometry

Redox potentiometry was carried out according to the method presented by Dutton (1971). The sample was maintained at 10^0C using a Churchill thermostatic system, stirred, and kept under anaerobic conditions by passing a continuous stream of O_2-free nitrogen over it. To ensure the absence of oxygen the nitrogen was first passed through a solution of 1% (w/v) sodium dithionite, 0.005% (w/v) methyl viologen,

100mM Tris-HCl pH 9 in a Drechsel bottle then rough a second flask containing 100mM Tris-HCl pH 9.

The redox potential was measured with a platinum electrode used in conjunction with a calomel reference electrode (P101 and K401 respectively, obtained from Radiometer, Copenhagen). The electrodes were calibrated using a saturated quinhydrone solution in 100mM KH_2P0_4 pH 7 (E_{m7} +286 mV, pH dependent) then an equimolar solution (5mM) of potassium ferricyanide and potassium ferrocyanide in 100mM Tris-HCl pH 8 (E_m +420 mV, pH independent) was used.

The redox potential of isolated iron sulphur centres A and B was adjusted by microlitre additions of a freshly prepared solution of 0.5% dithionite in the presence of 25% glycerol. Reduction by dithionite was mediated by 30 μM methyl viologen and triquat. After any adjustment the sample was left to equilibrate for at least 10 minutes before an EPR sample was taken. Each sample was frozen and stored in liquid nitrogen until required.

2.7 Polyacrylamide Gel Electrophoresis

The analysis of the polypeptide composition of the different preparations was performed using the Pharmacia 8-25% SDS-PAGE PhastSystem™ and Pharmacia native PhastGel. Gels were scanned using an LKB Ultroscan X densitometer and the data manipulated using LKB 2400 GelScan software.

Western blot analysis was carried out using a mini-gel system

(Hoefer SE 250), where optimum band resolution was found using 15% acrylamide resolving gels.

	RESOLVING	STACKING
30% acrylamide/.08% bis-acryl	10.00 ml	1.65 ml
1.5 M Tris-Hcl (pH 8.9)	5.00 ml	--------
0.5 M Tris-HCl (pH 6.7)	--------	2.50 ml
Glycerol	0.75 ml	--------
20% (w/v) SDS	0.20 ml	0.1 ml
H_2O	5.68 ml	5.63 ml
TEMED	20 µl	20 µl
10% (w/v) ammonium persulphate	200 µl	100 µl
TOTAL	20 ml	10 ml

Table 2.1

Composition of the 15% SDS Gel

The samples were solubilised by mixing 1:1 with 4% (w/v) SDS, 5% (v/v) 2-mercaptoethanol, 0.1% (w/v) bromophenol blue, 6 M urea, 7.5% (v/v) glycerol, 100mM Tris-HCl pH 6.8 and boiling for 2 minutes. The gel composition for the mini-gel is shown in Table 2.1. The gels were run at a constant current of 30 mA for 40-60 minutes. TEMED and 40% acrylamide/1.07% bis-acrylamide (w/v) solution obtained from Sigma, ammonium persulphate was prepared fresh each time. The samples were run alongside Sigma Dalton Mark VII-L and stained with Coomassie blue.

2.8 Western Blot Analysis

Antibody labelling was carried out largely by the method of Towbin

et al. (1979). 15% slab gels were run as described in section 2.7. The gel was then equilibrated in 25mM Tris, 192mM glycine and 20% methanol (transfer buffer) for 20-30 minutes. After equilibration it was placed onto a piece of 3 mm filter paper and overlayed with a sheet of nitrocellulose (NC), a further sheet of filter paper was then placed over the NC. All sheets were thoroughly soaked with transfer buffer. The NC/gel sandwich was placed in the transfer apparatus and transferred at 100 V for 3-4 hours. After transfer the nitrocellulose was washed in 50mM Tris-HCl and 0.9% NaCl pH 7.4 (TBS) for 10 minutes, then further washed in 0.05% Nonidet, 0.05% Tween 20, 5% (w/v) Marvel™, 0.9% NaCl and 50mM Tris-HCl pH 7.4 (blocking buffer) for 30-60 minutes. The excess blocking buffer was removed with TBS buffer and the NC incubated in primary antibody overnight. The primary antibody had been diluted 2000X in washing buffer. Following incubation the NC was washed 4 X 15 minutes in 0.05% Nonidet, 0.05% Tween 20, 0.9% NaCl and 50mM Tris-HCl pH 7.4 (washing buffer) then incubated in the secondary antibody for 3 hours. The secondary antibody was a peroxidase conjugate of goat anti-rabbit antibody. After incubation in the secondary antibody the nitrocellulose was washed 2 X 15 minutes in washing buffer and 2 X 15 minutes in TBS. Any antibody binding was indicated by incubation in colour development solution (see below) followed by washing with H_20.

Colour Development Solution

Solution 1) 30 mg 4-chloro-1-napthol and 10ml ice cold

methanol

Solution 2) 24 µl 30% H_2O_2 in 40 ml TBS

Both solutions were mixed together immediately prior to nitrocellulose incubation and the development took between 5 and 30 minutes.

2.9 Electron Paramagnetic Resonance

2.9.1 EPR Theory

Electron paramagnetic resonance (EPR) spectroscopy is a technique used for the detection and characterisation of paramagnetic species, i.e. molecules containing unpaired electrons. Like optical spectroscopy it utilises electromagnetic radiation to induce a change in energy state of a sample; however in the case of EPR there is no change in the electronic state but an alteration of the systems spin state.

The spin of each electron within the system creates a magnetic field termed the magnetic dipole moment. In an electron pair the spins are opposed thus the resultant magnetic moment is zero. However, in a paramagnetic species the magnetic moment of the unpaired electron is "free" to interact with an externally applied magnetic field. The application of a magnetic field to a paramagnetic species results in the orientation of the unpaired electrons into either a high or low energy state (M_S = +\-½) dependant on the direction of electron spin (fig 2.2). The high energy state is unfavourable and thus there is an asymmetric distribution of electrons.

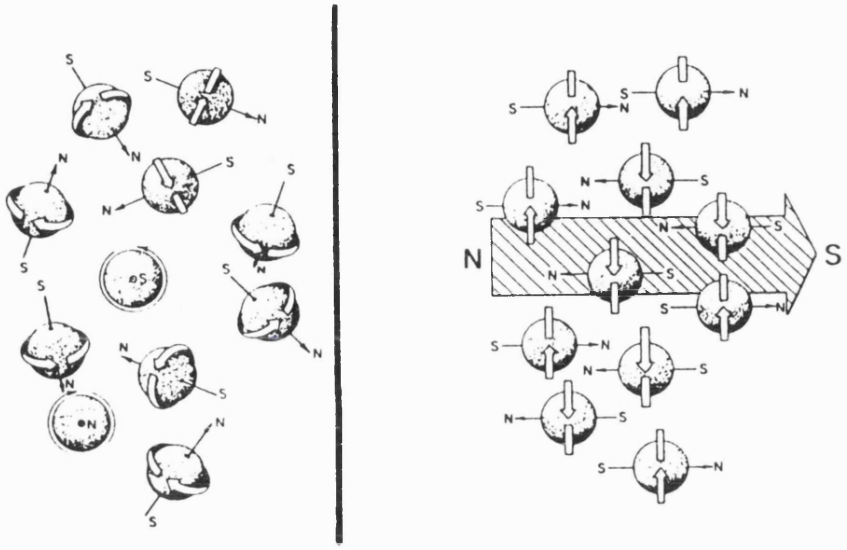

Figure 2.2

The Behaviour of Electrons in an Externally Applied Magnetic Field.

In the absence of a magnetic field the magnetic dipole moment of an electron is random. However, when an external magnetic field is applied to the system the electron magnetic dipole moment can take up one of two possible orientations; either parallel or anti-parallel to the field. The former is a low energy state and as such more favourable, whereas the latter is a higher energy state and therefore has a lower population of electrons. The distribution of electrons in these sub-populations is determined by the Boltzmann distribution. [Diagram from Swartz Bolton and Borg; Biological Applications of EPR, Wiley interscience]

Application of electromagnetic radiation of an appropriate energy induces a transition between the two energy levels according to the relationship:

1) $$E = h.v$$

where:

E = The difference in energy between the two states.

h = Planck's constant (6.626×10^{-34} J s)

v = the frequency of radiation.

The energy difference between the two states is linearly related to the magnitude of the applied magnetic field H:

2.) $$h.v = g.B.H$$

where:

B = The Bohr magneton (9.27408×10^{-24} J/T).

g = an EPR characteristic of the measured sample.

Thus the frequency required to observe resonance is dependent on the magnetic field and can be obtained by either varying the frequency at a fixed magnetic field or vice versa (fig 2.3).

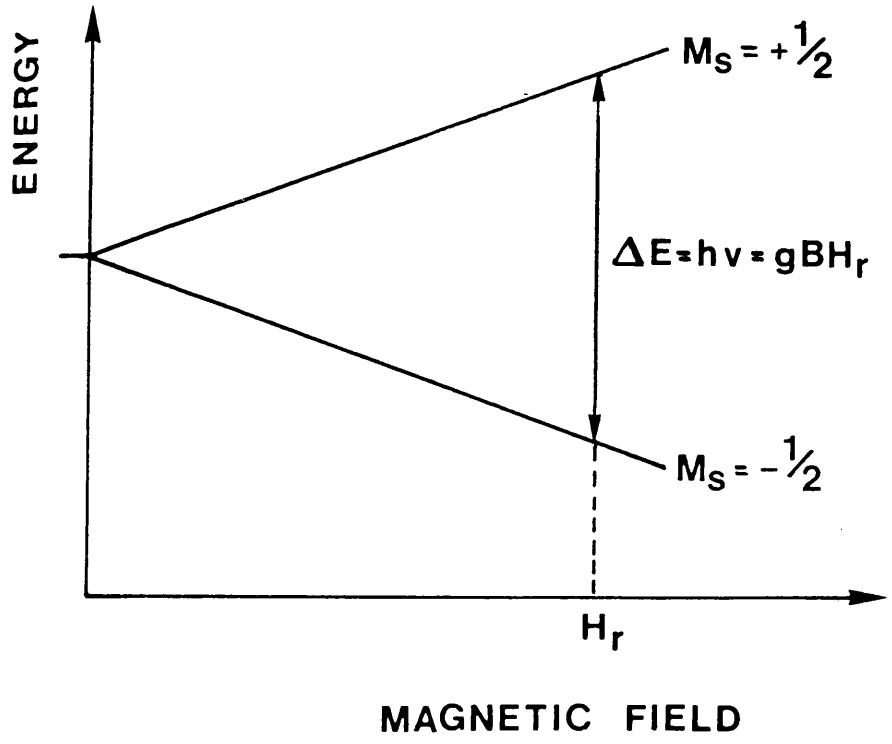

Figure 2.3

Electron Energy Levels as a Function of the Magnetic Field Strength.

The energy difference between the possible electron orientations increases with increasing magnetic field strength. Resonance can either be achieved by varying the magnetic field at fixed microwave frequency or vice versa.

E = Energy difference
h = Plank's constant
v = frequency of radiation
g = g-value
B = Bohr magneton
H_r= Magnetic field resonance
M_s= Electron spin quantum number
[Diagram from Swartz Bolton and Borg; Biological Applications of EPR, Wiley interscience]

In practice the frequency is kept at a constant value and the magnetic field is scanned until resonance occurs, i.e. the magnitude of the energy difference between the states is adjusted through a range which will cause a resonance with the constant microwave frequency.

To gain a net absorption of microwaves there must be a preference for electrons to occupy the lower energy state. The ratio of electrons in the higher and lower energy state is given by the Boltzmann distribution:

$$N_{+½} / N_{-½} = 1 - (h.v/k.t)$$

where:

N = the number of electrons in each state.

T = the absolute temperature.

k = Boltzmann's constant (1.381×10^{-23} J/K)

Thus the number of electrons in the low energy state is inversely proportional to the temperature resulting in an increased microwave absorption and greater EPR signal intensity at cryogenic temperatures. Despite this the $N_{+½} / N_{-½}$ ratio at 5 K and microwave frequency of 9.05 GHz is only 0.9132 and therefore the net absorption is due only to a small population of unpaired electrons. The small population difference results in a very low sensitivity and leads to a requirement for high sample concentrations. The signal to noise ratio is improved by superimposing an AC sinusoidal magnetic modulation over the DC field scan. The signal is

then obtained from a sinusoidal output with the same frequency as the modulation thereby removing the effects of random noise. A consequence of this is that the EPR spectra are recorded as the first derivative of their absorption.

The EPR signal of a particular component is characterised by: the line width i.e. a measurement in gauss or mT from the maxima to the minima of the spectra, the line shape or spectral structure and the g-value.

The area of the microwave absorption curve, found by integration of the first derivative spectra, is proportional to the number of spins giving rise to the spectra. The g-value of an electron effected solely by the applied magnetic field is 2.00232 ("free electron g-value"), however, in systems where the unpaired electron is affected by local magnetic interactions the g-value is shifted up field or down field of the free electron value. Local magnetic interference comes from parent and neighbouring nuclei and in the case of transition metals from the ligand electrons. The g-value therefore acts as a specific marker for a particular component.

2.9.2 EPR Experimental Details

EPR spectra were obtained at cryogenic temperatures using a Jeol X-band spectrometer with 100 kHz field modulation and an Oxford instruments ESR 9 liquid helium cryostat. Samples were placed in calibrated quartz tubes with a 3 mm internal diameter. Each EPR sample contained approximately 0.3 ml of material at a chlorophyll concentration of at least 0.5 mg/ml. All redox manipulations were carried out under

oxygen-free nitrogen or argon.

Samples with P700 reduced and all other centres oxidised were prepared by the addition of sodium ascorbate to 20mM, dark adapted at room temperature for 20 minutes then frozen in liquid nitrogen in the dark. An irreversible one electron transfer forming $P700^{+}/Fe\text{-}S_A^{-}$ was achieved by illumination of this sample at cryogenic temperatures whereas illumination at room temperature and freezing under illumination results in the reduction of both iron sulphur A and B.

Samples with P700 reduced and $Fe\text{-}S_{A/B}$ reduced were prepared by the addition of Tris-HCl pH 9.0 to 100mM. The sample was then flushed with oxygen-free nitrogen for 20 minutes in the dark before the addition of sodium dithionite to 0.2% w/v. After a 30 min equilibration in the dark the samples were frozen in liquid nitrogen.

Photoreduction of redox centres A_1 and A_0 was achieved by illumination of dithionite reduced samples at 200 K in an unsilvered dewar using a solid CO_2/ethanol mixture with illumination provided by a 650 W light source. EPR spectra illuminated at this temperature were recorded immediately after illumination.

In order to double reduce A_1 photosystem-I samples were reduced with sodium dithionite in 200mM glycine-KOH pH 10.0 then illuminated at 4^0C in an unsilvered dewar for an appropriate time, dark adapted for 30 seconds and then frozen in the dark under liquid nitrogen.

Further information on specific preparations can be found in the relevant results section.

EPR spectra were recorded on a Dell microcomputer using ASYST software written by M.C.W. Evans.

3.0 RESULTS

3.1 Characterisation of Photosystem-I

3.1.1 Digitonin Photosystem-I

Digitonin photosystem-I was isolated by the method described in section 2.1.4 and characterised by room temperature kinetic spectra, low temperature EPR spectroscopy and SDS-PAGE analysis. Oxidised-minus-reduced difference spectra indicated a P700:chlorophyll ratio of 1:150-200 and EPR analysis showed the complex to have a full complement of normally oriented redox components.

Figure 3.1 shows a densitometric scan of the polypeptide content of isolated Digitonin photosystem-I particles resolved by 8-25% SDS-polyacrylamide gel electrophoresis. There were variations in the number and relative intensity of polypeptide bands depending on the preparation, however, there were invariably 11 bands: 2 at 60 kDa, 1 at 35 kDa, four between 22 and 28 kDa, one at 21 kDa, two at approximately 17 kDa and one at 9 kDa. There also appeared to be some lower molecular weight polypeptides below 9 kDa but the gel system and interference by free pigment chlorophyll did not allow the resolution of these into discrete polypeptide bands.

The two high molecular weight polypeptide bands formed a broad heavily stained band with an apparent molecular weight centred at approximately 55 kDa. They were therefore identified as the two major core complex subunits PSI-A and PSI-B.

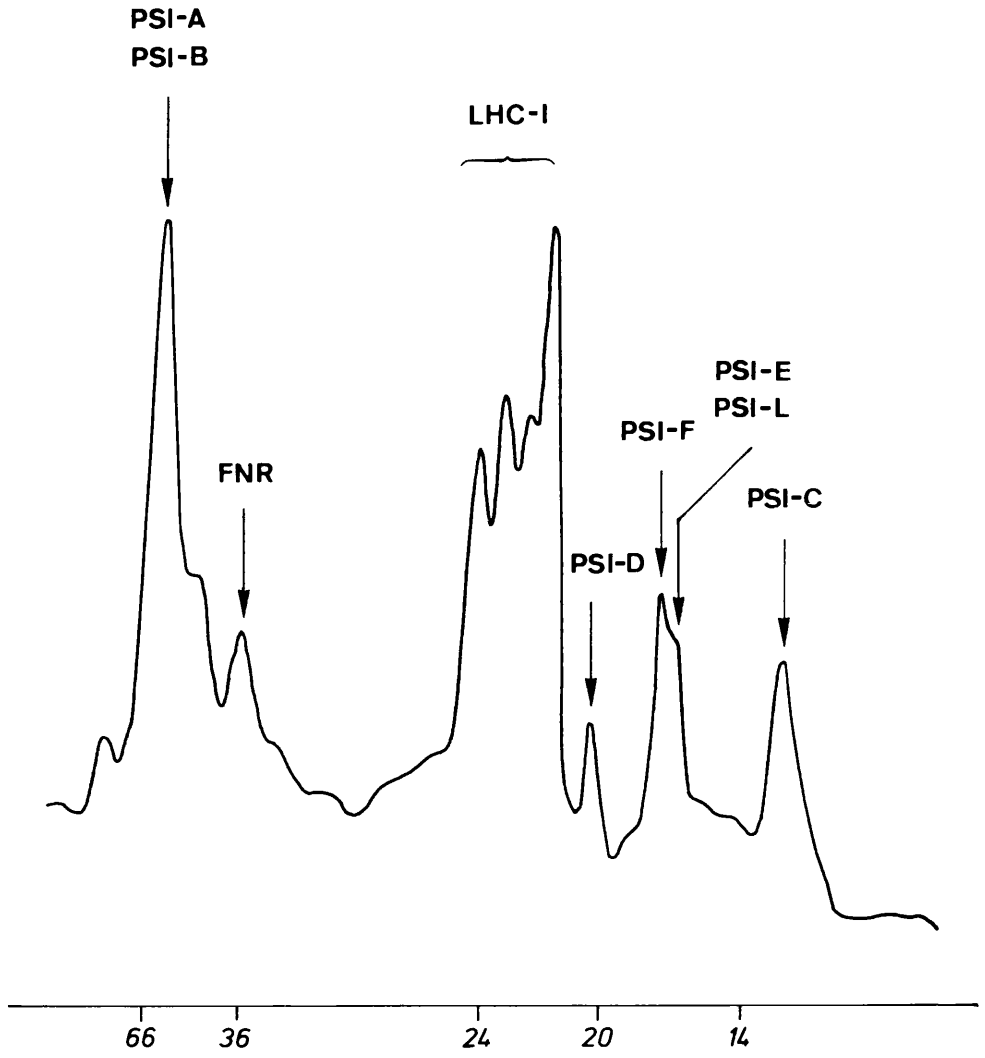

Figure 3.1

Polypeptide Composition of Digitonin Isolated Photosystem-I.

Laser densitometric trace of photosystem-I isolated using Digitonin by the method in materials and methods section 2.1.4. SDS-PAGE polypeptide separation was performed with an 8-25% polyacrylamide gradient using the Pharmacia PhastGel system. Approximately 0.5 µg of chlorophyll was loaded per lane.

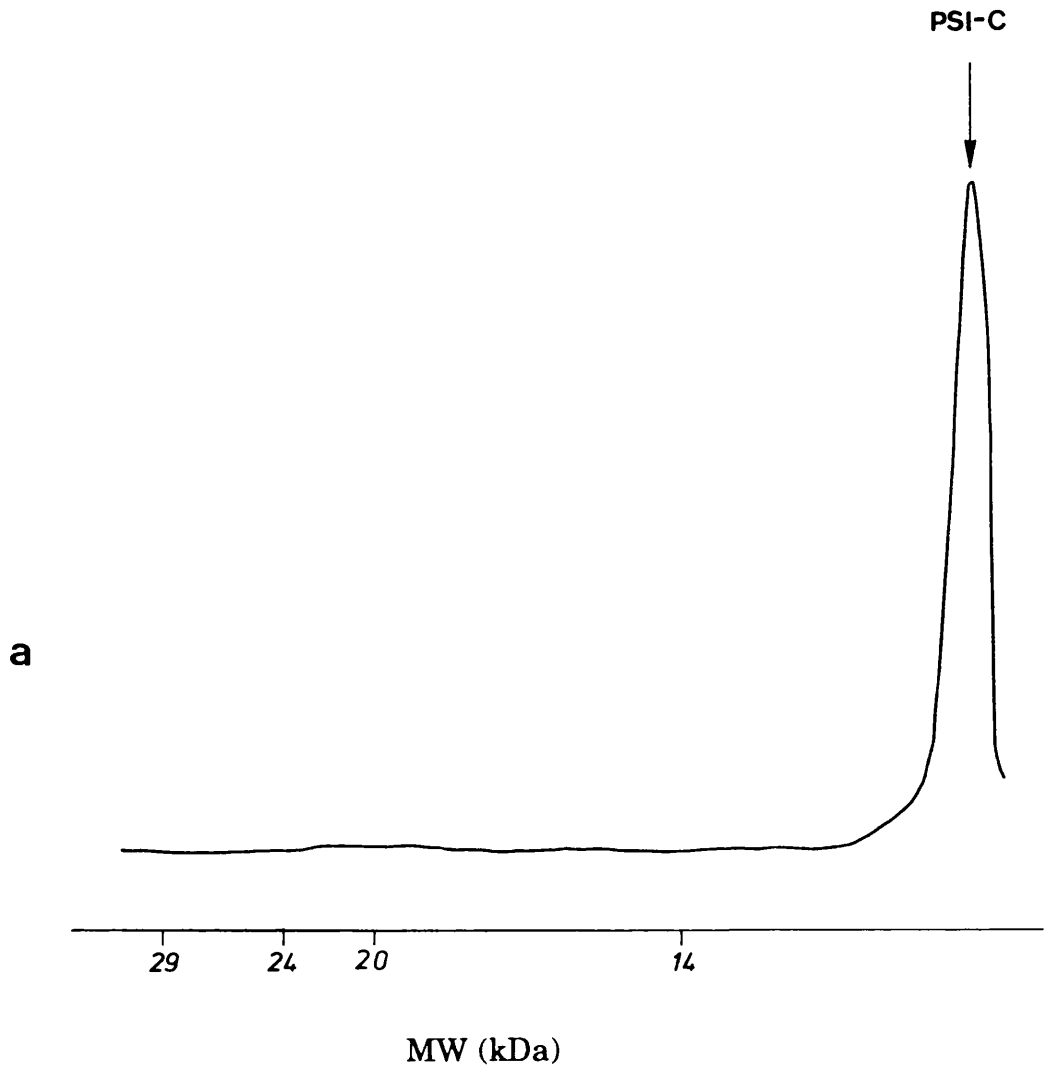

Figure 3.2

a.) Western Blot Analysis of Photosystem-I Polypeptides Labelled With Antibodies Raised Against PSI-C.

The polypeptides were initially resolved using 15% polyacrylamide SDS-PAGE by the method outlined in section 2.7. Approximately 5-10 µg of chlorophyll was loaded per lane. Western blot analysis was carried out according to the method in section 2.8.

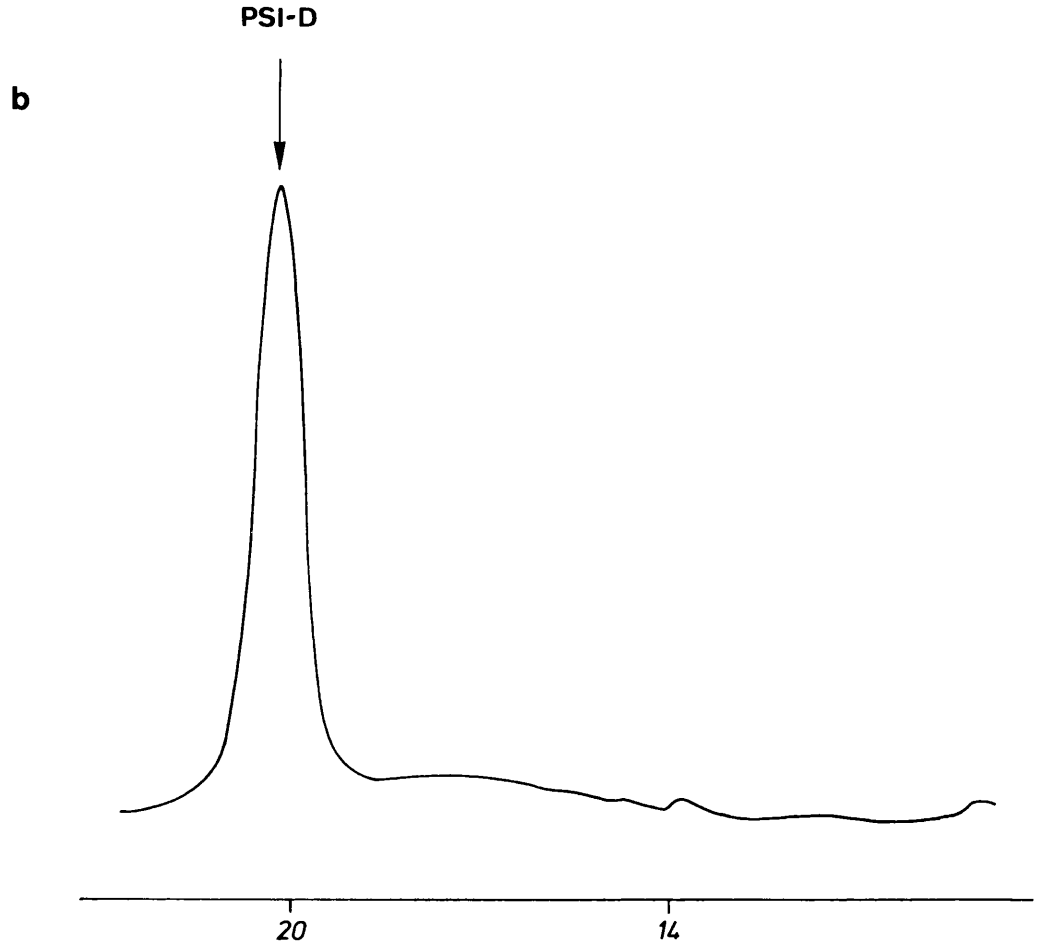

Figure 3.2

b.) Western Blot Analysis of Photosystem-I Polypeptides Labelled With Antibodies Raised Against PSI-D.

The polypeptides were initially resolved using 15% polyacrylamide SDS-PAGE by the method outlined in section 2.7. Approximately 5-10 µg of chlorophyll was loaded per lane. Western blot analysis was carried out according to the method in section 2.8.

The slightly diffuse band centred at 35 kDa was identified as bound FNR which had not been removed during the Digitonin isolation procedure. Identification as bound FNR was based on comparison of its electrophoretic properties with those of previously characterised soluble spinach FNR. The diffuse and lightly stained nature of the 35 kDa polypeptide (and on occasion its almost complete absence) indicated that it had been depleted during Digitonin isolation and was therefore probably not present in stoichiometric quantities. Four bands which migrated to between 22 and 28 kDa were identified as the light harvesting complex LHC-I (Andersen *et al.*, 1992_b; Staffan and Andersson, 1991). The poorly stained band at 21 kDa was identified by Western blot analysis as PSI-D (fig. 3.2). This appeared on the densitometric scan as a small peak following the heavily stained light harvesting complex polypeptides; although ill-defined on the gel scan, it formed a clearly visible electrophoretic band. The densitometric scan also showed a broad peak centred at approximately 17 kDa which comprised two regions forming a higher molecular weight peak with a lower molecular weight shoulder; this peak formed two visibly discrete bands on the SDS gel. The leading edge of the peak probably constitutes PSI-F, the plastocyanin docking protein, whilst the lower molecular weight region can reasonably be identified as a mixture of PSI-E and PSI-L which frequently co-migrate (Andersen *et al.*, 1992_{ab}; Staffan and Andersson, 1991; Zilber and Malkin, 1992). The intense region at 9 kDa was identified by western blot analysis as PSI-C, the Fe-$S_{A/B}$ binding protein (fig. 3.2). The intensity, width and line shape of this band in the

low molecular weight region suggests the presence of other low molecular weight proteins but the PhastGel SDS-PAGE system used here did not clearly resolve them. There was also occasionally a weak polypeptide band at 14 kDa which remains unidentified.

3.1.2 Triton X-100 Photosystem-I

Triton X-100 particles were prepared by the method described in section 2.1.2 and further purified on a hydroxyapatite column by the method outlined in section 2.1.3. The purified photosystem-I had a chlorophyll a:b ratio of >7 and oxidised-minus-reduced difference spectra showed it to have a P700:chlorophyll ratio of 35-65. This is consistent with a purified preparation depleted in light harvesting complex chlorophyll.

Figure 3.3_{ab} shows densitometric scans of two Triton X-100 photosystem-I preparations resolved by 8-25% gradient SDS polyacrylamide gel electrophoresis. It can be seen that there was variation between preparations in the number and relative intensity of some of the polypeptide bands although each preparation invariably contained 5 distinct bands attributable to the two major core polypeptides, PSI-A and PSI-B and three low molecular weight polypeptides at 21 kDa, 17 kDa and 9 kDa. The densitometric peaks at 9 kDa and 21 kDa were identified by Western blot analysis as PSI-D and PSI-C respectively. The 17 kDa band was comparable to that observed in Digitonin samples but it could no longer be differentiated into two discrete polypeptides.

a

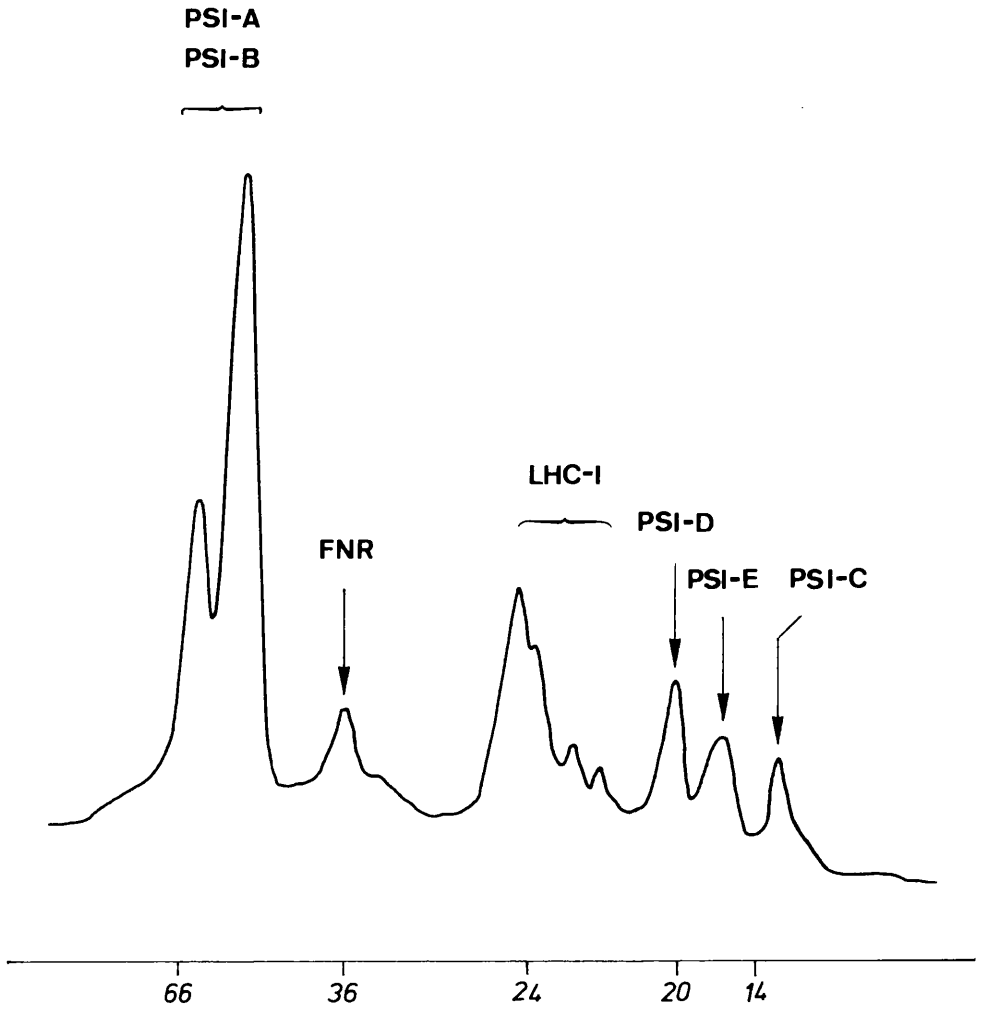

Figure 3.3

a.) Polypeptide Composition of Triton X-100 Isolated Photosystem-I.

Laser densitometric trace of photosystem-I isolated using Triton X-100 by the method in materials and methods section 2.1.2, the photosystem-I was further purified by application to a hydroxyapatite column (Section 2.1.3) and washed with low concentrations of Triton X-100. SDS-PAGE polypeptide separation was performed with an 8-25% polyacrylamide gradient using the Pharmacia PhastGel system. Approximately 0.5 µg of chlorophyll was loaded per lane.

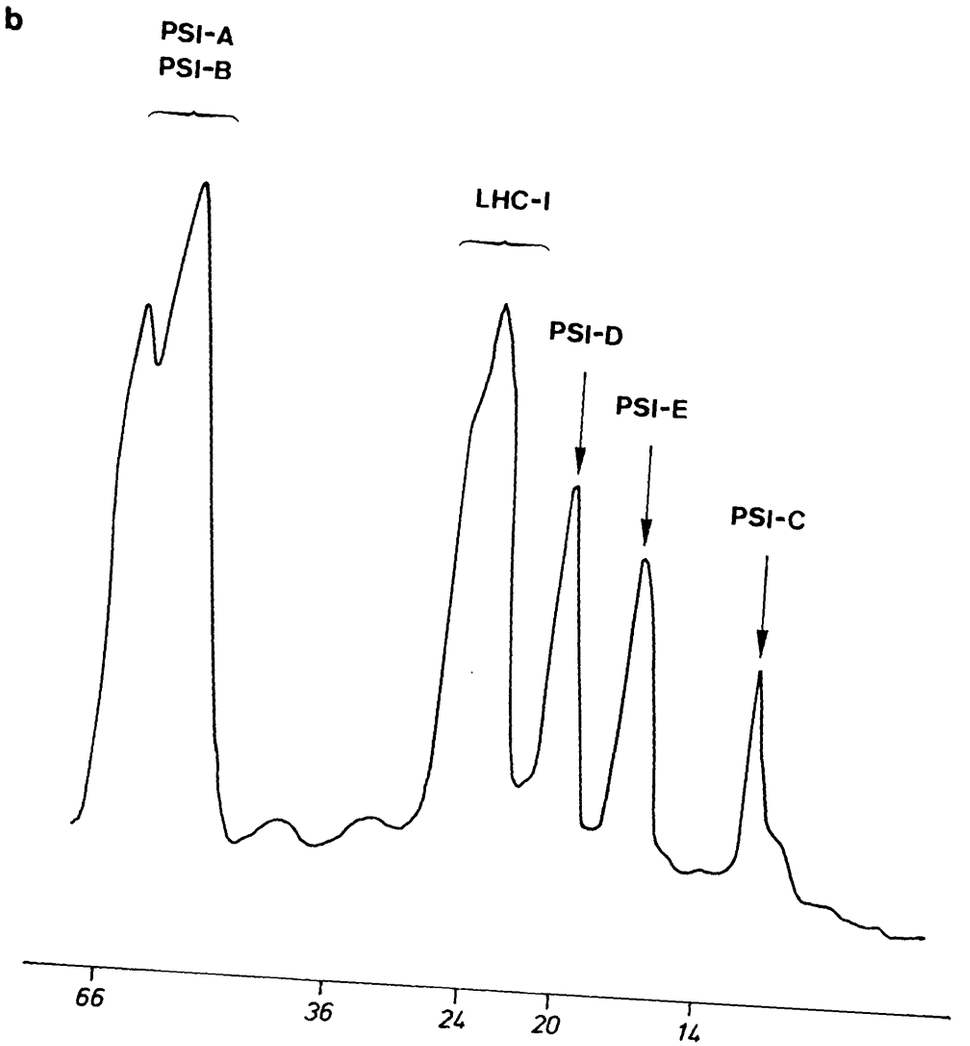

Figure 3.3

b.) Polypeptide Composition of Triton X-100 Isolated Photosystem-I.

Legend as figure 3.3_a

The remaining 17 kDa polypeptide band was most likely to be composed of PSI-E as it has been reported that the majority of the PSI-F and PSI-L is lost on extraction and purification of photosystem-I with Triton X-100 (Bengis and Nelson, 1977; Ishikawa *et al.*, 1992).

In addition to PSI-A, B, C, D and E there also remained varying concentrations of other polypeptides. A band identified as bound FNR seemed difficult to remove from the photosystem-I reaction centre complex and was retained at a low concentration even following prolonged washing with 0.5% Triton X-100 on an hydroxyapatite column. It was equally difficult to remove all of the polypeptides associated with the LHC-I complex which formed a densely stained and diffuse area between 22 and 28 kDa. However, this region was depleted as compared to the analogous molecular weight bands seen in the Digitonin photosystem-I densitometric scan and the four polypeptides comprising LHC-I could no longer be clearly differentiated. This indicated at least partial removal of the LHC-I polypeptides by Triton extraction (figs 3.1 and 3.3_{ab}). The retention of light harvesting complex polypeptides in Triton photosystem-I was not altogether surprising as they also remained bound to the core complex following treatment with 6.8 M urea; LHC-I can therefore be considered as very hydrophobic and a strongly bound integral membrane polypeptide unit. The low P700:chlorophyll ratio suggested that despite the retention of LHC-I polypeptides the vast majority of its associated chlorophyll had been removed by Triton washing.

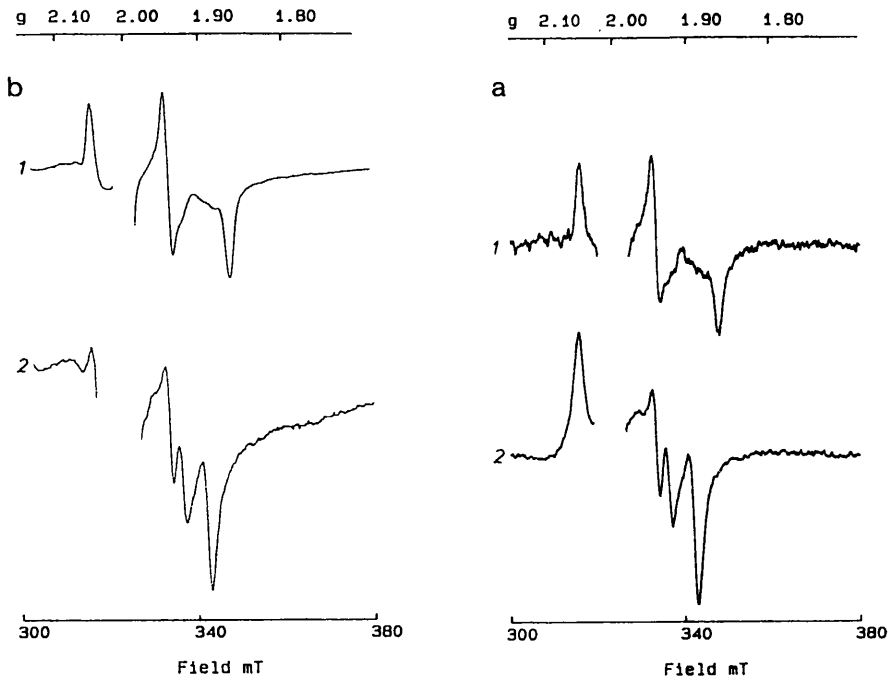

Figure 3.4

a. Fe-$S_A^-{}_B^-$ and Fe-S_A^- EPR Spectra of Digitonin Photosystem-I Particles.

1a) FeS_A^-. Light minus dark difference spectra of samples reduced with 30mM sodium ascorbate, frozen in the dark and illuminated at 15K in the EPR cavity.
2a) Fe-$S_A^-{}_B^-$. Spectra of samples reduced with sodium ascorbate, illuminated at room temperature and frozen under illumination.

EPR conditions: Microwave power 10 mW, temperature 15K, modulation width 1.25 mT. The g = 2.00 region of the spectra has been deleted for clarity.

b. Fe-$S_A^-{}_B^-$ and Fe-S_A^- EPR Spectra of Triton X-100 Photosystem-I Particles.

1b) FeS_A^-. Light minus dark difference spectra of samples reduced with 30mM sodium ascorbate, frozen in the dark and illuminated at 15K in the EPR cavity.
2b) Fe-$S_A^-{}_B^-$. Spectra of samples reduced with sodium ascorbate, illuminated at room temperature and frozen under illumination.

EPR conditions: Microwave power 10 mW, temperature 15K, modulation width 1.25 mT. The g = 2.00 region of the spectra has been deleted for clarity.

Triton and Digitonin particles had the same low temperature EPR spectra for both photoreduced iron-sulphur centre A, with principle g values of 1.94 and 1.87, and interactive EPR spectra for photoreduced centres A and B with g values of 1.94, 1.92 and 1.89, this indicated that Triton X-100 extraction did not perturb these centres (fig. 3.4_{ab}). Both preparations also exhibited the same $P700^{+}/Fe\text{-}S_{(A/B)}^{-}$ room temperature re-reduction kinetics although the Triton X-100 photosystem-I particles, unlike the Digitonin extracted material, had lost the ability to utilise plastocyanin as an electron donor to $P700^{+}$. This provided additional evidence that PSI-F was extracted from photosystem-I by treatment with Triton X-100, consistent with the findings of Bengis and Nelson (1977) and Li *et al.* (1991_a), and further suggested the identification of the remaining 17 kDa electrophoretic polypeptide band observed by 8-25% SDS-PAGE as PSI-E.

3.2 The Photosystem-I Core Complex

$Fe\text{-}S_A$ and $Fe\text{-}S_B$ are 4Fe-4S centres bound to a 9 kDa polypeptide which forms part of the photosystem-I reaction centre complex (Oh-oka *et al.*, 1987; Wynn and Malkin, 1988_a). The $Fe\text{-}S_{A/B}$ protein can be removed from photosystem-I by a number of procedures including the use of chaotropes such as urea. Urea treatment reversibly denatures the extrinsic polypeptides thereby releasing them from photosystem-I reaction centre complex. This treatment thus enables the isolation and purification of a photosystem-I core complex containing P700, A_0, A_1 and $Fe\text{-}S_X$. The

core complex is depleted of its terminal bound redox components and other stromally oriented polypeptides which are thought to be involved in interactions with soluble protein intermediates.

3.2.1 Characterisation of The Photosystem-I Core Complex

The core complex was isolated from Digitonin photosystem-I by the chaotrope extraction method described in section 2.1.5. Depletion of the Fe-$S_{A/B}$ holoprotein was monitored by change in the $P700^+$ back reaction from electron acceptor components following laser flash illumination. After 30 minutes incubation with 6.8 M urea the back reaction time reduced from 20 ms to 1 ms indicative of a photosystem-I core complex (fig. 3.5). Golbeck and Cornelius (1986) have previously identified the 1 ms optical transient as representing the back reaction between $P700^+$ and Fe-S_X^-. This therefore indicates the removal of the peripheral Fe-$S_{A/B}$ holoprotein yielding a core complex composed of centres P700, A_0, A_1, and Fe-S_X. Chaotrope induced depletion of iron-sulphur centres A and B was confirmed by measurement of photo-induced iron-sulphur centre EPR spectra. These spectra demonstrated that low temperature single electron photo-reduction of Fe-S_A (fig. 3.6) and room temperature photo-reduction of both centres A and B (fig. 3.7) was decreased by 85-90% as compared to the control values. The isolated core particle retains approximately 10% of the EPR signal attributed to Fe-$S_{A/B}$ and approximately 5% $NADP^+$ reduction activity of control photosystem-I.

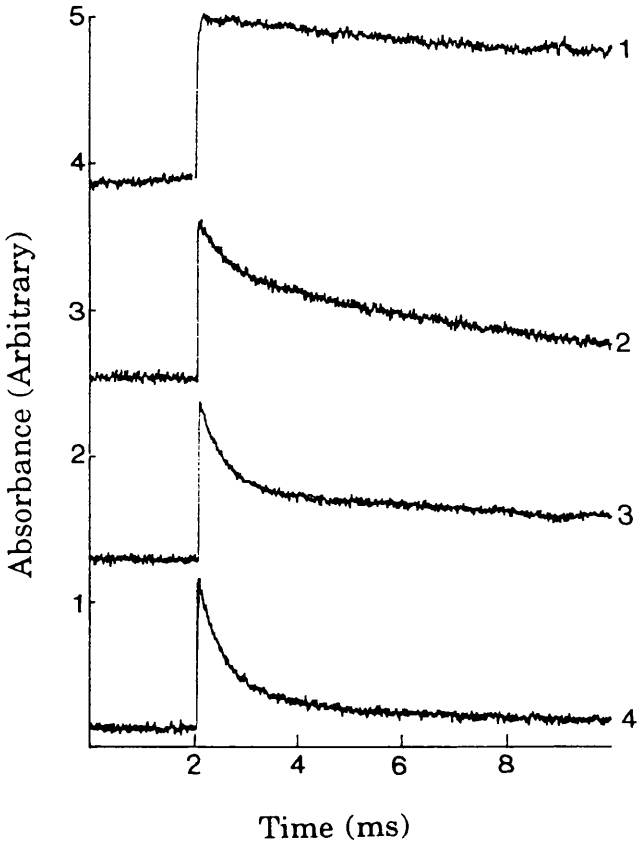

Figure 3.5

Re-reduction Kinetics of P700+ Following Oxidation by Laser Flash Illumination.

Control Digitonin photosystem-I particles incubated in 6.8M urea to remove the Fe-$S_{A/B}$ holoprotein and other peripheral polypeptides as described in materials and methods section 2.1.5. Incubation time 1.) 0 Minutes, 2.)10 minutes, 3.) 20 minutes, 4.) 25 minutes.

The reaction mixture contained: photosystem-I particles 25µg chlorophyll/ml in 20mM Tricine-KOH pH 8.0, 6.7mM sodium ascorbate and 68 µM dichlorophenolindophenol. 30 repetitions were averaged at 0.5 Hz flash repetition rate.

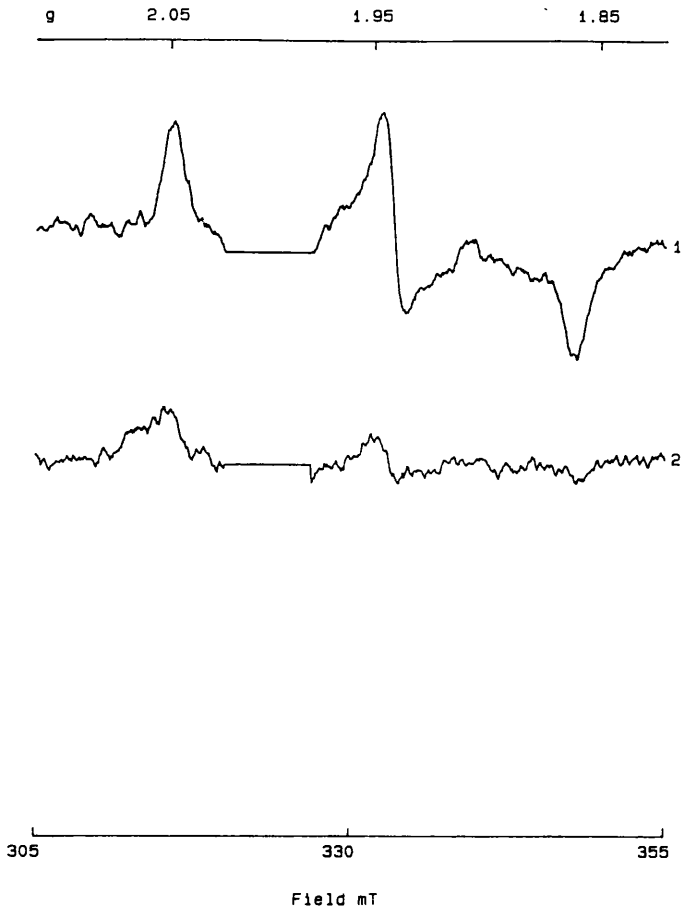

Figure 3.6

Fe-S_A^- EPR Spectra of Control and Urea Treated Digitonin Photosystem-I Particles.

Light-minus-dark EPR difference spectra of Fe-S_A achieved by reduction of samples with 30mM sodium ascorbate, freezing in the dark then illumination at 15K in the EPR cavity.

1) Control samples of Digitonin photosystem-I particles before treatment.
2) Urea treated particles with the Fe-$S_{A/B}$ holoprotein removed. Urea treatment is described in section 2.1.5. Each sample contained 500µg/chlorophyll/ml.

EPR conditions: Microwave power 10 mW, temperature 15K, modulation width 1.25 mT, Instrument gain 500. The g = 2.00 region of the spectra has been deleted for clarity.

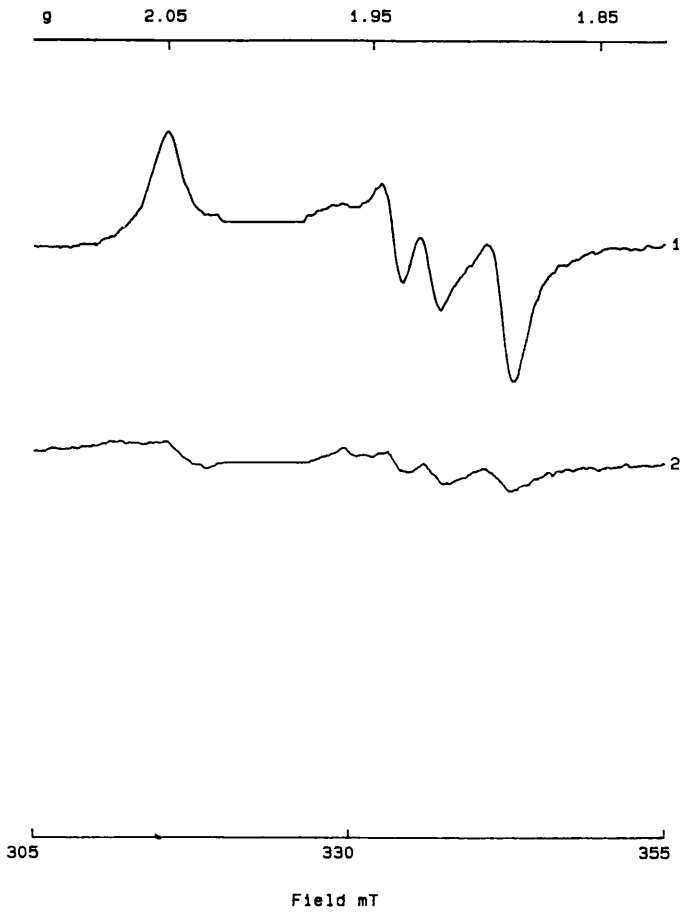

Figure 3.7

Fe-$S_{A}^{-}{}_{B}^{-}$ EPR Spectra of control and Urea Treated Digitonin Photosystem-I Particles.

Light-minus-dark EPR difference spectra of Fe-$S_{A/B}$ achieved by reduction of samples with 30mM sodium ascorbate, illumination at room temperature and freezing under illumination.

1) Control samples of Digitonin photosystem-I particles before treatment.

2) Urea treated particles with the Fe-$S_{A/B}$ protein removed. Urea treatment is described in section 2.1.5. Each sample contained 500µg/chlorophyll/ml.

EPR conditions: Microwave power 10 mW, temperature 15K, modulation width 1.25 mT, Instrument gain 500. The g = 2.00 region of the spectra has been deleted for clarity.

The ability to rebind the Fe-$S_{A/B}$ holoprotein to the core complex during reconstitution experiments is dependant on the retention of Fe-S_X which can also be damaged during urea treatment. A balance had to be struck between removing as much of the Fe-$S_{A/B}$ as possible, whilst retaining functional Fe-S_X, in order to secure high levels of reconstitution. Removal of 100% of Fe-$S_{A/B}$ resulted in high levels of Fe-S_X damage, this was reflected in the loss of 1 ms kinetics and the preparations inability to rebind isolated PSI-C. To maintain the structure of Fe-S_X the urea/PS-I reaction mixture was kept anaerobic at all times and diluted 10X in oxygen free Tris-HCl buffer immediately after the 1 ms kinetics had been reached. After complete removal of urea (by either dialysis against 50mM Tris-HCl pH 8.3 or centrifugation of the core complex and resuspension in 50mM Tris-HCl pH 8.3) and addition of 0.1% 2-mercaptoethanol Fe-S_X was stabilised and would remain intact at 4^0C over an 8 hour period.

EPR Characteristics of Core Complex Photosystem-I

It was extremely difficult to observe the photo-reduction of Fe-S_X in the core complex by EPR. This may be a result of EPR spectrum broadening caused by a change in the micro-environment of Fe-S_X^- or an alteration in ligand orientation brought about by a modification in the structure of PSI-A and B at the acceptor side. Such structural changes are likely if the PSI-C, D and E, removed by chaotrope action, play a role in structural integrity of the acceptor side of photosystem-I. The designation of Fe-S_X in the core particle was based on the 1 ms $P700^+$ re-reduction

transient observed at room temperature which had previously been identified by optical difference spectra as the remaining iron-sulphur centre (Golbeck and Cornelius, 1986).

Identification of the other redox components, previously described in photosystem-I, was achieved by photo-accumulation experiments using the method of Bonnerjea and Evans (1982). Core particle preparations were dark adapted for 30 minutes at room temperature in the presence of 0.2% (w/v) sodium dithionite at pH 10.0 then frozen in the dark and stored in liquid nitrogen. The redox state after this treatment was apparently P700, A_0, A_1 and Fe-S_X^- and the sample had no g = 2.00 EPR signal at this stage. The samples were then illuminated for 30 seconds at 200K. This gave rise to an asymmetric g = 2.00 EPR signal 0.89 mT wide typical of the photo-reduced secondary electron acceptor A_1^- (fig. 3.8) as previously described (Bonnerjea and Evans, 1982; Gast *et al.*, 1983). The redox state after 30 seconds of 200K illumination was therefore P700, A_0, A_1^- and Fe-S_X^-, although a slight shoulder on the high field side of the spectrum did indicate a small proportion of A_0 had been reduced. Further illumination at 200K for progressively longer periods caused the gradual broadening of the g = 2.00 EPR spectra. After a total of 13 minutes illumination at 200K the g = 2.00 photo-accumulated EPR signal had broadened to 1.4 mT concomitant with the reduction of both A_1 and A_0 (fig. 3.9) (Bonnerjea and Evans, 1982).

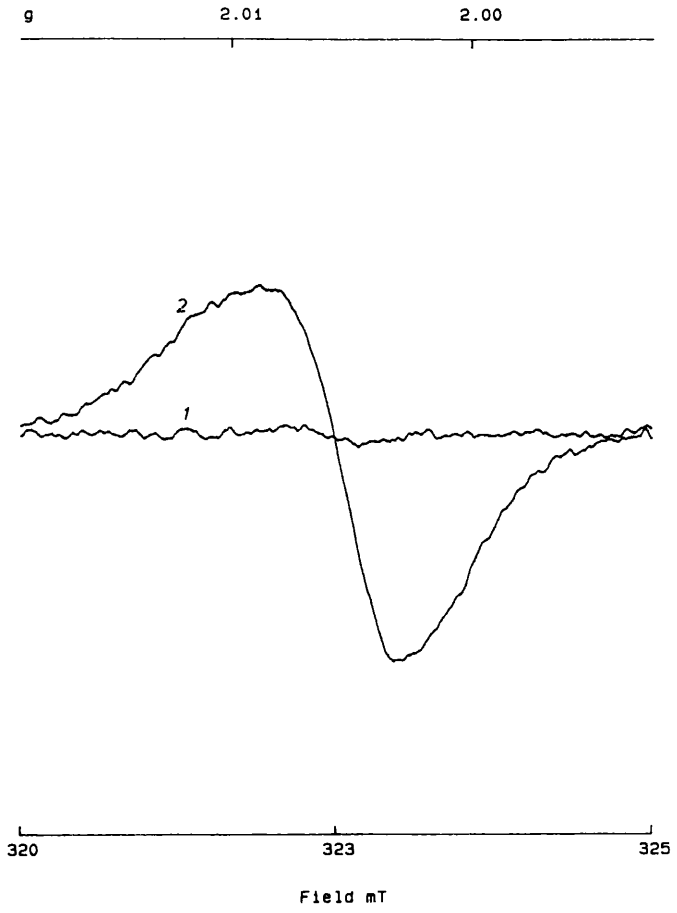

Figure 3.8

The EPR Spectrum of A_1^- in Digitonin Photosystem-I Core Particles.

Samples were prepared as described in the materials and methods section 2.9.2. The spectra was obtained by 200K illumination of Digitonin photosystem-I core particles which had been previously incubated with 0.2% (w/v) sodium dithionite at pH 10.0 and frozen in the dark. Illumination time: 1)Dark and 2)0.5 min. After 0.5 minute illumination the sample was removed to the EPR spectrometer and the spectra recorded.

EPR conditions: Microwave power 5 μW, modulation width 0.1 mT, recording temperature 75K.

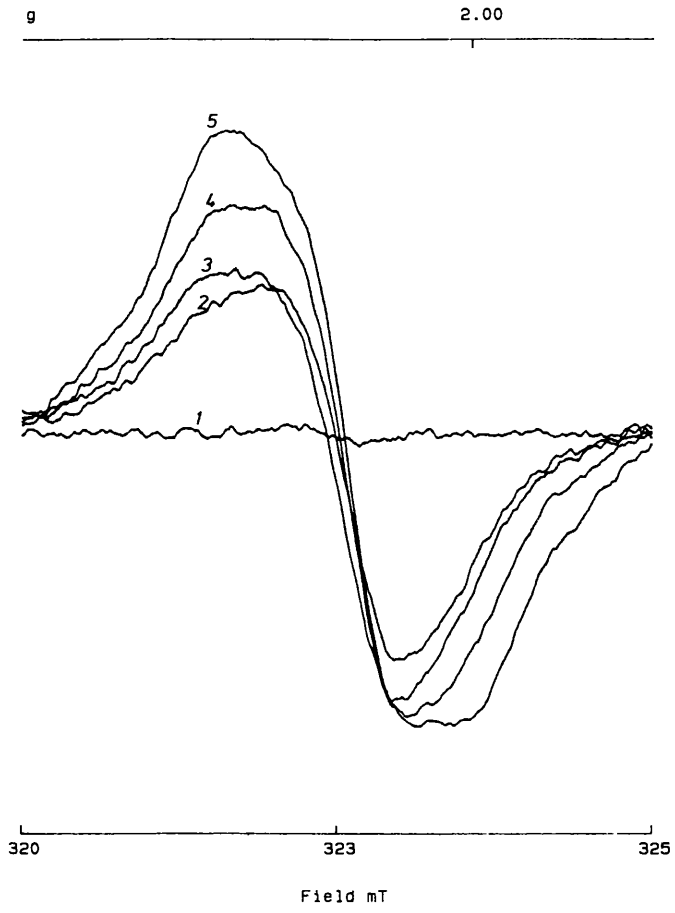

Figure 3.9

The EPR Spectra of A_0^- and A_1^- for Digitonin Photosystem-I Core Particles.

Samples were prepared as described in the materials and methods section 2.9.2. The spectra were obtained by progressively longer periods of 200K illumination of Digitonin photosystem-I particles which had been previously incubated with 0.2% (w/v) sodium dithionite at pH 10.0 and frozen in the dark.

Illumination time: 1) Dark, 2) 0.5 min, 3) 1 min, 4) 3 min and 5) 13 min. At intervals during the illumination the samples were removed to the EPR spectrometer and the spectra recorded.

EPR conditions: Microwave power 5 μW, modulation width 0.1 mT, recording temperature 75K.

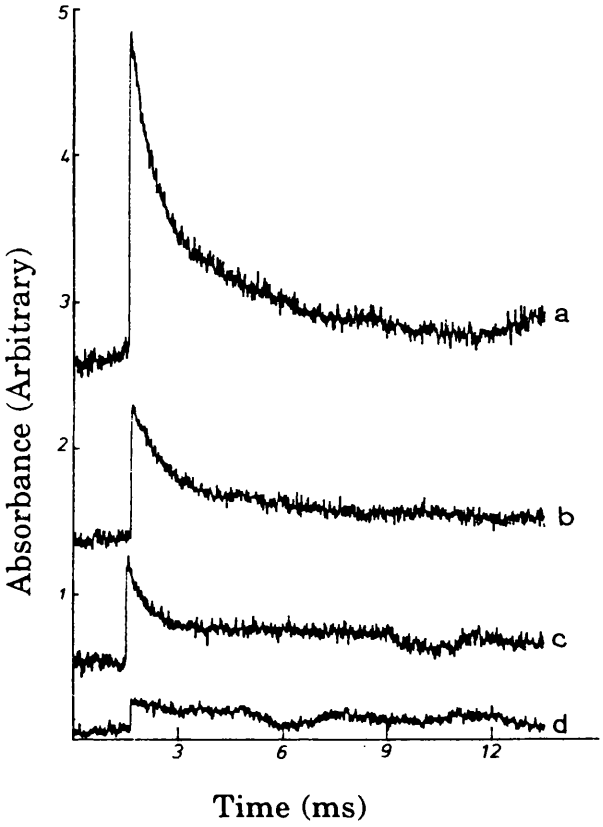

Figure 3.10

Re-reduction Kinetics of $P700^+$ Following Oxidation by Laser Flash Illumination during the oxidative destruction of Fe-S_X.

The oxidative destruction of Fe-S_X was achieved by incubation of the photosystem-I core particle in 3 M urea and 5mM potassium ferricyanide as described in material and methods section 2.1.5. a) 0 minutes incubation, b) 5 minutes incubation, c) 10 minutes incubation, d) 25 minutes incubation.

The reaction mixture contained: photosystem-I particles 25µg chlorophyll/ml in 20mM Tricine-KOH pH 8.0, 20mM sodium ascorbate and 68µM dichlorophenolindophenol. 30 repetitions were averaged at 0.5 Hz flash repetition rate.

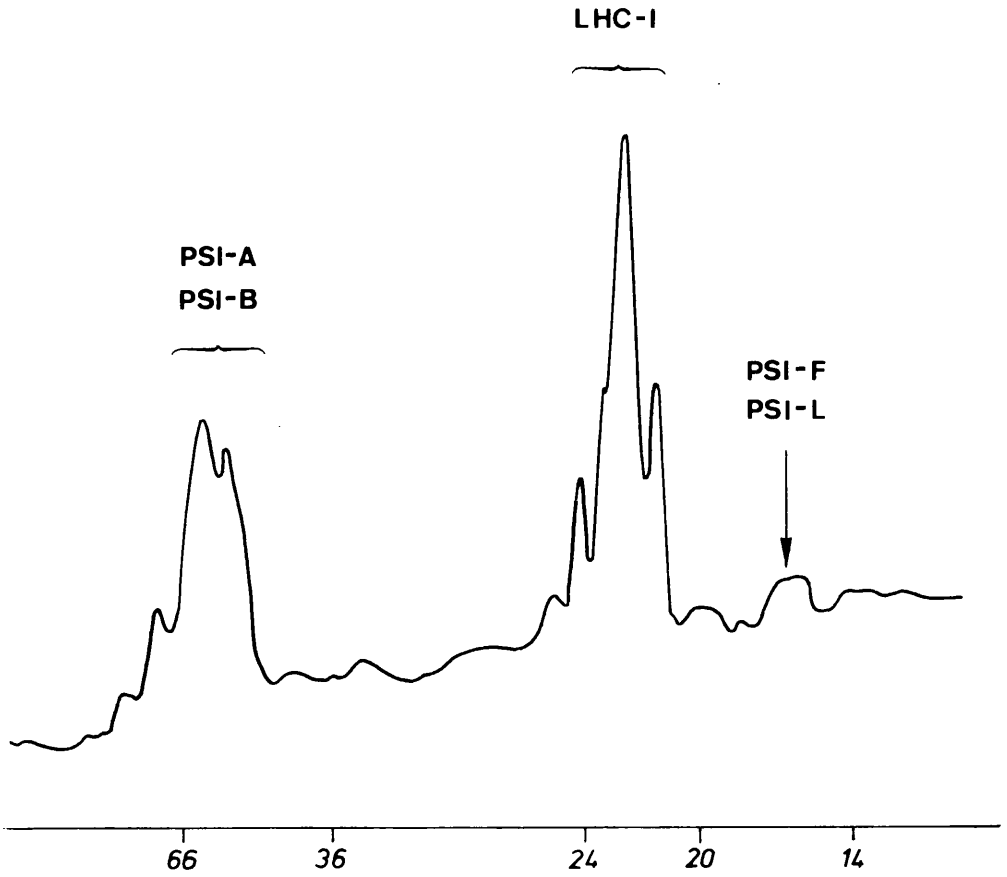

Figure 3.11

Polypeptide Composition of Digitonin Isolated Photosystem-I Core Complex.

Laser densitometric trace of photosystem-I isolated using Digitonin then stripped of peripheral polypeptides by the method in section 2.1.5. SDS-PAGE polypeptide separation was performed with an 8-25% polyacrylamide gradient using the Pharmacia PhastGel system. Approximately 0.5 μg of chlorophyll were loaded per lane.

Removal of Fe-S_X from the Photosystem-I Core Particle

Incubation of the core particle in 5mM potassium ferricyanide, 3 M urea and 20mM Tris-HCl at 50 µg chl/ml for 30 minutes at room temperature resulted in the loss of the 1 ms $P700^+/Fe\text{-}S_X^-$ back reaction kinetics replacing it with a $T_{½}$ too short to resolve on the equipment available (fig. 3.10). This indicated the oxidative destruction of Fe-S_X to the level of zero valence sulphur reported by Warren *et al.* (1990).

Illumination of these samples at 200K in the presence of dithionite at pH 10.0 for between 30 seconds and 13 minutes gave identical EPR spectra to those observed in both the core particle and control photosystem-I. The g = 2.00 EPR spectrum after 30 seconds illumination was .89 mT wide broadening to 1.4 mT with further 200K illumination. This is indicative of a particle containing P700, A_0 and A_1 but depleted of iron-sulphur centres Fe-$S_{A/B}$ and Fe-S_X.

SDS-PAGE Analysis of the Core Particle

The densitometric scan of the 8-25% SDS-polyacrylamide gel of the P700/Fe-S_X core particle isolated from Digitonin photosystem-I is shown in (fig. 3.11). It shows a major band at approximately 60 kDa and four bands from 22-28 kDa indicating a particle comprised primarily of the major core proteins PSI-A and PSI-B and the light harvesting complex (LHC-I). There was depletion of the low molecular weight extrinsic polypeptides in the 8-21 kDa range and the bound FNR at 35 kDa.

The 21 kDa and the 9 kDa proteins, identified by western blot as

PSI-D and PSI-C respectively, were almost completely absent, although a small residual fraction of both proteins did remain. By comparison with the results of low temperature EPR spectroscopy and the rate of photo-reduction of $NADP^+$ by the core particle one would expect the residual acceptor side protein content to be 5-15 % of that observed in the starting material.

There remained a diffuse band at 17 kDa but this is probably a mixture of PSI-F and PSI-L both of which have an apparent molecular weight of 17 kDa and are hydrophobic intrinsic polypeptides not extractable from the core complex by chaotrope treatment (Li *et al.*, 1991_a; Okkels *et al.*, 1991).

Further evidence of the identity of polypeptides extracted from Digitonin photosystem-I by urea treatment comes from analysis of polypeptides retrieved from the YM100 filtrate following concentration of the core complex. Concentration of the filtrate over an Amicon YM2 membrane followed by analysis of electrophoretic properties and antibody labelling revealed the proteins to be PSI-C, PSI-D, PSI-E and a small quantity of LHC-I (fig. $3.12,3.13_{ab}$). However, western blot analysis indicated that PSI-D suffered varying amounts protein degradation during chaotrope extraction which rendered it useless for the purpose of further purification (fig. 3.13_b). The iron sulphur centres of PSI-C had also degraded during the urea isolation.

An attempt was made to reconstitute the iron-sulphur centres by additions of $FeCl_3$ and Na_2S to the extracted PSI-C apoprotein under

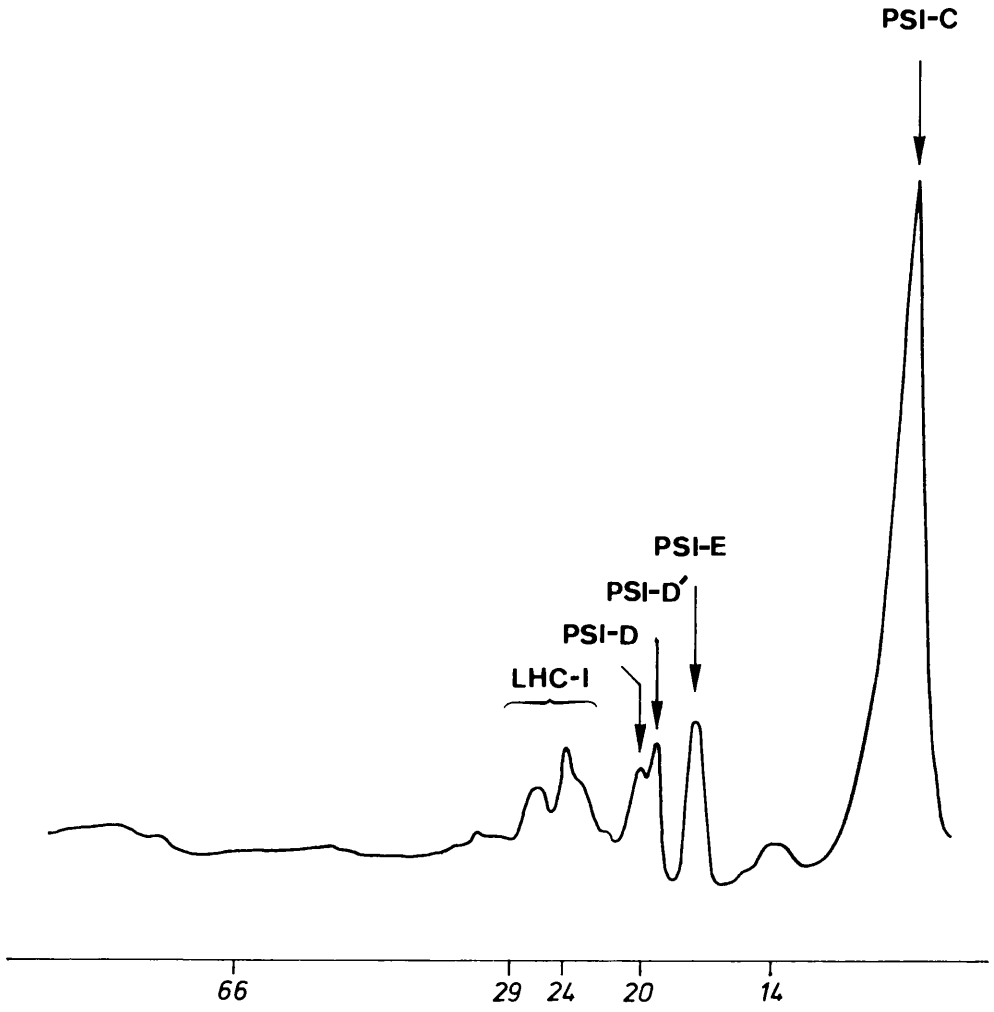

Figure 3.12

Polypeptide Composition of Low Molecular Mass Polypeptides Released from Digitonin Isolated Photosystem-I Following Urea Treatment.

The released proteins were separated from the core complex by YM100 ultra filtration and then concentrated over an Amicon YM2 membrane. SDS-PAGE polypeptide separation was performed with an 8-25% polyacrylamide gradient using the Pharmacia PhastGel system. D' denoted PSI-D breakdown product.

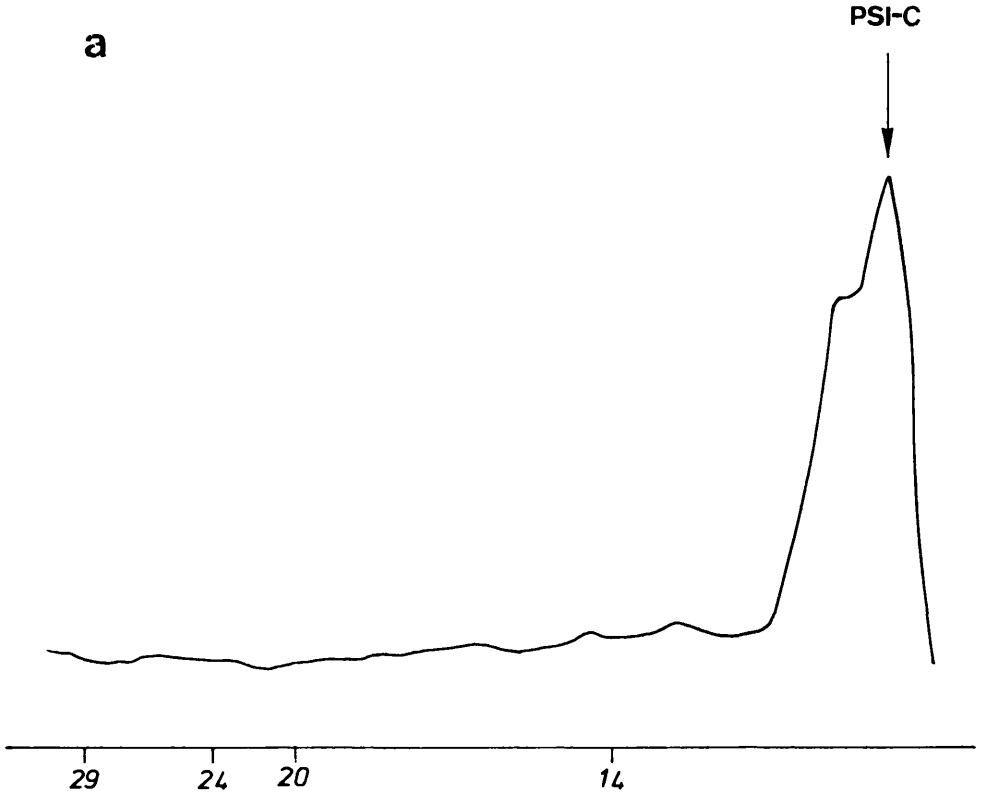

Figure 3.13

a.) Western Blot Analysis of Photosystem-I Polypeptides Released by Treatment with 6.8 M Urea Labelled With Antibodies Raised Against PSI-C.

Laser densitometric trace of the polypeptides released from photosystem-I by urea treatment labelled with antibodies raised against PSI-C. The released proteins were separated from the core complex by YM100 ultra filtration and then concentrated over an Amicon YM2 membrane. SDS-PAGE polypeptide separation was performed using 15% polyacrylamide resolving gel by the method outlined in section 2.7. Approximately 5-10 µg of chlorophyll was loaded per lane. Western blot analysis was carried out according to the method in section 2.8.

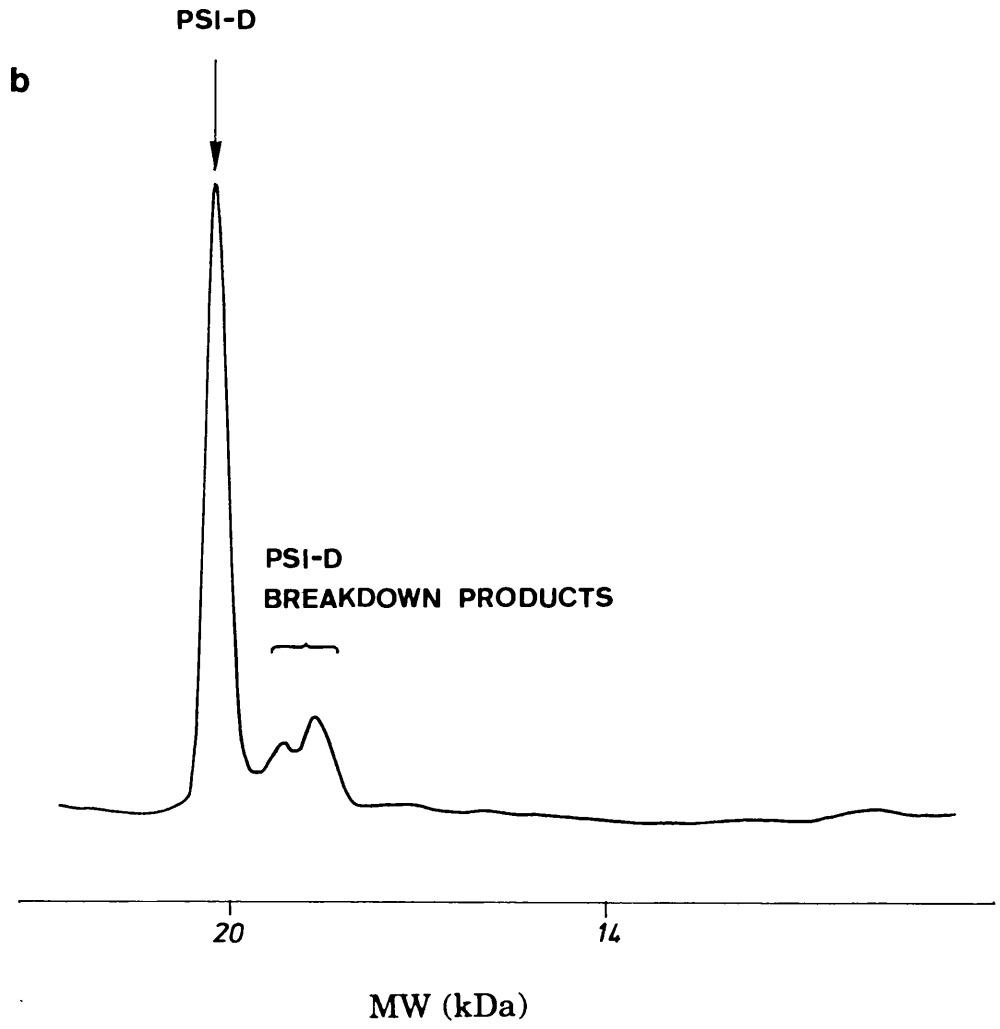

Figure 3.13

b.) Western Blot Analysis of Photosystem-I Polypeptides Released by Treatment with 6.8 M Urea Labelled With Antibodies Raised Against PSI-D.

Laser densitometric trace of the polypeptides released from photosystem-I by urea treatment labelled with antibodies raised against PSI-D. The released proteins were separated from the core complex by YM100 ultra filtration and then concentrated over an Amicon YM2 membrane. SDS-PAGE polypeptide separation was performed using 15% polyacrylamide resolving gel by the method outlined in section 2.7. Approximately 5-10 µg of chlorophyll was loaded per lane. Western blot analysis was carried out according to the method in section 2.8.

reducing conditions but this proved to be unsuccessful. Extrinsic polypeptides derived by solvent treatment seemed less perturbed than those extracted by chaotropes. It was therefore decided to use *n*-butanol extraction as a preliminary stage in the purification of stromally oriented extrinsic polypeptides which may be required during reconstitution experiments.

3.3 The Role of Bound Iron-Sulphur Centres A and B

PSI-C, the iron sulphur centre A and B containing polypeptide, can be isolated by treatment with solvents such as acetone (Wynn and Malkin, 1988_a) or *n*-butanol (Oh-oka *et al.*, 1988_b) which partition the peripheral hydrophi lic proteins into the aqueous phase. This isolation procedure does not perturb the tertiary structure of the polypeptides in the manner observed in chaotrope washing, consequently, the iron-sulphur protein can be further purified with the labile redox components still intact. The resultant PSI-C has EPR and optical difference spectra typical of a 2 X {4Fe-4S} ferredoxin (Wynn and Malkin, 1988_a), although the EPR spectrum of the isolated holoprotein is somewhat broader than that observed for Fe-$S_{A/B}$ bound to the photosystem-I complex.

Golbeck and his co-workers have utilised these isolation techniques in a series of experiments which go some way in the elucidation of the structure and function of the photosystem-I stromally oriented peripheral polypeptides. They have demonstrated that incubation of core photosystem-I with the isolated Fe-$S_{A/B}$ protein, in conjunction with other

stromally oriented photosystem-I polypeptides, results in a recovery of the optical kinetics and EPR characteristics of the native photosystem-I complex.

Their results show:

1.) The ferredoxin isolated by Wynn and Malkin forms the bound iron-sulphur complex responsible for the Fe-$S_{A}^{-}{}_{B}^{-}$ EPR spectra and the optical back reaction kinetics between $P700^{+}$ and the terminal redox component. The kinetics and EPR spectra indicated that the Fe-$S_{A/B}$ holoprotein had reconstituted to a normal configuration.

2.) Chaotrope treatment of photosystem-I removes PSI-C, D and E, all of which rebound onto the core complex in equal amounts on reconstitution.

3.) Cross species reconstitution, i.e. spinach Fe-$S_{A/B}$ with cyanobacterial core complex, resulted in a spinach Fe-$S_{A}^{-}{}_{B}^{-}$ type EPR spectra. This indicates that the Fe-$S_{A/B}$ EPR signal is inherent in the protein and dependant on PSI-C being bound to a core complex, although the spectra does not seem to be directly influenced by the species of core complex.

4.) Reconstitution in the absence of PSI-D resulted in an EPR Fe-$S_{A/B}$ spectrum indicative of altered iron-sulphur centre orientation.

Centrifugation of samples reconstituted in the absence of PSI-D results in the loss of the Fe-$S_{A}^{-}{}_{B}^{-}$ EPR spectrum although the Fe-$S_{A/B}$ apoprotein remained bound to the core complex. Addition of PSI-D during reconstitution results in native type EPR spectra and prevents Fe-$S_{A/B}$ degradation during centrifugation. This suggests a structural role for PSI-D in stabilisation and orientation of PSI-C and the redox components Fe-$S_{A/B}$.

Although chemical and photo-reduced photosystem-I redox components have been extensively characterised by biophysical and biochemical means at both cryogenic and room temperature, the role of iron-sulphur centres A and B in room temperature $NADP^+$ photo-reduction had not been directly demonstrated. A modified version of Golbeck's reconstitution system was used during this work as a basis for the investigation of the role that the Fe-$S_{A/B}$ holoprotein and other stromally oriented peripheral polypeptides play in room temperature forward electron transfer to $NADP^+$ involving ferredoxin and FNR. The results indicate that iron-sulphur centres A and B, in conjunction with stromal oriented polypeptides PSI-D and PSI-E, are essential for electron transfer to $NADP^+$ to take place.

3.3.1 Isolation and Characterisation of the Fe-$S_{A/B}$ Holoprotein

Butanol extraction of peripheral photosystem-I polypeptides was carried out by a modified version of the method of Oh-oka *et al.* (1987) detailed in section 2.3.

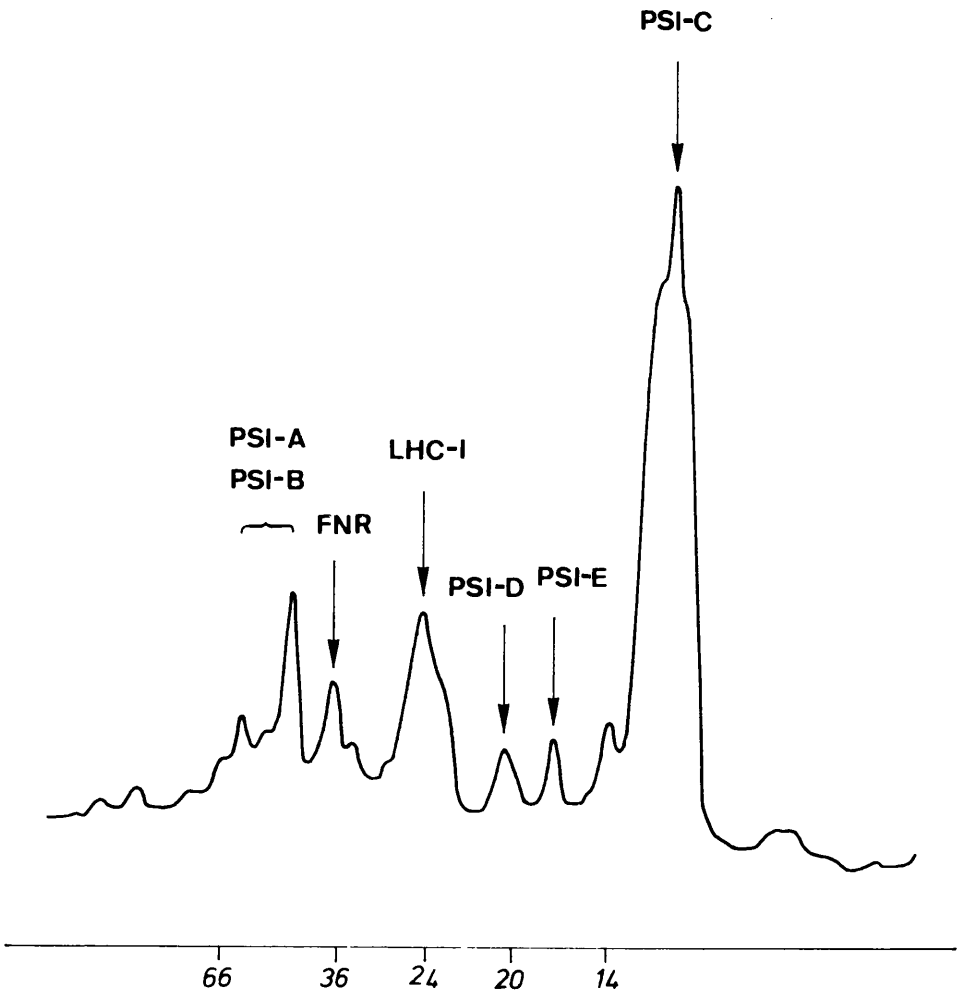

Figure 3.14

Polypeptide Composition of Low Molecular Mass Polypeptides Released from Triton Isolated Photosystem-I Following *n*-butanol Treatment.

Laser densitometric trace of the polypeptides released from the Triton X-100 isolated photosystem-I by butanol extraction (Method section 2.3). The released proteins were concentrated over an Amicon YM2 membrane under Argon. SDS-PAGE polypeptide separation was performed with an 8-25% polyacrylamide gradient using the Pharmacia PhastGel system.

Triton X-100 photosystem-I particles purified on a hydroxyapatite column were used for the extractions in order to restrict the polypeptides extracted to those shown to have an involvement in events at the acceptor side of photosystem-I.

Following *n*-butanol extraction the Fe-$S_{A/B}$ holoprotein was contained in the yellow-brown aqueous phase but it was fairly heavily contaminated with higher molecular weight polypeptides. Figure 3.14 shows the densitometric trace of the protein content in the *n*-butanol extracted material following electrophoresis on a 8-25% SDS-gel. It contained a range of polypeptides from 66 kDa to 9 kDa including a small proportion of PSI-A and PSI-B, bound FNR and unpigmented LHC-I.

Western blot and SDS-PAGE analysis indicated the presence of a comparatively high proportion of PSI-C, PSI-D and PSI-E. The identification of the 17 kDa band as PSI-E was based principally on its electrophoretic properties and the knowledge that PSI-F (which also has an apparent molecular weight of approximately 17 kDa) will not partition into the aqueous phase during solvent extraction (Oh-oka *et al.*, 1988_a). PSI-L, another possible contaminant, is hydrophobic and therefore unlikely to be butanol extractable. It had also been established that most of the PSI-F and PSI-L was removed from photosystem-I by 0.5% Triton X-100 washing, very low levels of contamination by these polypeptides would therefore be expected.

Oh-oka *et al.* (1987) reported that the ionic strength of the photosystem-I buffer solution prior to *n*-butanol extraction effected the

relative amounts of higher molecular weight polypeptide contamination following solvent partitioning. In the experiments presented here variation of the ionic strength between 25 and 300mM NaCl made little difference to the purity of the end product.

The intention during this work was to demonstrate the necessity of Fe-$S_{A/B}$ in forward electron transfer to $NADP^+$ and to investigate the role of other peripheral acceptor side polypeptides in the mediation of those events. This required further purification of the *n*-butanol extract in order to clearly define the respective functions of PSI-C, PSI-D and PSI-E. Purification was achieved by a number of chromatographic procedures each of which will be discussed in turn.

Ion exchange chromatography (Preparation 1)

Figure 3.15 shows a densitometric scan of the polypeptides obtained after DEAE Fractogel ion exchange chromatography of the *n*-butanol extracted material. The constituent polypeptides were resolved by 8-25% SDS-PAGE.

Ion exchange chromatography of the *n*-butanol extracted material on DEAE fractogel served two main purposes:

1.) It lowered the relative concentration of the PSI-A, PSI-B, FNR and LHC-I with a concomitant concentration of PSI-C, D and E.

2.) Washing the material with 50mM Tris-HCl pH 8.1 whilst bound

to the column removed the *n*-butanol in the aqueous solution. Removal of *n*-butanol was essential as it acted as a barrier to reconstitution of the extrinsic polypeptides to the photosystem-I core complex.

The disadvantage of ion exchange chromatography was the loss of valuable polypeptides during the washing procedure. Up to 50% of the extracted material was lost in the washings which included high levels of PSI-C, D and E. There also remained a low level of 22-28 and 35 kDa polypeptide contamination in the eluted end product. To be certain that these played no role in reconstitution or had an involvement in cofactor binding during $NADP^+$ photo-reduction they had to be removed.

Sephacryl S-200 HR Gel filtration (Preparation 2)

The *n*-butanol extracted material was passed down an oxygen free 40 cm X 2.2 cm sephacryl S-200 HR column and eluted over a 1-2 hour time period. This step was introduced to free solvent extracted material of *n*-butanol and to remove the high molecular weight contaminants whilst maintaining the EPR characteristics of the iron-sulphur redox centres of PSI-C. The material eluted in two fractions measured by the absorbance at 280 nm (fig. 3.16). The first fraction (fraction 1), which was dark brown in colour, formed 60-70% of the total eluted material.
It passed down the column at a rate indicative of a high molecular weight polypeptide or multi-protein unit. The second fraction formed a diffuse band and was yellow in colouration.

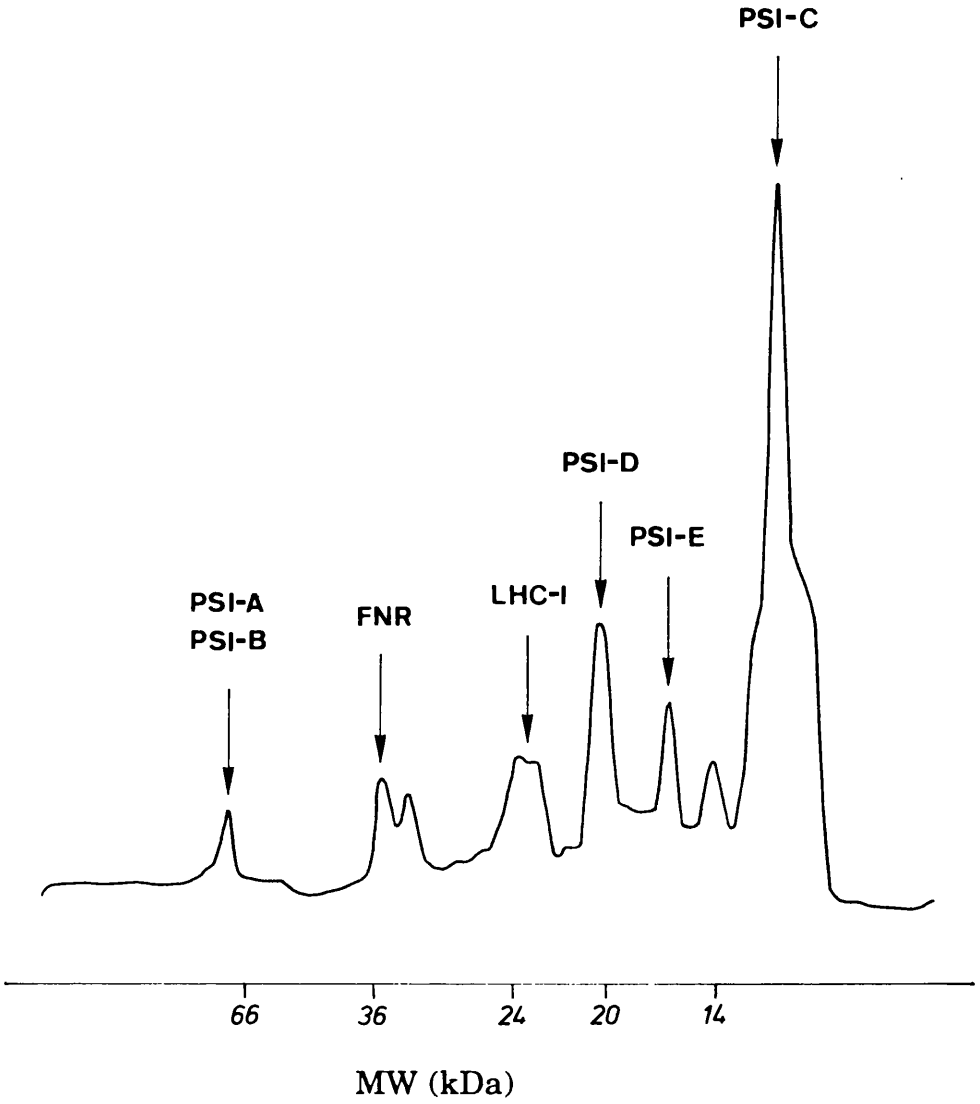

Figure 3.15

Polypeptide Composition of *n*-butanol Extracted Material Following Purification on a DEAE Fractogel Column.

Laser densitometric trace of polypeptides after initial purification on DEAE fractogel by the method in section 2.3. The eluted material was concentrated over an Amicon YM2 membrane under Argon. SDS-PAGE polypeptide separation was performed with an 8-25% polyacrylamide gradient using the Pharmacia PhastGel system.

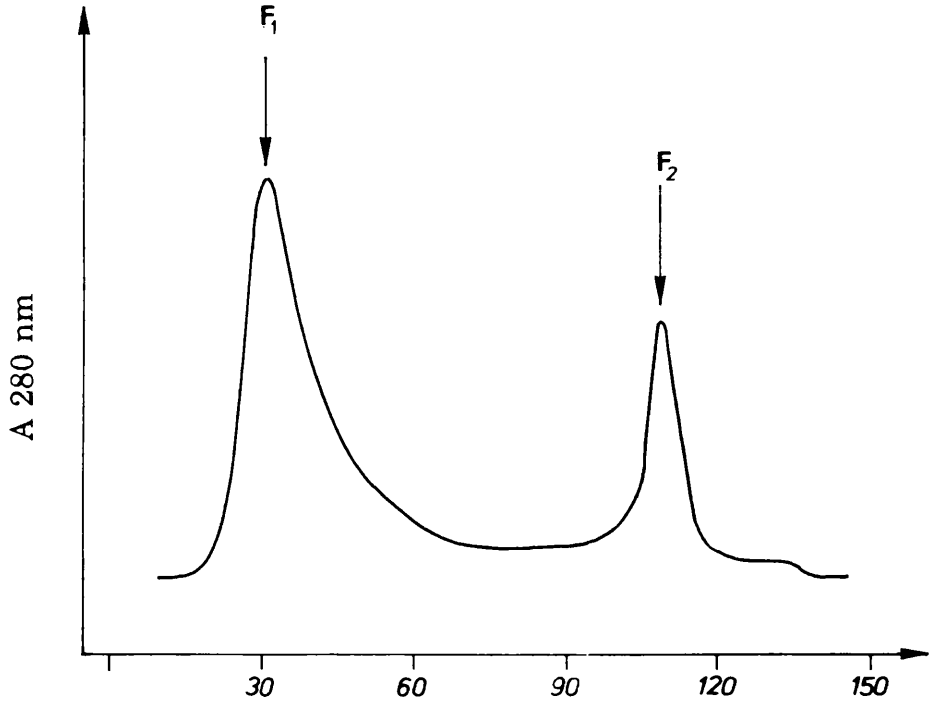

Figure 3.16

Elution Profile of Butanol Extracted Material Passed Through a Sephacryl S-200 HR Column.

The butanol extracted material was concentrated over an Amicon YM2 membrane under Argon. It was then size fractionated by passage through a 2.6 X 40 cm S-200 HR gel filtration column in 20mM Tris-HCl pH 8.0, 5mM dithiothreitol and 100mM NaCl and eluted over a 1-2 hour time period. Eluted material was monitored using a 280 nm single path U.V. monitor.

Thorough degassing of both the column packing material and running buffers and addition of dithiothreitol at all stages of the purification procedure was essential. Failure to carry out these measures resulted in the gradual disappearance of the yellow colouration in protein fraction 2. EPR analysis indicated that the loss of colouration was caused by degradation of the iron-sulphur centres of PSI-C although the binding protein itself remained intact.

SDS-PAGE and low temperature EPR spectroscopic analysis was carried out on both fractions. SDS-PAGE revealed that the high molecular weight fraction 1 was composed of all the *n*-butanol extracted polypeptides (PSI-A, B, C, D, E, FNR and LHC-I) which, despite the large range in molecular weights, co-migrated down the column.

Fraction 2 contained PSI-C, D and E which, due to the lack of resolution of the column media, eluted in one diffuse band (fig. 3.17). EPR spectra and western blot analysis confirmed the presence of the iron-sulphur holoprotein (PSI-C) in both fractions 1 and 2 but in fraction 1 the low temperature EPR spectrum was altered with principle g values of 2.10, 2.08, 2.01, 1.985 and 1.917 (fig. 3.18). The iron-sulphur centres in this fraction were unaffected by oxygen.

Clumping of the proteins in the manner observed in fraction 1 was very costly in terms of polypeptide loss. In order to retrieve some of these proteins various attempts were made to solubilise fraction 1. Native page gel electrophoresis indicated that treatment of the *n*-butanol extract with 7 M urea for 30 minutes resulted in the release of the constituent fraction

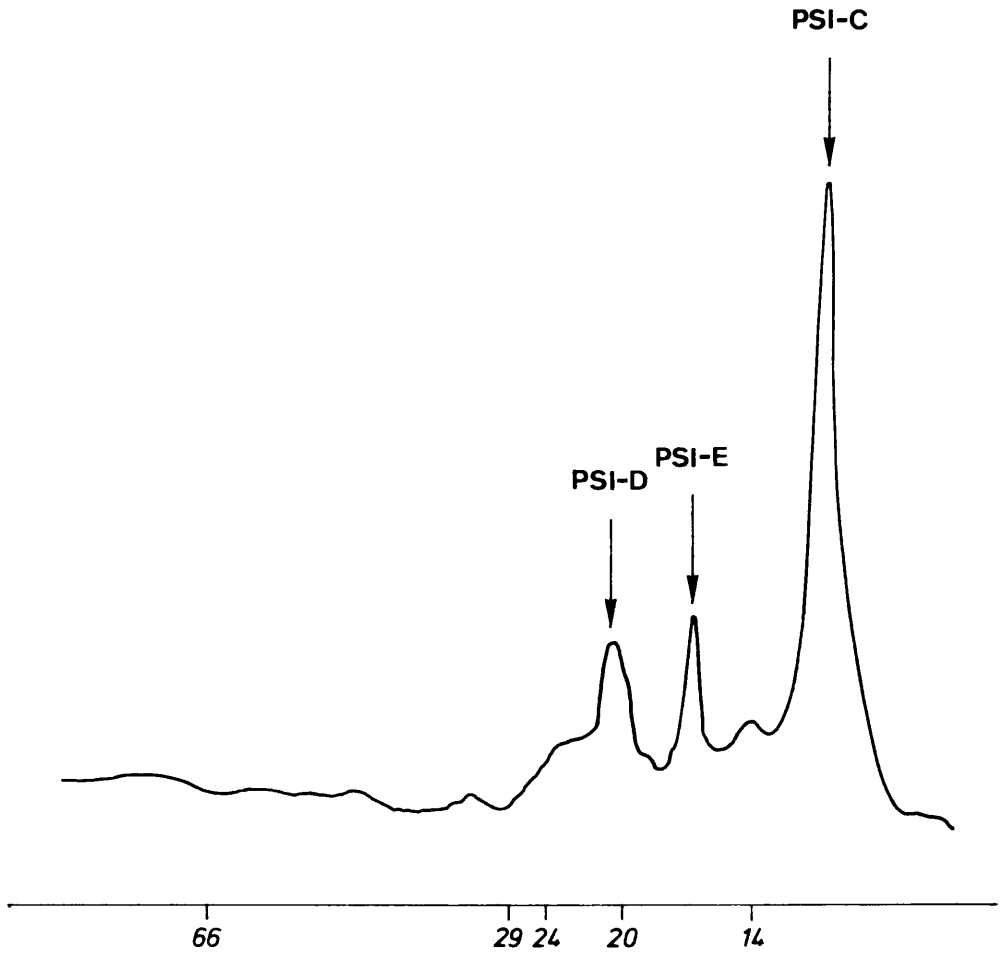

Figure 3.17

Polypeptide Composition of Preparation 2 (S-200 HR) Fraction 2.

Laser densitometric trace of the polypeptides contained in the second fraction eluted from the S-200 HR gel filtration column. The column was run by the method in section 2.3. The eluted material was concentrated over an Amicon YM2 membrane under Argon.

SDS-PAGE polypeptide separation was performed with an 8-25% polyacrylamide gradient using the Pharmacia PhastGel system.

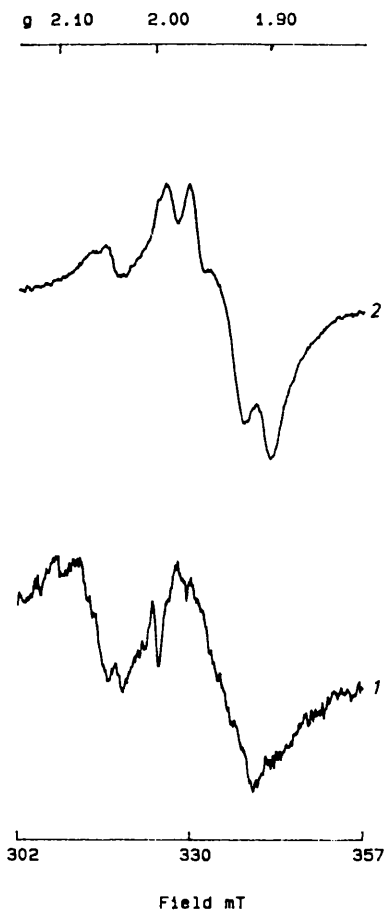

Figure 3.18

The EPR Spectra of Fractions 1 and 2 Eluted from the Sephacryl S-200 HR Column.

The protein material in 20mM Tris-HCl pH 8.0, 5mM Dithiothreitol and 100mM NaCl was reduced with 0.2% sodium dithionite pH 9.0 for 5 minutes. before freezing under liquid nitrogen.

1.) Fraction 1.

2.) Fraction 2.

EPR conditions: microwave power 10 mW., temperature 15K, modulation width 1 mT. instrument gain 250.

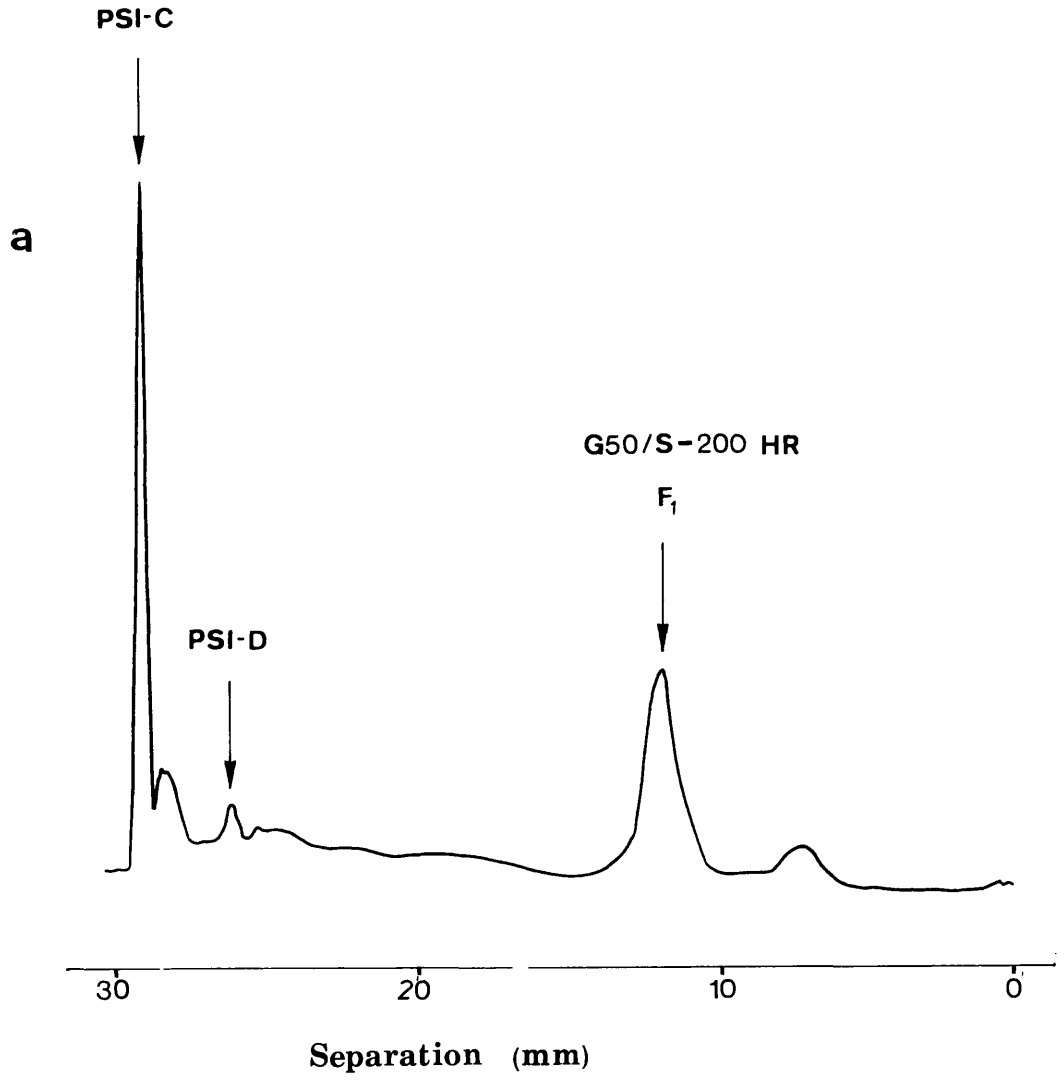

Figure 3.19

a.) Native-PAGE Analysis of *n*-butanol Extracted Material.

Laser densitometric trace of the polypeptides released from the Triton X-100 isolated photosystem-I by butanol extraction (Method section 2.3). The released proteins were concentrated over an Amicon YM2 membrane under Argon. Polypeptide separation was performed by native-PAGE using the Pharmacia PhastGel system.

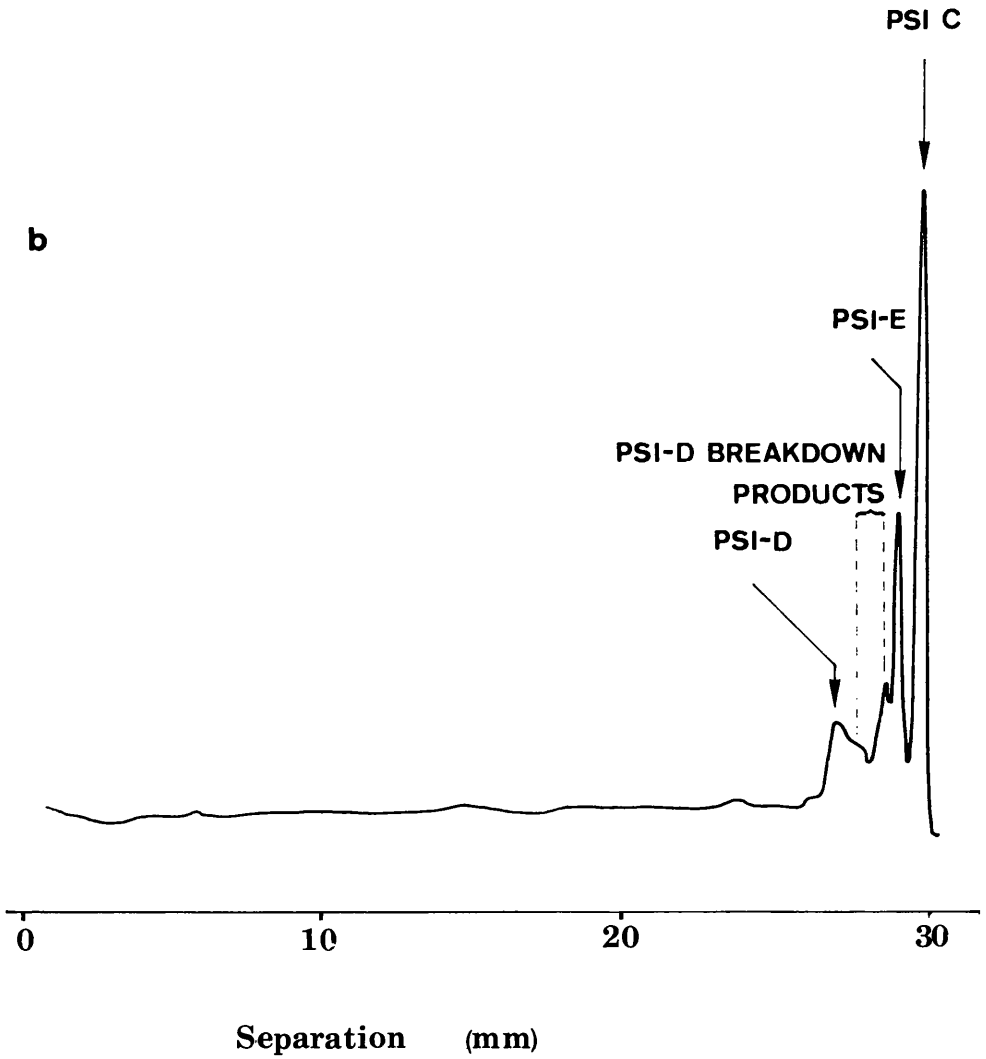

Figure 3.19

b.) Native-PAGE Analysis of *n*-butanol Extracted Polypeptides Treated with 7 M Urea.

Laser densitometric trace of the polypeptides released from the Triton X-100 isolated photosystem-I by butanol extraction (Method section 2.3). The released proteins were concentrated over an Amicon YM2 membrane under Argon then incubate in 7M urea for 30 minutes at room temperature. Polypeptide separation was performed by native-PAGE using the Pharmacia PhastGel system.

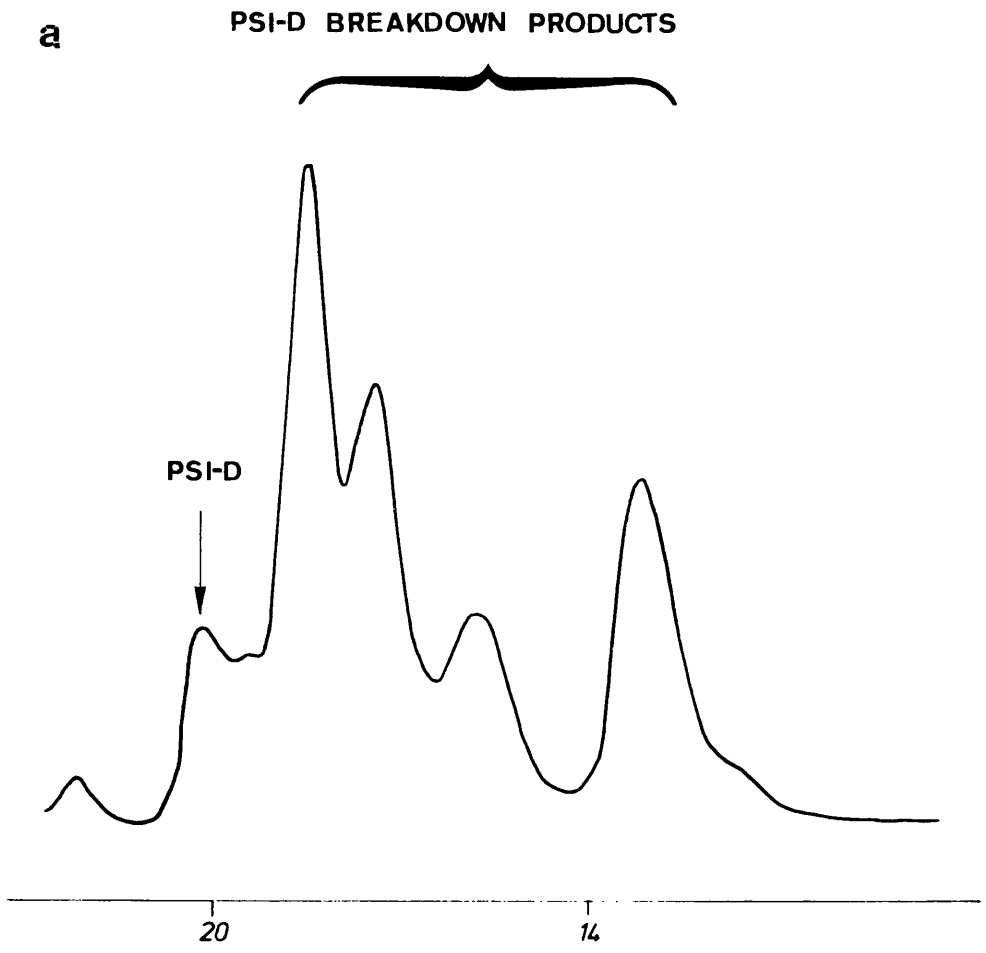

Figure 3.20

a.) Western Blot Analysis of *n*-butanol Extracted Polypeptides Treated with 7 M Urea Labelled With Antibodies Raised Against PSI-D.

The *n*-butanol extracted material was treated with a range of Urea concentrations in order to disperse the constituent polypeptides of fraction 1 and increase the yield of proteins following gel filtration. After 7M urea treatment the polypeptides were size fractionated on a Sephacryl S-200 HR. The resultant fraction 2 resolved by 15% SDS-PAGE (method section 2.7) and labelled with antibodies raised against PSI-D (methods section 2.8).

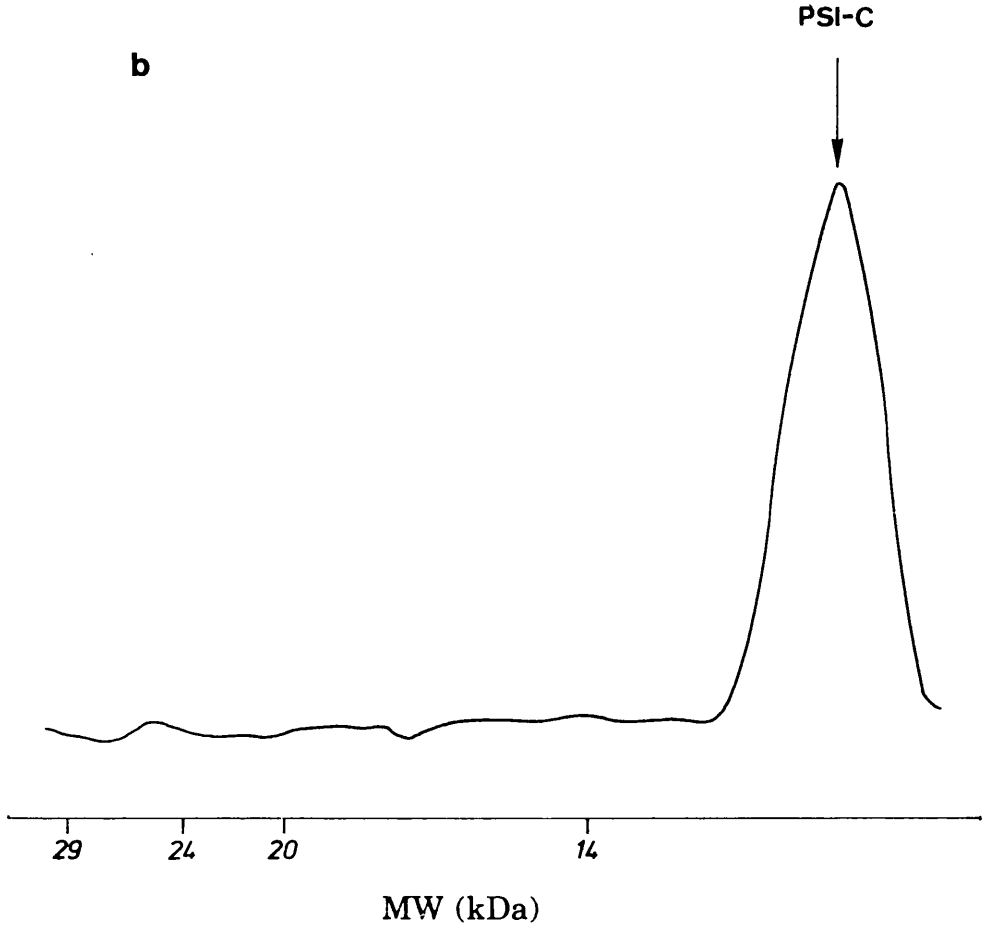

Figure 3.20

b.) Western Blot Analysis of *n*-butanol Extracted Polypeptides Treated with 7 M Urea Labelled With Antibodies Raised Against PSI-C.

The *n*-butanol extracted material was treated with a range of Urea concentrations in order to disperse the constituent polypeptides of fraction 1 and increase the yield of proteins following gel filtration. After 7M urea treatment the polypeptides were size fractionated on a Sephacryl S-200 HR. The resultant fraction 2 resolved by 15% SDS-PAGE (method section 2.7) and labelled with antibodies raised against PSI-C (methods section 2.8).

1 polypeptides (fig. 3.19_{ab}). However, a repeat of these experimental conditions using pre-equilibrated gel filtration columns to isolate individual fraction 1 polypeptides did not significantly disperse fraction 1 or increase the yield of PSI-C, D or E. In fact, the resulting low molecular weight fraction (gel filtration fraction 2) was greatly depleted in the band attributed to PSI-D with concomitant increase in the number of lower molecular weight bands. Western blot analysis revealed that the disappearance of PSI-D was caused by the same protein degradation observed in the YM100 filtrate following urea treatment of photosystem-I (fig. 3.20_a). Despite the loss of proteins in fraction I it was decided to carry out a rapid isolation and purification of stromally orientated polypeptides from fraction 2 in an attempt to avoid PSI-D degradation.

Sephadex G 50 Gel Filtration (Preparation 3)

Sephadex G 50 gel filtration was utilised to gain a greater resolution in order to separate the lower molecular weight polypeptides. A Sephadex G 50 gel filtration column (100 cm X 1.6 mm) was degassed and equilibrated with Tris-HCl, 5mM dithiothreitol, 100mM NaCl pH 8.1. It was loaded with concentrated *n*-butanol extract and developed over a 24-48 hour period. The polypeptides eluted in 4 fractions as measured by 280 nm absorbance (fig. 3.21). The peak of each fraction was collected under argon and stored in liquid nitrogen. The polypeptide content of each fraction was assayed by low temperature EPR spectroscopy, western blot analysis and SDS-polyacrylamide gel electrophoresis:

Fraction 1 contained a mass of polypeptides from 8 kDa to 63 kDa. It had EPR and antibody binding properties identical to S-200 HR fraction 1.

Fraction 2 contained a mixture of PSI-E and PSI-D .

Fraction 3 contained a mixture of PSI-E and PSI-C.

Fraction 4 contained solely the 9 kDa gene product of *psa*C previously identified as the protein binding iron-sulphur centres A and B (Wynn and Malkin, 1988_a).

Figure 3.22 shows the densitometric scan of the G 50 fractions resolved by 8-25% SDS-PAGE. The peak containing PSI-E ran at a higher molecular weight thanexpected, this may be the result of dimer formation. The EPR spectra of the highly purified PSI-C holoprotein (contained in G 50 fraction 4) reduced by addition of 0.2% (w/v) dithionite is shown in fig. 3.23. It has g values at 1.90, 1.92, 1.95, 1.98, 2.00, 2.06 and 2.07 and is 28.5 mT wide. The spectrum is somewhat broader than that observed for Fe-$S_{A/B}$ in native photosystem-I. Broadening of the spectra in this manner may be a result of extraction into an artificial environment or an increase in flexibility of the free holoprotein. Such an increase in flexibility could result in variation of the orientation or distance between iron-sulphur centre A and iron-sulphur centre B thereby altering the interactive EPR spectrum. The spectral characteristics indicated that the isolated protein was a 2 X [4Fe-4S] ferredoxin and the absorbance spectrum (fig. 3.24) is typical of a bacterial ferredoxin. This is consistent with the identification of the purified 9 kDa polypeptide as the protein housing Fe-$S_{A/B}$ (Wynn and Malkin, 1988_a; Oh-oka *et al.*, 1987).

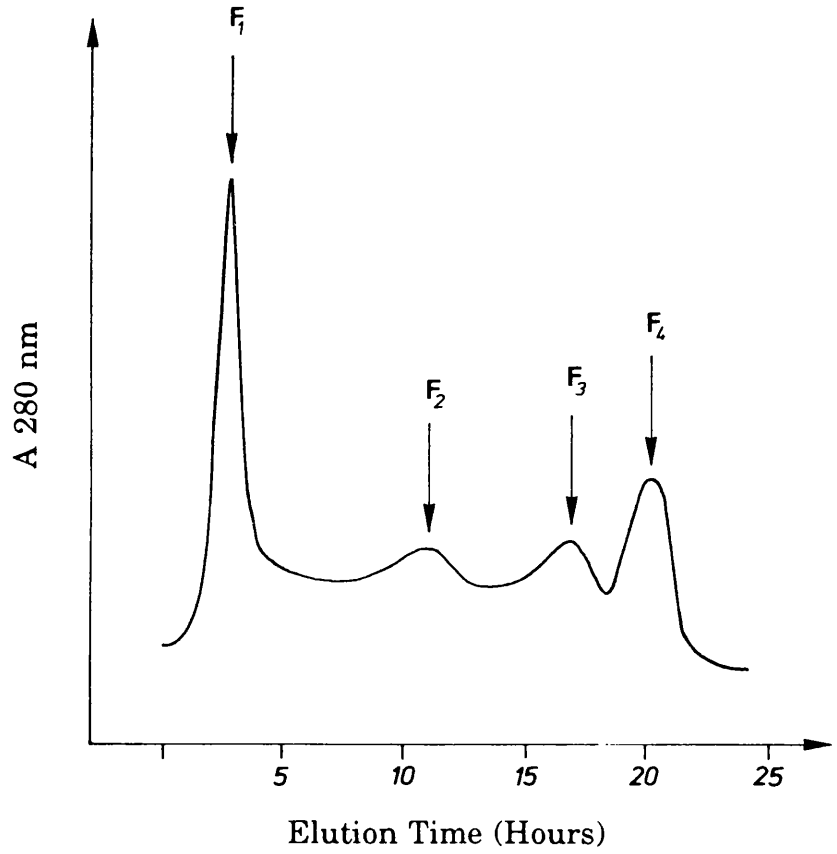

Figure 3.21

Elution Profile of Butanol Extracted Material Passed Through a Sephadex G 50 Gel Filtration Column.

The butanol extracted material was concentrated over an Amicon YM2 membrane under Argon then size fractionated by passage through a 2.2 X 100 cm G 50 gel filtration column in 20mM Tris-HCl pH 8.0, 5mM Dithiothreitol and 100mM NaCl and eluted over a 24-48 hour time period (methods section 2.3). Eluted material was monitored using a 280 nm single path U.V. monitor.

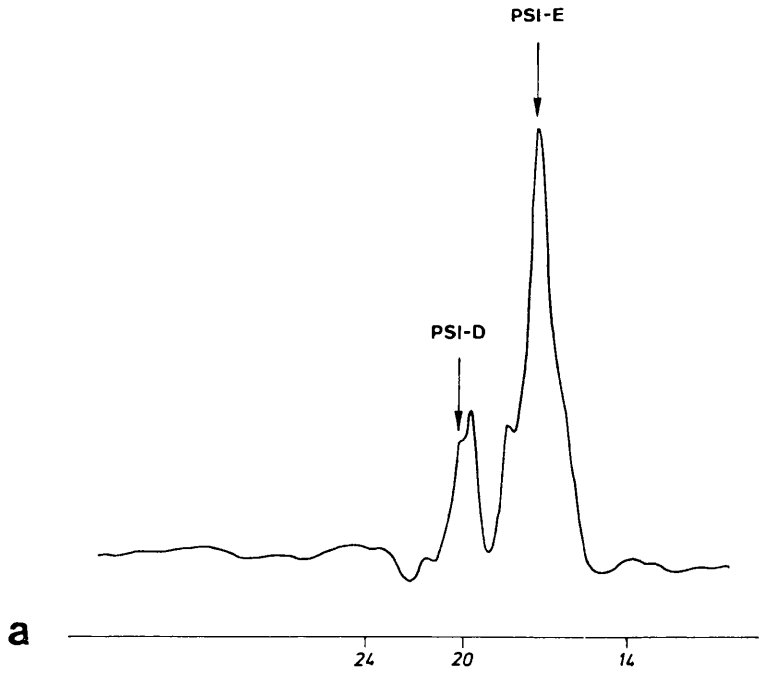

Figure 3.22

Polypeptide Composition of Preparation 3 (Sephadex G 50) Fractions.

Laser densitometric trace of the polypeptides contained in the each of the fractions eluted from the G 50 gel filtration column. The columns were run by the method in section 2.3. The eluted material was concentrated over an Amicon YM2 membrane under Argon.

SDS-PAGE polypeptide separation was performed with an 8-25% polyacrylamide gradient using the Pharmacia PhastGel system.

a.) Fraction 2
b.) Fraction 3
c.) Fraction 4

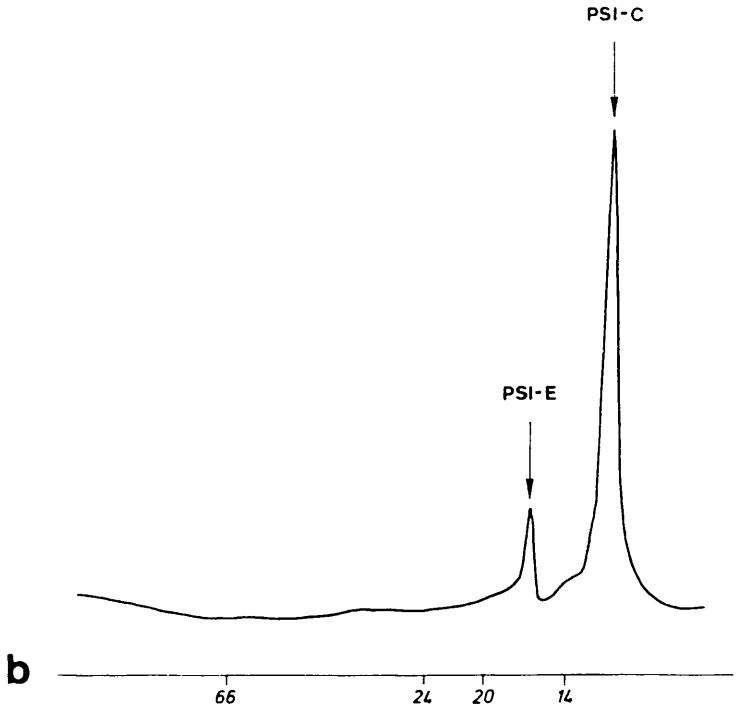
PSI-C
PSI-E
b
66
24
20
14
MW (kDa)

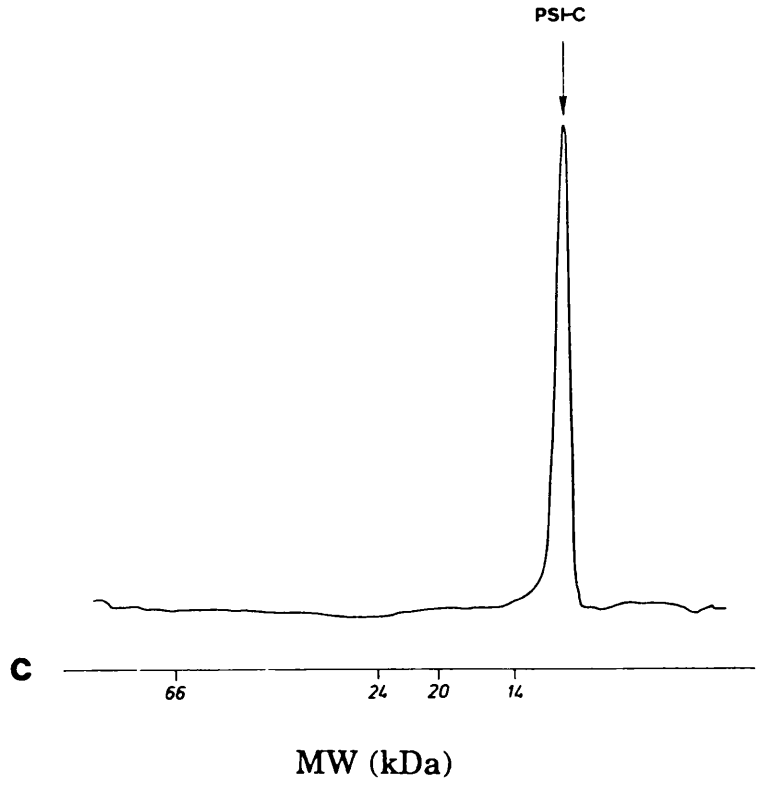
PSI-C
c
66
24
20
14
MW (kDa)

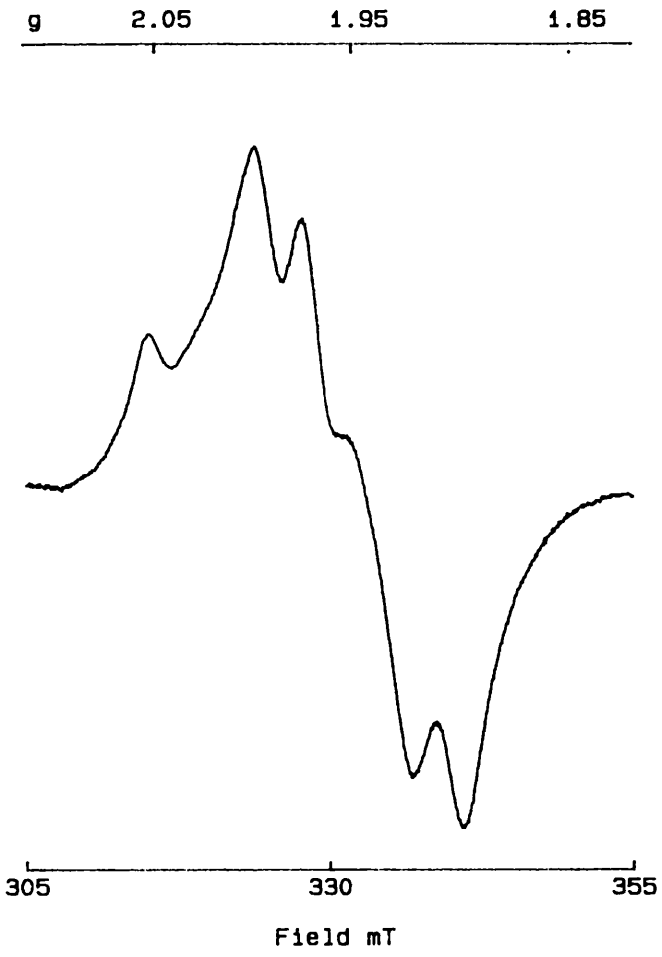

Figure 3.23

The EPR Spectrum of the Isolated Fe-$S_{A/B}$ Holoprotein.

The protein, in 20mM Tris-HCl pH 8.0, 5mM Dithiothreitol and 0.1 M NaCl, was reduced with 0.2% sodium dithionite pH 9.0 for 5 minutes before freezing.

EPR conditions: microwave power 10 mW., temperature 15K, modulation width 1 mT. instrument gain 250.

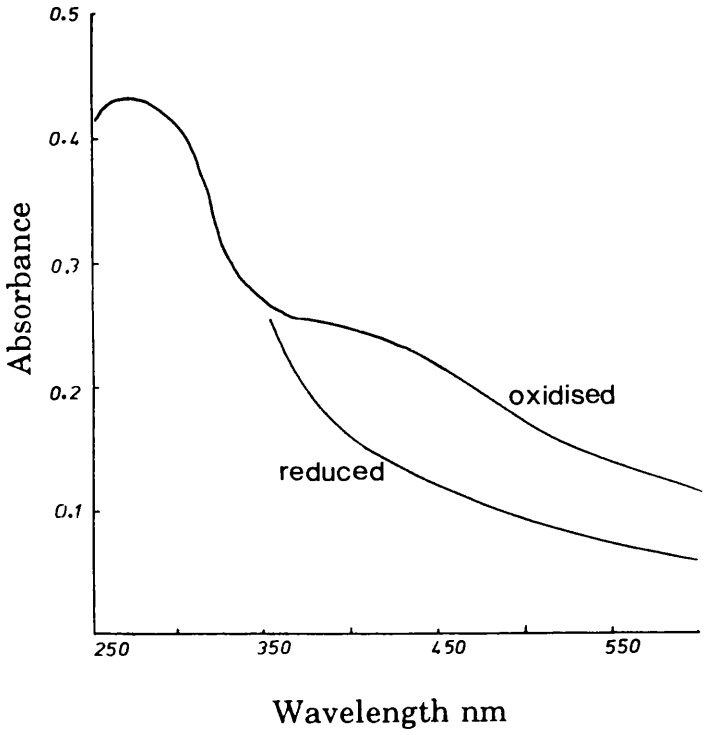

Figure 3.24
Absorption Spectra of the Purified G 50 Fe-$S_{A/B}$ Protein.
The spectra were recorded at 25°C in a 1 cm path cuvette. The protein was reduced by the addition of 0.2% (w/v) sodium dithionite.

Oh-oka *et al.* (1991) have reported the redox potential of the centres to be -480 and -540mV, the two centres being distinguished by differences in temperature dependence of their EPR signals. Redox titrations on the preparation obtained by *n*-butanol extraction were carried in the presence of 25% glycerol to stabilise the iron-sulphur centres. In the absence of glycerol the samples rapidly lost their EPR signals and it was apparent that the centres were being oxidised. In these titrations a single wave was observed on the titration with Em≈-510 mV. There was no major effect of temperature on the relative signal sizes at different potentials and there was no evidence for different potentials for the two centres. Plotting the titration curve for different parts of the spectrum or at 10K or 40K did not affect the midpoint potential. The preparation essentially showed the properties of the higher potential component described by Oh-Oka *et al.* (1991). It has previously been shown that glycerol affects the properties of the Fe-$S_{A/B}$ centres *in situ* (Evans and Heathcote, 1980) so it may be that while stabilising the centres it changes the environment sufficiently to remove the differences reported by Oh-Oka *et al.* (1991). The results confirm that the low potential of the Fe-$S_{A/B}$ centres in the reaction centre are a property of the Fe-$S_{A/B}$ protein itself, but indicate that the characteristic EPR spectrum of the two centres *in vivo* is the result of binding to photosystem-I.

Further attempts to purify PSI-D and PSI-E, contained in G 50 fractions 2 and 3, to homogeneity resulted in the disappearance of the SDS-PAGE polypeptide band attributed to PSI-D and the appearance of 4-

5 additional bands. These bands were identified by western blot analysis as the breakdown products of PSI-D. It became obvious that the conditions utilised for the removal and purification of the extrinsic polypeptides predisposed them to degradation by a protease and any prolonged or multi-step isolation procedure resulted in the almost total break down of PSI-D. This type of protein degradation was also observed by Golbeck and his co-workers during reconstitution experiments. It occurs once PSI-D has been released from the photosystem-I reaction centre complex by either solvent or chaotrope extraction, but it is rapidly accelerated by the presence of denaturing quantities of urea. It was therefore decided to carry out the reconstitution experiments using fractions already gained from ion exchange and gel filtration chromatography in order to ascertain a function for the stromally oriented polypeptides.

3.4 Reconstitution of Photosystem-I

$P700^+$ Re-reduction Kinetics

The role of the Fe-$S_{A/B}$ protein in electron transport was investigated using photosystem-I core particles isolated from Digitonin photosystem-I. Similar reconstitution of the Fe-$S_{A/B}$ holoprotein to the core complex was obtained with Triton X-100 particles but the ability of each of the control Triton preparations to photo-reduce $NADP^+$ was inconsistent. Such inconsistency was probably a result of the removal of varying amounts of the plastocyanin docking protein PSI-F by Triton X-100 during isolation and purification thereby limiting the rate of P700 turnover.

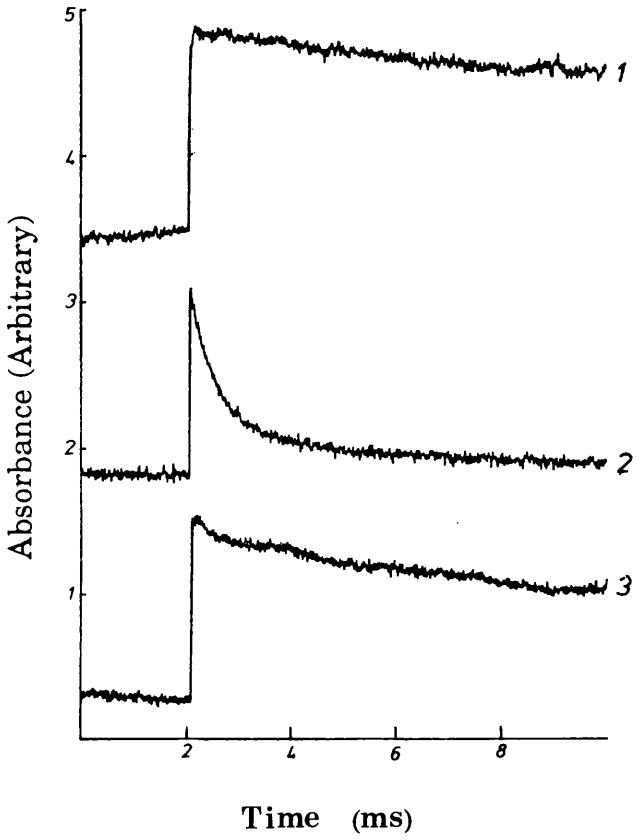

Figure 3.25

Re-reduction Kinetics of $P700^+$ following oxidation by laser flash illumination.

1) Digitonin photosystem-I particles.

2) Digitonin photosystem-I particles following urea treatment to remove Fe-$S_{A/B}$ as described in section 2.1.5.

3) Urea treated Digitonin particles reconstituted with Fe-$S_{A/B}$ preparations described in materials and methods section 2.4.

The reaction mixture contained: photosystem-I particles 25µg chlorophyll/ml in 20mM Tricine-KOH pH 8.0, 6.7mM sodium ascorbate and 68 µM dichlorophenolindophenol. 30 repetitions were averaged at 0.5 Hz flash repetition rate.

Golbeck and his co-workers have also reported that Triton X-100 damages redox centre A_1 after removal of Fe-S_X but in the work reported here incubation of urea treated Triton photosystem-I particles with 1% Triton X-100 for 1 hour at room temperature did not affect the 200K photo-accumulation of the A_1^- EPR signal.

Reconstitution of the Fe-$S_{A/B}$ containing fractions onto the photosystem-I core complex was initially monitored by measurement of the re-reduction of $P700^+$ by back reaction from the electron acceptors following laser flash illumination. Incubation of the isolated photosystem-I core complex with either the highly purified PSI-C holoprotein or any of the polypeptide fractions containing the free Fe-$S_{A/B}$ holoprotein (ion exchange, S-200 HR fraction 2 and G 50 fraction 3) resulted in a recovery of the $P700^+$ re-reduction kinetics from 1 ms to approximately 19.0 ms (fig. 3.25). This value is not significantly shorter than the observed control value of 20 ms. The slight difference in kinetics between control and reconstituted samples is probably indicative of destruction of a small proportion of iron-sulphur centre X and polypeptide damage at the acceptor side of PSI-A and PSI-B preventing PSI-C rebinding. Both of these factors would contribute to a fast phase of $P700^+$ re-reduction.

The majority of the Fe-$S_{A/B}$ holoprotein rebound to the core complex within a few seconds and reconstitution was complete after 10 minutes. Prolonged incubation of the core photosystem-I and the isolated Fe-$S_{A/B}$ for up to 3 hours under reducing conditions at room temperature under argon did not improve the kinetics beyond that observed after 10 minutes.

Incubation of the photosystem-I core complex with the highly purified Fe-$S_{A/B}$ (G 50 fraction 4), in the absence of all other stromal polypeptides, did not alter the time period of reconstitution or affect the recovered $P700^+$ re-reduction kinetics as compared to photosystem-I reconstituted with a full complement of stromally oriented polypeptides.

No reconstitution was observed using the n-butanol extracted material without further purification, this was probably a result of the presence of *n*-butanol in the unrefined extract. There was also no recovery of native $P700^+$ back reaction kinetics in samples which had the Fe-$S_{A/B}$ centres denatured by bubbling with oxygen.

Although gel filtration fraction 1 had both antibody binding and EPR characteristics of the PSI-C holoprotein it also did not recover native $P700^+$ re-reduction kinetics.

Table 3.1 gives a detailed account of the effect of reconstitution with each fraction on the recovery of $P700^+$ re-reduction kinetics.

EPR Analysis of Reconstituted photosystem-I.

Recovery of the photo-induced Fe-$S_{A}^{-}{}_{B}^{-}$ EPR spectra was only achieved by reconstitution with the ion exchange preparation (Preparation 1) and the Sephacryl S-200 HR preparation fraction 2 both of which contained polypeptides PSI-C, D and E.

Low temperature illumination demonstrated that photo-oxidation of P700 was again coupled to Fe-S_A reduction. The signal size of Fe-S_A was restored to about 80% of that observed in the starting material (fig. 3.26).

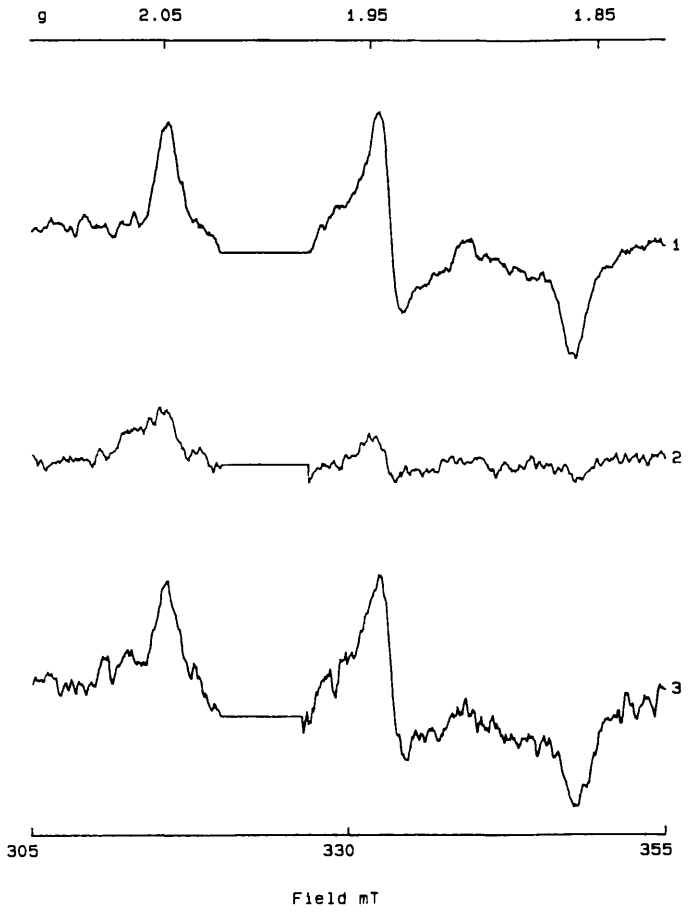

Figure 3.26

Fe-S_A^- EPR Spectra of Control, Urea Treated and Reconstituted Digitonin Photosystem-I Particles.

Light minus dark EPR difference spectra of Fe-S_A. Samples were reduced with 30mM sodium ascorbate, frozen in the dark and illuminated at 15K in the EPR cavity.

1) Control samples of Digitonin photosystem-I particles before treatment.
2) Urea treated particles with the Fe-$S_{A/B}$ holoprotein removed.
3) Urea treated particles after reconstitution with the Fe-$S_{A/B}$ protein preparations.

Each sample contained 500µg/chlorophyll/ml. Urea treatment and reconstitution are described in materials and methods sections 2.1.5 and 2.5 respectively. EPR conditions: Microwave power 10 mW, temperature 15K, modulation width 1.25 mT, Instrument gain 500. The g = 2.00 region of the spectra has been deleted for clarity.

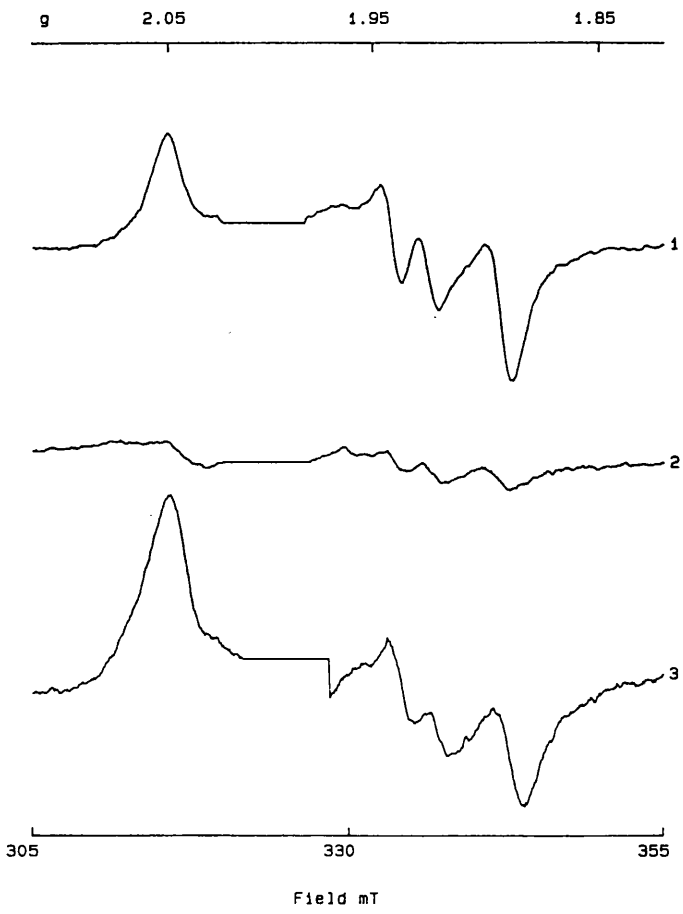

Figure 3.27

Fe-$S_{A}^{\cdot}{}_{B}$ EPR Spectra of Control, Urea Treated and Reconstituted Digitonin Photosystem-I Particles.

Light minus dark EPR difference spectra of Fe-$S_{A/B}$. Samples were reduced with 30mM sodium ascorbate, illuminated at room temperature and frozen under illumination.

1) Control samples of Digitonin photosystem-I particles before treatment.
2) Urea treated particles with the Fe-$S_{A/B}$ protein removed.
3) Urea treated particles after reconstitution with the Fe-$S_{A/B}$ protein preparations.

Each sample contained 500µg/chlorophyll/ml. Urea treatment and reconstitution are described in materials and methods sections 2.1.5 and 2.4 respectively. EPR conditions: Microwave power 10 mW, temperature 15K, modulation width 1.25 mT, Instrument gain 500. The g = 2.00 region of the spectra has been deleted for clarity.

Room temperature illumination and freezing under illumination resulted in the photo-reduction of Fe-S_A and Fe-S_B demonstrating that Fe-S_B had also recovered. The signal size of the Fe-$S_A^-B^-$ spectra also indicated an 80% recovery (fig. 3.27). The g values, line shape and line width of the reconstituted photo-induced Fe-$S_{A/B}$ EPR spectra were identical to those of the control photosystem-I. This indicated that PSI-C and the core photosystem-I had reconstituted to a native configuration.

Rebinding of the highly purified Fe-$S_{A/B}$ to the core complex, demonstrated by the recovery of the room temperature $P700^+$ re-reduction kinetics, did not result in the recovery of the EPR signals attributed to either Fe-S_A or Fe-S_B.

Attempted reconstitution with the high molecular weight multi-protein fraction 1 from gel filtration isolation preparations 2 or 3 did not result in the recovery of the photo-induced EPR spectra for iron-sulphur centre A or B.

3.4.1 The Role of the Fe-$S_{A/B}$ Holoprotein in $NADP^+$ Reduction by Photosystem-I

$NADP^+$ reduction by washed spinach thylakoids required the addition of soluble 2Fe-2S ferredoxin, all other protein components being bound to the stromal side of the thylakoid. After isolation of photosystem-I by Digitonin additions of plastocyanin and soluble FNR were required in addition to ferredoxin. The Digitonin preparation contains an SDS-PAGE band indicative of the presence of bound FNR (see section 3.1.1). The

requirement for exogenous FNR indicated damage to the bound enzyme during Digitonin isolation or its partial removal resulting in less than stoichiometric amounts.

Urea treatment of Digitonin particles resulted in almost complete loss of $NADP^+$ photo-reduction activity (Table 3.2). The residual activity was about 5% which was rather lower than the residual 10-15% Fe-$S_{A/B}$ photo-reduction observed by EPR. The difference in activity between $NADP^+$ and Fe-$S_{A/B}$ photo-reduction is indicative of damage to the residual extrinsic stromal polypeptides remaining bound to the core complex after urea treatment. This protein damage results in a loss of ability to bind the soluble stromal polypeptides required to allow $NADP^+$ reduction but does not affect the residual Fe-$S_{A/B}$ photo-reduction observed by low temperature EPR.

Recovery of $NADP^+$ photo-reduction activity was achieved by incubation of either Fe-$S_{A/B}$ protein preparation 1 (ion exchange) or preparation 2 (S-200 HR, Fraction 2) with the isolated core particle photosystem-I (fig. 3.28). Incubation of both G 50 fraction 2 (PSI-D and PSI-E) and fraction 3 (PSI-C and PSI-E) together with the core complex also resulted in some recovery of $NADP^+$ photoreduction but it was never greater than 20-25% that observed with preparations 1 or 2.

The highly purified Fe-$S_{A/B}$ holoprotein, which reconstituted $P700^+$ re-reduction kinetics, did not result in recovery $NADP^+$ photo-reduction (Table 3.1).

Fraction	Recovery of $P700^+$ re-reduction kinetics	Recovery of control Fe-S_{A}^{-} $_{B}^{-}$ EPR signals	Recovery of control $NADP^+$ photoreduction rate
n-butanol extract	-	-	-
DEAE purified	+	+	+
S-200 HR F1	-	-	-
S-200 HR F2 (PSI-C,D and E)	+	+	+
G 50 F1	-	-	_
G 50 F2 (PSI-D and E)	-	-	-
G 50 F3 (PSI-C and E)	+	_	-
G 50 F3 (PSI-C)	+	-	-
G 50 F4 + F2(PSI-C,D and E)	+	+/-	+/-

Table 3.1

The Effect of Incubation of the Core Complex with Each of the Polypeptide Fractions Isolated by the Methods Outlined in Section 2.3.

+ Full reconstitution
- No reconstitution
+/- Partial reconstitution

Sample Type	Rate of NADP+ Reduction µmoles/mg chlorophyll/h
Native photosystem-I	718
Urea treated photosystem-I	28
Urea treated Photosystem-I reconstituted with Fe-$S_{A/B}$ plus PSI-E and PSI-D	673
Urea treated Photosystem-I reconstituted with oxidised Fe-$S_{A/B}$ plus PSI-E and PSI-D	30
Reconstituted photosystem-I minus ferredoxin	0
Reconstituted photosystem-I minus ferredoxin and ferredoxin-NADP oxidoreductase	0

Table 3.2

$NADP^+$ Reduction by Digitonin Photosystem-I Particles.

NADP+ photo-reduction was followed by measuring the change in OD340 at 30 second intervals following illumination by saturating white light. The reaction mixture contained 25mM Tricine-KOH pH 7.8, 6.7mM Sodium Ascorbate, 68 µM dichlorophenolindophenol, 0.07% Triton X-100 X-100, 0.1% 2-mercaptoethanol, Digitonin photosystem-I particles 10µg chlorophyll/ml., 1.5 µM plastocyanin, 5 µM ferredoxin, 0.5mM NADP+, ferredoxin-NADP+ oxidoreductase and Fe-$S_{A/B}$ protein in excess.

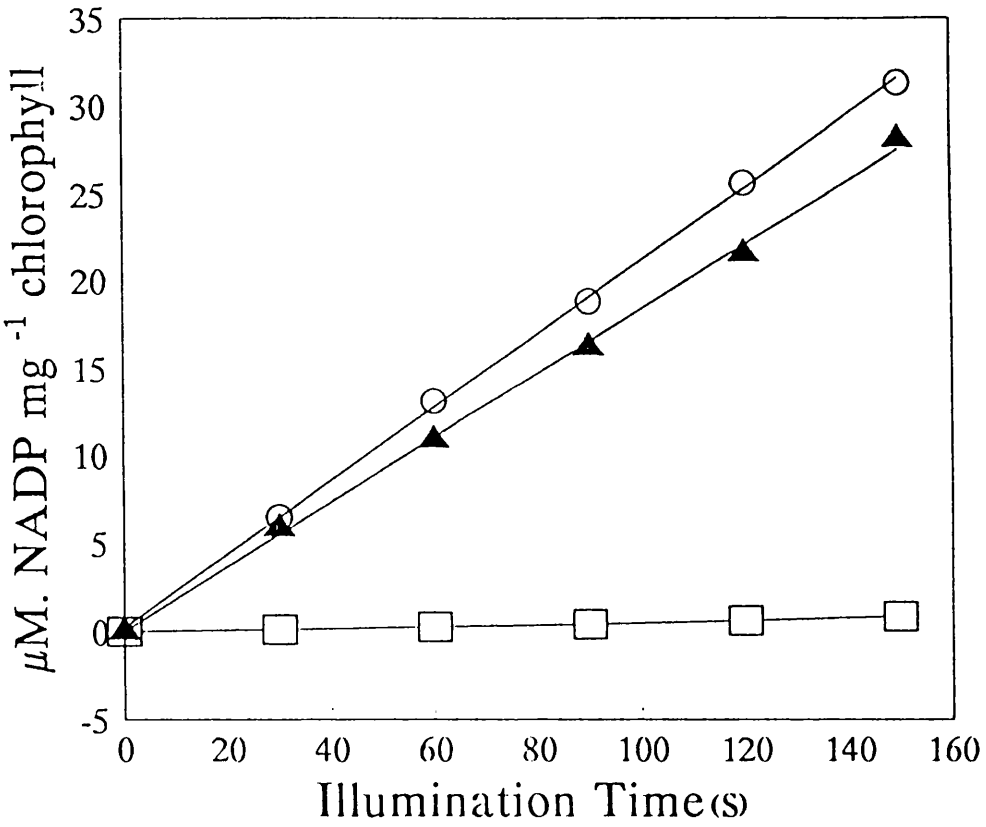

o Control

▲ Reconstituted

□ Urea treated

Figure 3.28

NADP⁺ Reduction by Digitonin Photosystem-I Particles.

NADP+ reduction was followed by measuring the change in OD340 at 30 second intervals following illumination by saturating white light. The reaction mixture contained 25mM Tricine-KOH pH 7.8, 6.7mM Sodium Ascorbate, 68 µM dichlorophenolindophenol, 0.07% Triton X-100, 0.1% 2-mercaptoethanol, Digitonin photosystem-I particles (10µg chlorophyll/ml.), 1.5 µM plastocyanin, 5 µM ferredoxin, 0.5mM NADP+, ferredoxin-NADP+ oxidoreductase and Fe-$S_{A/B}$ protein preparations in excess.

Attempted reconstitution using the high molecular weight multi-protein unit from preparations 2 and 3 did not result in the reconstitution of room temperature $NADP^+$ photo-reduction.

These results indicate that a minimum of the $Fe\text{-}S_{A/B}$ holoprotein in conjunction with PSI-D and probably PSI-E is required to interact with soluble intermediates in order to bring about reduction of $NADP^+$. Following reconstitution the $NADP^+$ reduction activity was restored to about 90% of the control value, a similar recovery to that observed for the $Fe\text{-}S_{A/B}$ by EPR (fig. 3.28).

Reconstitution experiments were also attempted using photosystem-I core particles depleted of $Fe\text{-}S_X$. There was no reconstitution of the $P700^+/Fe\text{-}S_{(A/B)}^-$ back reaction kinetics or retrieval of $NADP^+$ photo-reduction activity. Concentration of the sample over an Amicon YM100 ultra filtration membrane followed by gel electrophoresis indicated that PSI-C had not rebound. This demonstrates that removal of $Fe\text{-}S_X$ alters the structure of the core complex acceptor side thereby preventing $Fe\text{-}S_{A/B}$ holoprotein binding.

The destruction of the iron-sulphur centres A and B by exposing them to oxygen prevents $NADP^+$ photo-reduction in the presence of PSI-D and PSI-E confirming that the $Fe\text{-}S_{A/B}$ centres are essential for forward electron transfer.

An attempt was made to recover $NADP^+$ reduction activity in the core particle using purified $Fe\text{-}S_{A/B}$ protein from spinach and PSI-D from cyanobacteria but there was no evidence that cyanobacterial PSI-D would

aid reconstitution of $NADP^+$ photo-reduction in the spinach photosystem-I core complex. This indicated that:

1.) Cyanobacterial PSI-D would not facilitate the stable reconstitution of spinach holoprotein.

2.) The acceptor side of photosystem-I requires more than PSI-D and PSI-C in order to bind ferredoxin and FNR.

3.) Cyanobacterial PSI-D will not interact with ferredoxin or FNR from spinach.

Attempted concentration of samples reconstituted with purified Fe-$S_{A/B}$ and cyanobacterial PSI-D by either centrifugation or Amicon YM100 ultra filtration resulted in a return to the 1 ms back reaction kinetics and the inability to raise the photo-reduced Fe-$S_{A/B}$ EPR spectra at cryogenic or room temperatures. This showed that cyanobacterial PSI-D was ineffectual in stabilisation of rebound spinach PSI-C.

Table 3.1 summarises the effect of reconstitution with each of the protein fractions on $P700^+$ re-reduction kinetics, photo-reduced iron-sulphur centre EPR spectra and $NADP^+$ photo-reduction.

3.5 Discussion

This work confirms the findings of Golbeck and his co-workers demonstrating that the presence of Fe-$S_{A/B}$ are essential for:

1.) 20 ms $P700^+$ re-reduction kinetics similar to those observed in control photosystem-I samples.

2.) Iron-sulphur centre photo-reduction observed by low temperature EPR.

Golbeck and his co-workers also demonstrated that whilst the purified Fe-$S_{A/B}$ holoprotein will rebind to the core complex and restore native $P700^+$ back reaction kinetics PSI-D is essential for stabilisation and correct orientation of the rebound protein.

In the results presented here rebinding of the iron-sulphur protein (PSI-C) to the core complex in the absence of PSI-E and/or PSI-D made no difference to the recovered $P700^+/Fe\text{-}S_{A/B}^-$ back reaction kinetics or the time period of total reconstitution which remained at 10 minutes. However, reconstitution using the Fe-$S_{A/B}$ holoprotein, or the Fe-$S_{A/B}$ holoprotein in conjunction with PSI-E, did not result in recovery of $NADP^+$ photo-reduction. Any attempt to concentrate a sample reconstituted with the pure Fe-$S_{A/B}$ by either centrifugation or Amicon YM100 ultra filtration resulted in a return to the 1 ms back reaction kinetics and the inability to raise the photo-reduced Fe-$S_{A/B}$ EPR spectra at cryogenic or room

temperature. These findings imply that once rebound PSI-C is stabilised by PSI-D (and possibly PSI-E) although neither facilitate the rate of Fe-$S_{A/B}$ rebinding or affect the back reaction between Fe-$S_{(A/B)}$- and $P700^+$.

In addition to the structural role for PSI-D (and possibly PSI-E) the inability of both Fe-$S_{A/B}$ and Fe-$S_{A/B}$ in conjunction with PSI-E to reconstitute $NADP^+$ reduction demonstrates that PSI-D, or PSI-D in conjunction with PSI-E, is also required in order to interact with the soluble stromal side polypeptides which mediate the flow of electrons from Fe-$S_{A/B}$ to $NADP^+$. Reconstitution experiments using polypeptides purified over a long period of time showed only partial recovery of $NADP^+$ photoreduction. This is probably indicative of polypeptide degradation.

The inability to recover $NADP^+$ photo-reduction using the PSI-C holoprotein devoid of iron-sulphur centres in conjunction with PSI-D and PSI-E confirms the necessity of the presence of iron sulphur centres A and B in forward electron transfer. Inoue *et al.* (1992) also demonstrated that, in the absence of Fe-S_B, Fe-S_A alone was unable to facilitate photo-reduction of $NADP^+$.

The work presented here does not allow designation of a specific role for PSI-D and PSI-E in FNR and ferredoxin binding or suggest a mechanism of mediation of electron flow to $NADP^+$. It does indicate, however, they are required to interact with soluble intermediates. Antibody labelling studies and cross linking experiments suggested the PSI-D was probably involved in ferredoxin binding and PSI-E FNR binding (Andersen *et al.*, 1991_{ab}; Zanetti and Merati, 1987)). However, more recent

data suggests that PSI-E may also promote interactions between the terminal bound iron-sulphur centres and soluble ferredoxin (Sonoike *et al.*, 1993; Sétif pers. comm.). These findings are difficult to reconcile with the work of Chitnis *et al.* (1989) who found control growth rates in *Synechoccus* sp. mutants depleted of PSI-E.

The roles of PSI-D and PSI-E are therefore not fully understood and further work is required before the functions of the peripheral acceptor side photosystem-I polypeptides can be assigned.

3.6 Intermediate Electron acceptors A_1 and A_0

The presence of two intermediate electron transport components acting between P700 and Fe-S_X was first suggested as a result of the observation of multiple back reaction times for the re-reduction of $P700^+$ following single turnover flash at room temperature. Bonnerjea and Evans (1982) and Gast *et al.* (1983) resolved two distinct components using low temperature EPR photo-accumulation techniques. The secondary electron acceptor, A_1, had a g value of 2.0051, a line width of 1.05 mT and was identified by its optical properties as a quinone. The primary electron acceptor, A_0, had a g value of 2.0024 and line width of 1.15 mT consistent with identification as a chlorophyll species. Solvent extraction demonstrated the presence of two molecules of phylloquinone per P700 although comparison of the A_0^- plus A_1^- photo-accumulated EPR signal to the maximum photo-accumulated $P700^+$ EPR signal indicated that only one molecule of A_0 and one molecule of A_1 is able to accept electrons in the photosystem-I reaction centre complex.

Although the EPR signal of A_0 is now generally accepted as an anionic chlorophyll monomer acting as the primary electron acceptor there is still controversy over the identity and function of A_1 (for discussion see section 1.5.3.).

Recently the weight of evidence has fallen in the favour of identification of A_1 as a quinone. Rustandi *et al.* (1990) have demonstrated that the electron spin polarised (ESP) EPR signal attributed to the $P700^+/A_1^-$ state is abolished on quinone extraction and narrowed on

exchange of the quinone with a deuterated quinone.

Sétif and Bottin showed that following illumination of photosystem-I particles in the presence of dithionite at pH 10 the $t_{½}$ 750 ns back reaction to $P700^+$, attributed to $P700^+/A_1^-$ back reaction, was replaced by the 25-30 ns back reaction from A_0^-. These kinetics were conserved even though some of the iron-sulphur centres had re-oxidised in the dark. Since the dark samples had no g = 2.00 EPR signal consistent with a quinone radical and the iron-sulphur centres had re-oxidised the authors concluded that the 25 ns kinetics had arisen as a result of quinone double reduction which created an obstacle to electron transfer past A_1. This work thus supported the identification of A_1 as a molecule of phylloquinone.

Recently Snyder *et al.* (1991) have also reported that preparations leading to double reduction of the quinone reversibly abolished the ESP EPR signal thereby supporting the findings of Sétif and Bottin.

The results discussed thus far do not however resolve the question of the origin of the photo-accumulated EPR signal at g = 2.0051 attributed to A_1 the identity of which has been recently called into question. In order to investigate this problem further the effect of conditions leading to quinone double reduction were examined with respect to the rise of the proposed A_1^- EPR signal by photo-accumulation.

3.6.1 The Effect of pH on g = 2.00 EPR Signals Attributed to A_1^- and A_0^-

Studies into the effect of ambient pH on photo-accumulation of A_0

and A_1 radicals were carried out on Digitonin photosystem-I prepared by the method in section 2.1.4. Digitonin particles were used as the orientation and EPR characteristics of their redox components most closely resemble those in the native membranes (Rutherford, 1990). In order to observe the photo-induced A_1^- EPR signal samples are usually prepared with dithionite and the pH adjusted to 10.0 in order to facilitate the dark reduction of iron-sulphur centres. However, it has been reported that such conditions can lead to the double reduction of the quinone molecule so, in order to avoid this, samples were prepared at pH 8.0 and dark adapted for 30 minutes.

Each of the samples prepared at pH 8.0 were compared to identical samples poised at pH 10.0. Figure 3.29 shows the EPR spectra of both sample types following a brief period of illumination at 205K in order to preferentially reduce A_1 (Mansfield and Evans, 1985,1886). At both pH 8.0 and 10.0 the g = 2.00 signal had the line width and g value previously attributed to A_1^- (Mansfield and Evans, 1988), although, in the pH 8.0 samples the g = 2.00 signal was 80% smaller than that at pH 10.0. The pH 8.0 sample also lacked the shoulder on the high field side of the peak which is observed at pH 10.0 after the same period of illumination (fig. 3.29). Samples were then illuminated for progressively longer periods at 230K in order to photo-reduce both A_1 and A_0. After 90 minutes illumination both samples had reached maximum signal size at g = 2.00 (fig. 3.30) and further illumination did not result in any further increase in signal size.

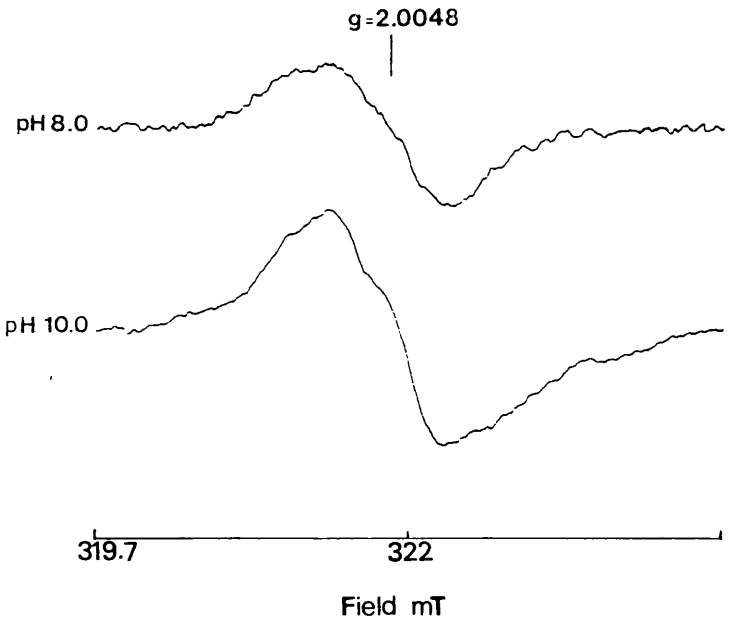

Figure 3.29

The EPR Spectra of A_1^- for Digitonin Particles.

The spectra were obtained by 205K illumination of Digitonin photosystem-I particles which had been previously incubated with 0.2% (w/v) sodium dithionite at pH 8.0 or pH 10.0 and frozen in the dark.

Samples, prepared as described in materials and methods sections 2.1.4 and 2.9.2, were illuminated for two minutes at 205K. Spectra are the average of two recordings.

EPR conditions: Microwave power 5 μW, modulation width 0.2 mT, recording temperature 75K.

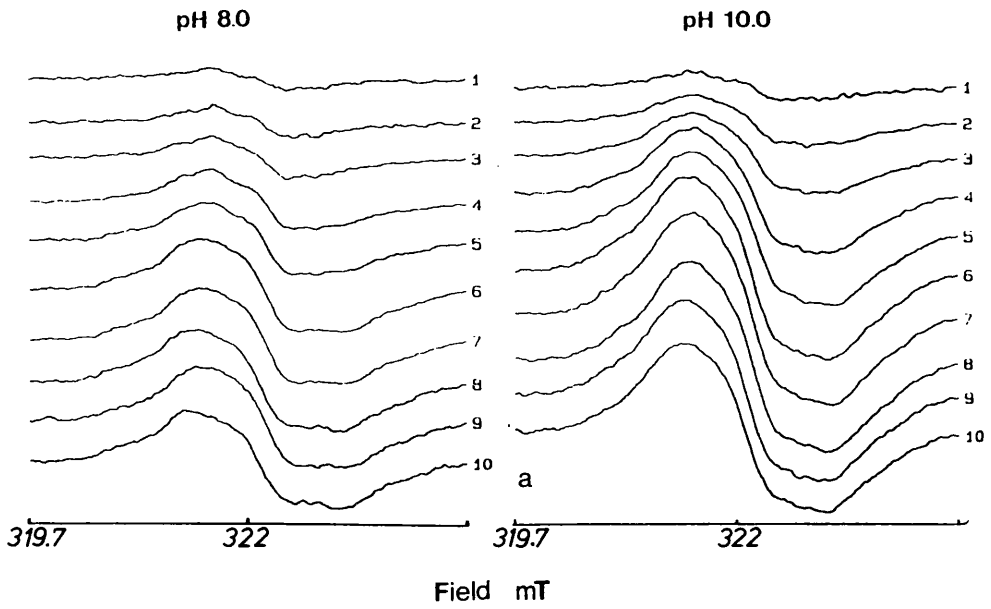

Figure 3.30

The EPR Spectra of A_0^- and A_1^- for Digitonin Particles.

The spectra were obtained by progressively longer periods of 230K illumination of Digitonin photosystem-I particles which had been previously incubated with 0.2% (w/v) sodium dithionite at pH 8.0 or pH 10.0 and frozen in the dark.

Samples, prepared as described in materials and methods sections 2.1.4 and 2.9.2, were illuminated at 230K for: 1)0.5 min, 2)1 min, 3)2 min, 4)5 min, 5)10 min, 6)30 min, 7)60 min, 8)90 min, 9)120 min and 10)180 min. At intervals during the illumination the samples were removed to the EPR spectrometer and the spectra recorded. Spectra are the average of two recordings.

EPR conditions: Microwave power 5 μW, modulation width 0.1 mT, recording temperature 75K.

Figure 3.30 shows that the pH 10.0 samples had considerably larger signals than those at pH 8.0 although both sets of signals had g values and line width consistent with identification of components A_1^- and A_0^-. The microwave power used was non saturating. Integration of the EPR spectrum gives the number of spin equivalents responsible for the EPR signal. Integration of the photo-induced g = 2.00 spectra at maximum size indicated that the pH 10.0 sample had approximately twice the number of spin equivalents (1.83) of its pH 8.0 counterpart (table 3.3).

To investigate this further the g = 2.00 EPR signal in a number of 230K photo-accumulated dithionite preparations, at pH 10.0 and pH 8.0, were compared to the g = 2.00 signal arising from a maximum $P700^+$ EPR spectra. Maximum P700 oxidation was achieved by illumination of samples at room temperature and freezing under illumination in the absence of a reductant. Samples prepared in this manner contained $P700^+$ in 100% of the photosystem-I reaction centres, since illumination at 15K did not generate any increase in the size of $P700^+$. Table 3.4 shows that the pH 10.0 samples contain approximately 4 spin equivalents per $P700^+$, 2 of which (one A_1^- and one A_0^-) accumulated within 5 minutes of 230K illumination (table 3.3), whereas the other two spins accumulated over the subsequent 55 minute period of illumination (Table 3.3). In contrast the pH 8.0 samples only accumulated two spin equivalents per $P700^+$ (table 3.4). This suggests that at pH 10.0 two sets of A_1 and A_0 can be photo-reduced whereas at pH 8.0 there is only a reduction of one set.

Cumulative period of 230K illumination (Min)	Spin intensity (arbitrary units)	
	pH 8.0	pH 10.0
0.5	209	420
1	325	838
2	515	1427
5	899	2232
10	1180	2769
30	1681	3338
60	1773	3489
90	1906	3432
120	1867	3312
180	1844	3064

Table 3.3

Spin Intensities of the g = 2.00 EPR Signals Photo-accumulated by 230K Illumination of Digitonin Photosystem-I Particles at pH 8.0 and pH 10.0.

The spin intensities were estimated by the double integration of the EPR spectra presented in figure 3.30.

Spin Intensity Relative to $P700^+$		
Preparation	pH 8.0	pH 10.0
Preparation 1	2.21	3.9
Preparation 2	1.98	3.73
Preparation 2	2.08	4.09

Table 3.4

The Number of Spins Photo-accumulated, relative to $P700^+$, in the Maximum g = 2.00 EPR Signal by 230K Illumination of Different Digitonin Photosystem-I Preparations at pH 8.0 and pH 10.0.

Samples, prepared as described in materials and methods section 2.9.2, were illuminated at 230K until the maximum g = 2.00 EPR signal had been attained. The spin intensity was estimated by double integration of the spectra and divided by the spin intensity in corresponding $P700^+$ samples.

These findings contradict the results of Gast *et al.* (1983) who reported that illumination of samples at room temperature in the presence of dithionite induced only one A_1^- and one A_0^- spin equivalent per $P700^+$. However, these experiments were carried out on Triton X-100 isolated particles and it has been suggested that this detergent perturbs the structure of the photosystem-I reaction centre (Mansfield and Evans, 1988).

In order to examine the effect of Triton X-100 isolation on the structure of photosystem-I Triton samples were prepared at pH 10.0 and pH 8.0 with dithionite and the photo-accumulated g = 2.00 EPR signals compared to those in Digitonin isolated photosystem-I.

Gast *et al.* (1983) originally photo-accumulated the g = 2.00 signals at room temperature in the presence of dithionite but it is now known that such treatment could lead to the double reduction of A_1 (Sétif and Bottin, 1989, 1991). Thus, for the purpose of Triton vs. Digitonin comparison all illumination was carried out at 230K. The results shown in figure 3.31 and table 3.5 clearly demonstrated that, like Digitonin samples, the Triton extracted material has a larger g = 2.00 at pH 10.0 and contains four spin equivalents per $P700^+$ whereas at pH 8.0 only two spins per $P700^+$ were observed. However, in Triton X-100 photosystem-I the A_0^- EPR signal is not as broad as that observed in Digitonin particles making it more difficult to distinguish from A_1^- and indicating possible perturbation of the photosystem-I reaction centre complex.

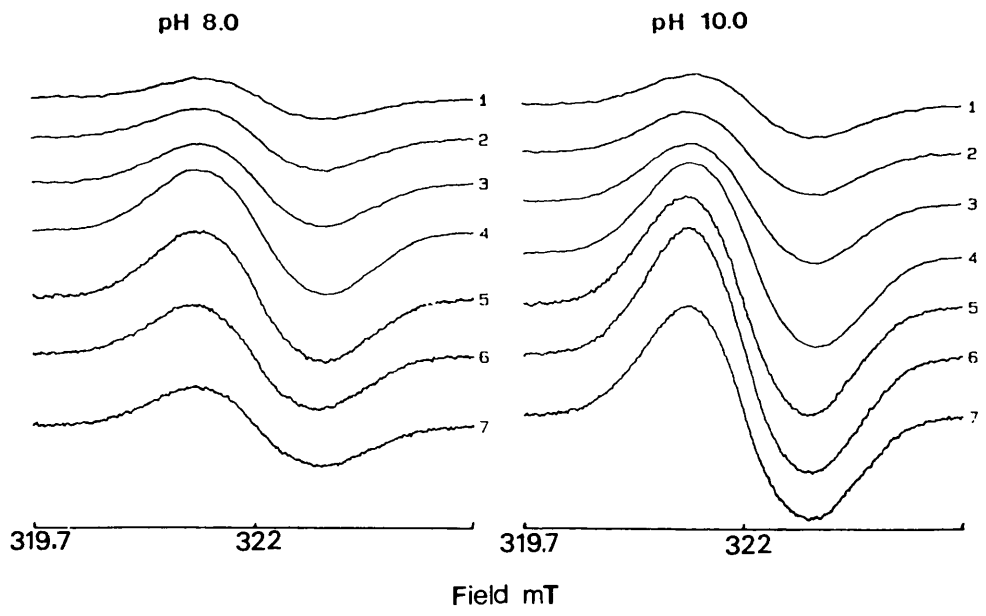

Figure 3.31

The EPR Spectra of A_0^- and A_1^- for Triton X-100 Particles.

The spectra were obtained by progressively longer periods of 230K illumination of Triton photosystem-I particles which had been previously incubated with sodium dithionite at pH 8.0 or pH 10.0 and frozen in the dark.

Samples, prepared as described in materials and methods sections 2.1.2, 2.1.3 and 2.9.2, were illuminated at 230K for: 1)0.5 min, 2)1 min, 3)2 min, 4)5 min, 5)10 min, 6)30 min and 7)60 min. At intervals during the illumination the samples were removed to the EPR spectrometer and the spectra recorded. Spectra are the average of two recordings.

EPR conditions: Microwave power 5 μW, modulation width 0.1 mT, recording temperature 75K.

Cumulative Period of 230K Illumination (Min)	Spin Intensity Relative to $P700^+$	
	pH 8.0	pH 10.0
0.5	0.633	0.959
1	0.935	1.256
2	1.279	1.840
5	1.943	2.902
10	2.004	3.300
30	1.602	3.681
60	1.208	3.239

Table 3.5

The Number of Spins, relative to $P700^+$, Photo-accumulated in the Maximum g = 2.00 EPR Signal by 230K Illumination of Triton X-100 Photosystem-I Preparations at pH 8.0 and pH 10.0.
Samples, prepared as described in materials and methods section 2.9.2, were illuminated at 230K until the maximum g = 2.00 EPR signal had been attained. The spin intensity was estimated by double integration of the spectra in figure and divided by the spin intensity in corresponding $P700^+$ samples.

3.6.2. The Effect of Quinone Double Reduction on the EPR Signal Attributed to A_1

In order to confirm the identity of the g = 2.00 photo-accumulated EPR signal attributed to the reduction of A_1 this signal was monitored under conditions which would lead to the gradual double reduction of the quinone. Double reduction was attempted in Digitonin photosystem-I poised at pH 8.0 in the presence of dithionite at 4°C but it was found that these conditions would only allow partial double reduction and so the samples had to be poised at pH 10.0. It would have been preferable to carry out this experiment at pH 8.0 as the results in section 3.6.1. indicate that only one of each A_1 and A_0 is photo-accumulated, thereby simplifying the situation.

Samples were illuminated at 4°C for gradually longer periods of time in order to progressively double reduce the quinone. They were then briefly dark adapted and frozen under liquid nitrogen. After short periods of illumination at 4°C the redox state of the samples was P700, A_0, A_1, Fe-S_X^-, Fe-S_A^- and Fe-S_B^- and the samples had no g = 2.00 EPR signal. A short period of subsequent 205K illumination at this stage induced the g = 2.00 EPR spectrum consistent with the photo-accumulation of A_1^- (fig. 3.32). However, after longer periods of 4°C illumination the subsequent 205K photo-induced signal became much broader. After 90 minutes of 4°C illumination the 205K photo-inducible A_1^- EPR signal had been totally replaced by a signal with a g-value of 2.0037 and a linewidth of 1.75 mT similar to a signal previously assigned to A_0^- (fig. 3.32) (Mansfield and

Evans, 1988). This indicated that illumination of Digitonin photosystem-I at pH 10.0 in dithionite at 4°C for 90 minutes doubly reduced A_1, rendering it EPR silent, and the subsequent 205K illumination led only to the photo-accumulation of A_0^-.

These experiments were repeated with Triton X-100 photosystem-I samples and the same results obtained with the exception that full double reduction was achieved with a shorter 4°C illumination time of 60 minutes.

Palace *et al.* (1987) and Ziegler *et al.* (1987) previously reported that prolonged u.v. illumination of photosystem-I results in inactivation of the quinone. To confirm that the loss of the 205K photo-induced A_1^- signal was not a result of quinone photo-damage the samples were dialysed against Tris-HCl pH 8.0 in the dark at 4°C in order to re-oxidise the quinol to quinone. Such samples were then frozen at pH 8.0 in the presence of dithionite then illuminated for 2 minutes at 205K to look for the re-emergence of the A_1^- EPR signal. After a 24 hour period of dialysis the EPR signal attributed to the reduced quinone returned although in some Digitonin photosystem-I preparations longer periods of dialysis were required.

Prolonged 230K illumination of Digitonin particles at pH 10.0 in the presence of dithionite suggested the presence of two quinone molecules. To investigate the effect of the double reduction procedure on each of these quinones, samples were selected at various points during the time course of A_1 double reduction and illuminated for 90 minutes at 230K in order to achieve the maximum g = 2.00 EPR signal (fig. 3.33).

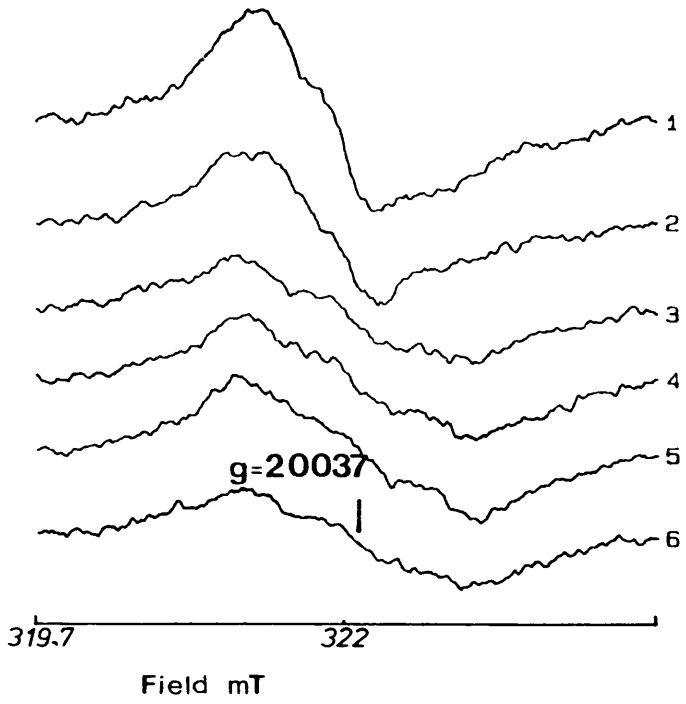

Figure 3.32

The Effect of Illumination at 4^{0}C for Progressively Longer Periods on the 205K Photoaccumulated EPR Spectra of A_1^- in Digitonin Photosystem-I at pH 10.0.

Samples, prepared as described in materials and methods sections 2.1.4 and 2.9.2, were illuminated at 4^{0}C for: 1)Dark, 2)2 min, 3)15 min, 4)30 min, 5)60 min and 6)90 min. After freezing samples were subsequently illuminated for 2 minutes at 205K .

EPR conditions: Microwave power 5 μW, modulation width 0.2 mT, recording temperature 75K.

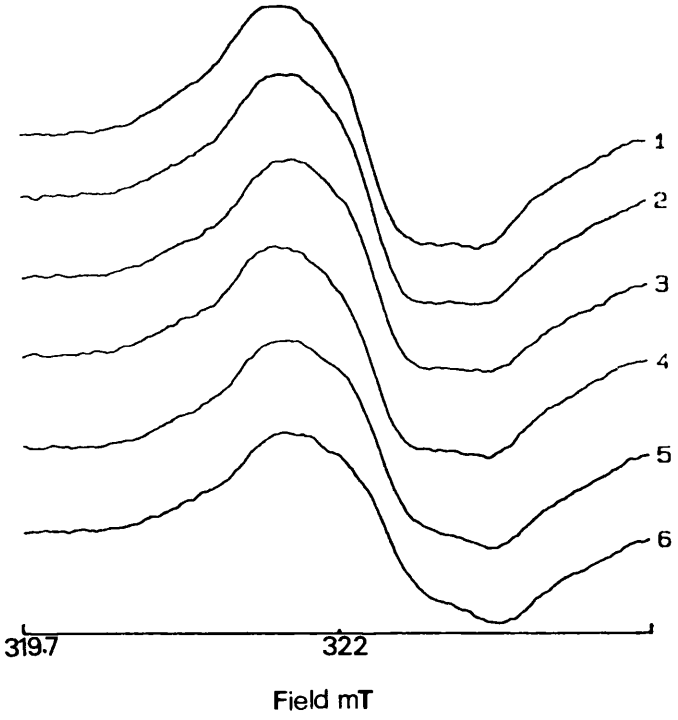

Figure 3.33

The Effect of Illumination at 4°C for Progressively Longer Periods on the 230K Photoaccumulated EPR Spectra of A_1^- and A_0^- plus A_1^- in Digitonin Photosystem-I at pH 10.0.

Samples, prepared as described in materials and methods sections 2.1.4 and 2.9.2, were illuminated at 4°C for: 1)Dark, 2)2 min, 3)15 min, 4)30 min, 5)60 min and 6)90 min. After freezing samples were subsequently illuminated at 230K until no further increase in signal size was observed.

EPR conditions: Microwave power 5 μW, modulation width 0.1 mT, recording temperature 75K.

Period of Illumination at 4^0	Spin Intensity Relative to $P700^+$
0	3.9
2	3.642
15	3.412
30	3.352
60	3.315
90	3.057

Table 3.6

Spin intensity of the Maximum g = 2.00 signals accumulated following 230K Illumination of Digitonin PS-I Particles at pH 10 Previously Illuminated at 4^0C in order to Double Reduce A_1.

Samples, prepared as described in materials and methods sections 2.1.4 and 2.9.2, were illuminated at 4^0 in order to double reduce A_1 then further illuminated at 230K until the maximum g = 2.00 EPR signal had been attained. The spin intensity was estimated by double integration of the spectra in figure 3.33 and divided by the spin intensity in corresponding $P700^+$ samples.

The acquired spectra were then double integrated in order to compare the photo-inducible spin intensity with that of a maximum $P700^+$ signal (table 3.6). As the 205K photo-accumulated A_0^- signal replaced the A_1^- signal, indicating quinone double reduction, the spin intensity dropped from 3.9 per $P700^+$ to 3.0 spins per $P700^+$. The spectra show that the component attributed to A_1^- is decreasing on double reduction but it is not completely abolished (fig. 3.33).

The results indicate that one of the quinone species is readily double reduced by prolonged illumination at 4^0C in the presence of dithionite at pH 10.0, whilst the other is not so easily double-reduced. The results also indicate that the A_1^- EPR signal, seen after brief illumination at 205K, is arising from the quinone that is more easily double-reduced as the other quinone requires longer periods of 205K illumination to be photo-accumulated.

3.7 Discussion

3.7.1 Quinone Double Reduction

The results show that the conditions which lead to the double reduction of the optically detected quinone and the appearance of the 25 ns A_0 transient also result in the disappearance of the photo-accumulated EPR signal attributed to A_1^-. This therefore confirms that the characteristics assigned to the secondary redox component of photosystem-I by various methods all refer to the same bound molecule of phylloquinone forming the A_1 electron transfer component. These characteristics are as

follows:

1.) The asymmetric g = 2.00 EPR signal formed by photo-accumulation at 205K (Bonnerjea and Evans, 1982; Gast *et al.*, 1983).

2.) The electron spin polarised signal attributed to the $P700^+/A_1^-$ radical pair (Thurnauer *et al.*, 1985; Rustandi *et al.*, 1990; Snyder *et al.*, 1991).

3.) 750 ns $P700^+$ re-reduction kinetics observed at room temperature (Sétif and Bottin, 1989,1991).

4.) The molecules of extractable vitamin K1 found in the photosystem-I reaction centre complex (Schroeder and Lockau, 1986)

Sétif and Bottin (1989) suggested that the photo-accumulated EPR signal attributed to A_1^- arose from a component following the double reduction of the quinone. The results reported here show this not to be the case as the photo-accumulated A_1^- spectra is gradually depleted during the time course of quinone double reduction. However, in the pH 10.0 samples, the 205K photo-induced A_1^- EPR spectrum does contain an additional shoulder on the high field side as compared to similar preparations at pH 8.0 (fig. 3.29). This is probably a contribution caused by the photo-reduction of A_0 and indicates that addition of dithionite at pH

10.0 double reduces some of the A_1 thereby giving rise to an A_0^- contribution after only a brief period of 205K illumination. This view is supported by measurements of spin intensity of the maximum g = 2.00 EPR spectra following illumination at 230K which are often less than four suggesting that a proportion of the quinone may have been double reduced. Mansfield and Evans (1988) also observed an additional contribution on the high field side of the A_1^- spectrum and concluded that illumination of samples at pH 10.0 in the presence of dithionite at 205K resulted in the reduction of both A_1 and A_0.

The results of Barry *et al.* (1988), which show no narrowing of the photo-accumulated A_1^- EPR spectra despite specific deuteration of the phylloquinone, are often cited as evidence that the A_1^- spectrum is that of a reporter species brought about by the reduction of the true A_1. However, the sample preparation during Barry's research involved the photo-accumulation of A_1^- by illumination at room temperature in the presence of dithionite. Such conditions have now been shown to result in the double reduction of A_1 and the resultant EPR spectrum contains a component from A_0^- thereby broadening the signal. Broadening of the signal in this manner may have acted to mask the expected narrowing caused by deuteration of the methyl protons of the quinone. In addition to this Barry and his co-workers used photosystem-I particles extracted by Triton X-100, a detergent now known to perturb the structure of photosystem-I.

3.7.2 Evidence for C_2 Symmetry in Higher Plant Photosystem-I

During the course of this work it was demonstrated that pH had an effect on the number of redox components being reduced by illumination at 230K. It was apparent that at pH 10.0 2 X A_1 and 2 X A_0 were being photo-reduced as compared to 1 X A_1 and 1 X A_0 at pH 8.0 as previously reported (Bonnerjea and Evans, 1982; Gast *et al.*, 1983). Once the maximum of two spins per $P700^+$ for the pH 8.0 sample or four spins per $P700^+$ for the pH 10.0 had been reached the signal size would not increase on further illumination. In fact further illumination reduced the amplitude of the signal indicating that even at 230K there may have been a small amount of A_1 double reduction.

This forms the first direct evidence that higher plant photosystem-I exhibits the same C_2 symmetry as other photosynthetic reaction centres (see Rutherford and Nitschke (1991) for a review). Although it had been previously demonstrated that two quinones are extractable from the reaction centre complex (Schroeder and Lockau, 1985) the existence of two primary chlorin acceptor molecules had not been established.

The reaction centres of purple bacteria exhibit a preference for redox events to take place up one of two symmetrical branches of electron transfer pathways (The A branch). On flash excitation only the bacteriopheophytin (H_A) located on the L polypeptide becomes reduced. Mar and Gringas (1990) demonstrated that it was possible to photo-trap the bacteriopheophytin (H_B) on the other branch (Branch B) by

illumination at 219K, although it occurs 274 times more slowly than its counter part on the A branch. A similar result is indicated for the photosystem-I reaction centre complex with one set of A_1 and A_0 redox components being readily reduced and the other requiring more prolonged 230K illumination. At higher temperature (4^0C) there is also a difference in the efficiency of electron transfer up each branch as demonstrated by the difficulty in doubly reducing the second A_1 by illumination in the presence of dithionite at pH 10.0. This was displayed by a drop in the number of spins from 4 to 3 following 90 minutes of 4^0C illumination indicating that one quinone and two chlorophyll molecules had been reduced. One would expect the spin value to have been 2 if both quinones had been doubly reduced.

Sétif and Bottin demonstrated that the 25 ns $P700^+/A_0^-$ re-reduction kinetics induced by quinone double reduction remained even when oxidation of iron-sulphur centres had occurred. Making an assumption that the second quinone had not been doubly reduced during the course of their experiment would also indicate that pathway 2 is highly inefficient and is incapable of reducing iron-sulphur centre X in the absence of the "primary pathway". The function of the second pathway therefore remains uncertain.

3.8 Summary of Results

1.) Treatment of photosystem-I with 6.8 M urea removes the peripheral polypeptides and terminal bound electron acceptors resulting in a photosystem-I core complex containing redox centres P700, A_0, A_1 and Fe-S_X, but largely depleted of Fe-$S_{A/B}$. SDS-PAGE analysis demonstrates that the core complex is depleted of subunits PSI-C (the Fe-$S_{A/B}$ binding protein), PSI-D and PSI-E. The isolated core complex is unable to photo-reduce $NADP^+$.

2.) Incubation of the core complex with an *n*-butanol extracted and purified PSI-C holoprotein preparation reconstitutes wild type $P700^+$ back reaction kinetics but to stabilise the rebound Fe-$S_{A/B}$ holoprotein and achieve a control photo-induced Fe-$S_{A/B}$ EPR spectrum PSI-D and possibly PSI-E are also required. This indicates a structural role for PSI-D and E.

3.) Recovery of $NADP^+$ photo-reduction requires a minimum of PSI-C, PSI-D and possibly PSI-E reconstituted onto the photosystem-I core complex. In the absence of PSI-C or PSI-D $NADP^+$ photo-reduction will not occur. This indicates an additional role for PSI-D and possibly PSI-E in the binding of ferredoxin and FNR and the mediation of electron transfer to $NADP^+$.

4.) Destruction of the PSI-C iron-sulphur centres by exposure to

oxygen results in an inability to reconstitute $NADP^+$ photo-reduction thereby confirming that Fe-$S_{A/B}$ are essential for forward electron transfer to ferredoxin.

5.) Illumination of photosystem-I at 4^0C in the presence of dithionite results in gradual double reduction of the proposed quinone secondary electron acceptor. Such treatment also results in a concomitant depletion of the photo-induced EPR spectrum previously assigned to A_1^-. This result indicates that the photo-accumulated asymmetric g = 2.00 EPR signal rises as a result of the reduction of A_1, the phylloquinone secondary electron acceptor.

6.) Maximum photo-accumulation of A_0^- and A_1^- EPR signals by illumination of photosystem-I at 230K results in 4 spins per $P700^+$. This suggests the reduction of 2 X A_1 and 2 X A_0 thereby indicating that higher plant photosystem-I may exhibit the C_2 symmetry observed in other types of reaction centre.

Andersen, B., Koch, B. and Scheller, H.V. (1992_a) Physiol. Plant. 84, 154-161.

Andersen, B., Koch, B., Scheller, H.V., Okkels, J.S. and Møller, B.L. (1990) in Current Research in Photosynthesis, (Baltschef fsky, M. ed.) Vol. 2 671-674. Kluwer, Dortrecht.

Andersen, B., Scheller, H.V. and Møller, B.L. (1992_b) FEBS Lett. 311, 169-173.

Arnon, D.I. (1949) Plant Physiol. 24, 1-15.

Arnon, D.I., Whatley, F.R. and Allen, M.B. (1954) J.Amer.Chem.Soc., 76, 6324-6325

Arnon, D.I, Whatley, F.R. and Allen, M.B. (1955) Biochim.Biophys.Acta, 16, 607-608

Barry, B.A., Bender, C.J., McIntosh, L., Ferguson-Miller, S. and Babcock, G.T. (1988) Israel J. Chem. 28, 129-132.

Bassham, J.A. and Calvin, M. (1957) The Path of Carbon in Photosynthesis, Englewood Cliffs, N.J., Prentice-Hall.

Bearden, A.J. and Malkin, R. (1972) Biochim. Biophys. Acta, 283, 456-468.

Bendall, D.S. and Davies, E.C. (1989) Physiol. Plant. 76, A87.

Bengis, C. and Nelson, N. (1977) J. Biol. Chem. 252, 4564-4569.

Berthold, D.A., Babcock, G.T. and Yocum, F. (1981) FEBS Lett. 134, 231-234.

Biggins, J. and Mathis, P. (1988) Biochem. 27, 1494-1499.

Biggins, J., Tanguay, N.A. and Frank, H.A. (1989) FEBS Lett. 250, 271-274.

Boardman, N.H. (1971) Methods Enzymol. 23, 268-276.

Bonnerjea, J. and Evans, M.C.W. (1982) FEBS Lett. 148, 313-316.

Bradford, M.M (1976) Anal. Biochem. 72, 248-254.

Brettel, K. (1989) Biochim. Biophys. Acta, 976, 246-249.

Brettel, K., Sétif, P. and Mathis, P. (1986) FEBS Lett. 203, 220-224.

Bryant D.A. (1992) The Photosystems: Structure, function and Molecular Biology. (Ed. J. Barber) Elsevier.

Bryant, D.A., Rhiel, E., de Lorimier, R., Zhou, J., Stirewalt, V.L., Gasparich, G.E., Dubbs, J.M. and Snyder, W. (1990) in Current Research in Photosysthesis, (Baltscheffsky, M. ed.) Vol. 2 pp. 1-9. Kluwer, Dortrecht.

Buchanan, B.B. and Arnon, D.I. (1973) Meth. Enzymol. 23, 413-440.

Cammack, R. and Evans, M.C.W. (1975) Biochem. Biophys. Res. Comm. 67, 544-549.

Chitnis, P.R., Purvis, D. and Nelson, N. (1991) J. Biol. Chem. 25, 1991-266.

Chitnis, P.R., Reilly, P.A., Meidel, M.C. and Nelson, N. (1989) J. Biol. Chem. 264, 18374-18380

Chamarovski, S.K. and Cammack, R. (1982) Photobiochem. Photobiophys. 4, 195-200.

Davenport, H.E. (1960) Biochem. J. 77, 471-477

Davis, I.H., Heathcote, P., Machlachlan, D.J.M. and Evans, M.C.W. (1993) Biochim. Biophys. Acta, In Press.

Dörnemann, D. and Senger, H. (1986) Photochem. Photobiol. 43, 573-581.

Dutton, P.L. (1971) Biochim. Biophys. Acta, 226, 63-68.

Duysens, L.N.M., Amesz, J. and Kemp, B.M. (1961) Nature, 190, 510-511.

Emerson, R.L., Chalmers, R.V. and Cederstrand, C. (1957) Proc. Natl. Acad. Sci. USA, 43, 133-143.

Evans, E.H., Rush, J.D., Johnson, C.E. and Evans, M.C.W. (1979) Biochem. J. 182, 861-865.

Evans, E.H., Rush, J.D., Johnson, C.E., Evans, M.C.W. and Dickson, D.P.E. (1981) Eur. J. Biochem. 118, 81-84.

Evans, M. C. W. and Heathcote, P. (1980) Biochim. Biophys. Acta. 590, 89-96

Evans, M.C.W., Reeves, S.G. and Cammack, R. (1974) FEBS Lett. 49, 111-114.

Evans, M.C.W., Sihra, C.K., Bolton, J.R. and Cammack, R. (1975) Nature,

256, 668-670.

Evans, M.C.W., Sihra, C.K. and Slabas, A.R. (1977) Biochem. J. 162, 75-85.

Evans, M.C.W., Telfer, A. and Lord, A.V. (1972) Biochim. Biophys. Acta, 267, 530-537.

Fish, L.E., Kuck, U. and Bogorad, L. (1985) J. Biol. Chem. 260, 1413-1421.

Ford, R.C. and Evans, M.C.W. (1983) FEBS Lett. 160, 159-164.

Frank, H.A., McLean, M.B. and Sauer, K. (1979) Proc. Natl. Acad. Sci. USA, 76, 5124-5128.

Gast, P., Swarthoff, T., Ebskamp, F.C.R. and Hoff, A.J. (1983) Biochim. Biophys. Acta, 722, 168-175.

Golbeck, J.H. (1992) Annu. Rev. Plant Physiol. and Mol Biol. 43, 293-324.

Golbeck, J.H. and Bryant, D.A. (1991) Current Topics in Bioenergetics Vol 16, 83-177.

Golbek, J.H. and Cornelius, J.M. (1986) Biochem. Biophys. Acta, 849 16-24.

Golbeck, J.H., Mehari, T., Parrett, K. and Ikegami, I. (1988) FEBS Lett. 240, 9-14.

Golbeck, J.H., Parrett, K.G. and McDermott, A.E. (1987) Biochim. Biophys. Acta, 893, 149-160.

Hanley, J.A., Kear, J., Bredenkamp, G., Li, G. Heathcote, P. and Evans, M.C.W. (1992_a) Biochim. Biophys. Acta, 1099, 152-156.

Hanley, J.A., Heathcote, P. and Evans M.C.W. (1992_b) in Current Research in Photosynthesis, (Murata, N. ed.) Vol. 1 577-580. Kluwer, Dortrecht.

Heathcote, P., Hanley, J.A. and Evans, M.C.W. (1993) Biochim. Biophys. Acta, In Press.

Hill, R. and Bendall, F. (1960) Nature, 186, 136-137.

Hill, R. and Scarisbrick, R. (1940) Nature, 146, 61-62

Hiyama, T. and Ke, B. (1971) Arch. Biochem. Biophys. 147, 99-108.
Hiyama, T. and Ke, B. (1972) Biochim. Biophys. Acta, 267, 160-171.

Høj, P.B. and Møller, B.L. (1986) J. Biol. Chem. 261, 14292-14300

Høj, P.B., Svendsen, I.B., Scheller, H.V. and Møller, B.L. (1987) J. Biol. Chem. 262, 12676-12684.

Ikegami, I. and Itoh, S. (1986) Biochim. Biophys. Acta, 851, 75-85.

Ikegami, I. and Itoh, S. (1987) Biochim. Biophys. Acta, 893, 517-523.

Ikegami, I. and Itoh, S. (1988) Biochim. Biophys. Acta, 934, 39-46.

Ikegami, I., Sétif, P. and Mathis, P. (1987) Biochim. Biophys. Acta, 894, 414-422.

Inoue, K., Kusumoto, N. and Sakuri, H. (1992) in Current Research in Photosynthesis, (Murata, N. ed.) Vol. 1 577-580. Kluwer, Dortrecht.

Ishikawa, H., Hibino, T. and Takabe, T. (1992) in Current Research in Photosynthesis, (Murata, N. ed.) Vol. 1 597-600. Kluwer, Dortrecht.

Itoh, S., Iwaki, M. and Ikegami, I. (1987) Biochim. Biophys. Acta, 893, 508-516.

Iwaki, M. and Itoh, S. (1989) FEBS Lett. 256, 11-16.

Jagendorf, A.T. and Uribe, E. (1966) Proc. Natl. Acad. Sci. USA, 55, 170-177.

Karapetyan, N.V., Shubin, V.V., Rakhimberdieva, M.G., Vashchenko, R.G. and Bolychevtseva, Y.V. (1984) FEBS Lett. 173, 209-212.

Katoh, S. (1973) Meth. Enzymol. 23, 408-413.

Ke, B. (1972) Biochim Biophysics Acta, 267, 595-599.

Ke, B., Hansen, R.E. and Beinert, H. (1973) Proc. Natl. Acad. Sci. USA, 70, 2941-2945.

Kim, D., Yoshihara, K. and Ikegami, I. (1989) Plant cell physiol. 30, 679-684.

Kirsch, W., Seyer, P. and Herrnmann R.G. (1986) Curr. Genet. 10, 843-855.

Klug, D.R., Giorgi, L.B., Crystall, B., Barber, J. and Porter, G. (1989) Photosynth. Res. 22, 277-284.

Koike, H. and Katoh, S. (1982) Photochem. Photobiol. 35, 527-531.

Kok, B. (1956) Biochim. Biophys. Acta, 22, 399-401.

Kok, B. (1957) Nature, 179, 583-584.

Kok, B. and Beirnert, H. (1962) Biochem. Biophys. Res. Comm. 9, 349-354

Krauss, N., Hinrichs, W., Witt, I., Fromme, P., Pritzkow, W., Dauter, Z., Bretzel, C., Wilson, K.W., Witt, H.S. and Senger, W. (1993) Nature, 361, 326-331.

Lagoutte, B., Sétif, P. and Duranton, J. (1984) FEBS Lett. 274, 24-29.

Li, N., Warren, P.V., Golbeck, J.H., Frank, G., Zuber, H. and Bryant, D.A. (1991_a) Biochim. Biophys. Acta, 1059, 215-225.

Li, N., Zhao,, J.D., Warren, P.V., Warden, J.T., Bryant, D.A. and Golbeck, J.H. (1991_b) Biochem. 30, 7863-7872.

MacKinney, G. (1941) J. Biol. Chem. 140, 315-322.

Malkin, R. (1986) FEBS Lett. 280, 2-317.

Malkin, R. and Berden, A.J. (1971) Proc. Natl. Acad. Sci. USA. 68, 16-19.

Mansfield, R.W. and Evans, M.C.W. (1985) FEBS Lett. 190, 237-241.

Mansfield, R.W. and Evans, M.C.W. (1986) FEBS Lett. 203, 225-229.

Mansfield, R.W. and Evans, M.C.W. (1988) Israel. J. Chem. 28, 97-102.

Mansfield, R.W., Hubbard, J.A.M., Nugent, J.H.A. and Evans, M.C.W. (1987_a) FEBS. Lett. 220, 74-78.

Mansfield, R.W., Nugent, J.H.A. and Evans, M.C.W. (1987_b) Biochim. Biophys. Acta, 894, 515-523.

Mar, T. and Gringas, G. (1990) Biochim. Biophys. Acta, 1017, 112-117.

Mathis, P. (1990) Biochim. Biophys. Acta, 1018, 163-167

Mathis, P., Ikegami, I. and Sétif, P. (1988) Photosynthesis Res. 16, 203-210.

McDermott, A.E., Yachandra, V.K., Guiles, R.D., Britt, R.D., Dexheimer, S.L., Sauer, K. and Klein, 1988 Biochem. 27, 4013-4020.

McDermott, A.E., Yachandra, V.K., Guiles, R.D., Sauer, K., Klein, M.P., Parrett, K.G. and Golbeck, J.H. 1989 Biochem. 28, 8056-8059.

Merati, G. and Zanetti, G. (1987) FEBS Lett. 215, 37-40.

Melis, A. and Brown, J.S (1980) Proc. Natl. Acad. Sci. USA, 77, 4712-4716.

Mitchell, P. (1966) Biological Reviews. 41, 445-502.

Möenne-loccoz, P., Robert, B., Ikegami, I. and Lutz, M. (1990) Biochem. 29, 4740-4746.

Nabedryke, E., Tavitian, B.A., Mantelr,W. and Breton, J. (1989). Physiol. Plant 76, Abstr. 441, A85.

Nitschke, W., Feiler, U. and Rutherford, A.W. (1990_a) Biochem. 29, 3834-3842.

Nitschke, W., Sétif, P., Liebl, U., Feiler, U. and Rutherford, A.W. (1990_b) Biochem. 29, 11079-11088.

Nitschke, W. and Rutherford, A.W. (1991) TIBS, 16, 241-245.

Norris, J.R., Uphaus, R.A., Crespi, H.L. and Katz, J.J. (1971) Proc. Natl. Acad. Sci. USA, 68, 625-629.

Nuijs, A.M., van Dorssen, R.J., Duysens, L.N.M. and Amesz, J. (1985_a) Biochim. Biophys. Acta. 807, 24-34.

Nuijs, A.M., van Dorssen, R.J., Duysens, L.N.M. and Amesz, J. (1985_b) Proc. Natl Acad. Sci. USA, 82, 6865-6868.

Oh-oka, H., Itoh, S., Saeki, K., Takahashi, Y. and Matsubara, H. (1991) Plant Cell Physiol. 32, 11-17

Oh-oka, H., Takahashi, Y., Kuriyama, K., Saeki, K. and Matsubara, H. (1988_a) J. Biochem. (Tokyo), 103, 963-968.

Oh-oka, H., Takahashi, Y. and Matsubara, H. (1989) Plant Cell Physiol. 30, 869-875.

Oh-oka, H., Takahashi, Y., Matsubara, H. and Itoh, S. (1988_b) FEBS Lett. 234, 291-294.

Oh-oka, H., Takahashi, Y., Wada, K., Matsubara, H., Ohyama, K. and Ozeki, H. (1987) FEBS Lett. 218, 52-54.

Okkels, J.S., Scheller, H.V., Jepsen, L.B. and Møller, B.L. (1989) FEBS Lett. 250, 575-579.

Okkels, J.S., Scheller, H.V., Svendsen, I. and Møller, B.L. (1991) J. Biol. Chem. 266, 6767-6773.

O'Malley, P.J. and Babcock, G.T. (1984) Proc. Natl. Acad. Sci. USA, 81, 1098-1101.

Palace, G.P., Franke, J.E. and Warden, J.T. (1987) FEBS Lett. 215, 58-62.

Parrett, K.G., Mehari, T., Warren, P. and Golbeck, J.H. (1989) Biochim. Biophys. Acta, 973, 324-332.

Parrett, K.G., Mehari, T. and Golbeck, J.H. (1990) Biochim. Biophys. Acta, 1015, 341-352.

Petrouleas, V., Brand, J.J., Parrett, K.G. and Golbeck, J.H. (1989) Biochem. 28, 8980-8983.

Philipson, K.D., Sato, V.L. and Sauer, K. (1972) Biochem. 11, 4591-4595.

Ruben, S., Randall, M., Kamen, M. and Hyde, J.L. (1941) J. Amer. Chem. Soc. 63, 877-879

Rustandi, R.R., Snyder, S.W., Feezel, L.L., Michalski, T.J., Norris, J.R., Thurnauer, M.C. and Biggins, J. (1990) Biochem. 2935, 8030-8032.

Rutherford, A.W. (1990) Biochim. Biophys. Acta, 1019, 128-132.

Rutherford, A.W. and Mullet, J.E. (1981) Biochim. Biophys. Acta, 635, 225-269.

Rutherford, A.W. and Nitschke, W. (1991) Trends Biochem. Sci. 16, 241-245.

Sakurai, H. and San Pietro, A. (1985) J. Biochem. (Tokyo), 98, 69-76.

San Pietro, A. and Lang, H.M. (1958) J.Biol.Chem. 231, 211-229

Sauer, K., Acker, S., Mathis, P. and Van Best, J.A. (1977) In "Bioenergetics of Membranes" (L. Packer Ed.), 351-359, Elsevier, Amsterdam.

Sauer, K., Acker, S., Mathis, P. and Van Best, J.A. (1979) Biochim. Biophys. Acta, 545, 466-472.

Scheer, H., Gross, E., Nitschte, B., Cmiel, E., Schneider, S., Schafer, W., Sciebel, H.-M. and Sculten H.-R. (1986) Photochem. Photobiol. 43, 559-571.

Scheller, H.V., Svendsen, I.B. and Møller, B.L. (1989) J. biol. chem. 264, 6929-6934.

Schroeder, H.U. and Lockau, W. (1986) FEBS. Lett. 199. 23-27

Senger, M., Dörnemann, D. and Senger, H. (1988). FEBS Lett. 234, 215-217

Sétif, P. and Bottin, H. (1989) Biochem. 28, 2689-2697.

Sétif, P. and Bottin, H. (1990) Biochim. Biophys. Acta, 1057, 331-336.

Sétif, P., Ikegami, I. and Biggins, J. (1987) Biochim. Biophys. Acta, 894, 146-156.

Sétif, P. and Mathis, P. (1980) Arch. Biochem. Biophys. 204, 477-485.

Shin, M. (1973) Meth. Enzymol. 23, 440-447.

Shuvalov, V.A., Ke, B. and Dolan, E. (1979_a) FEBS Lett. 100, 5-8.

Shuvalov, V.A., Klevanik, A.V., Shorkov, A.V., Kryukov, P.G. and Ke, B. (1979_b) FEBS Lett. 107 313-316.

Shuvalov, V.A., Nuijs, A.M., van Gorkom, H.J., Smit, H.W.J. and Duysens, L.N. M. (1986) Biochim. Biophys. Acta. 850, 319-323.

Smith, N.S., Mansfield, R.W., Nugent, J.H.A. and Evans, M.C.W. (1987) Biochim. Biophys. Acta. 892, 331-334.

Snyder, S.W., Rustandi, R.R., Biggins, J., Norris, J.R. and Thurnauer, M.C. (1991) Proc. Natl. Acad. Sci. USA, 88, 9895-9896.

Staffan, E.T. and Andersson, B. (1991) Photosynth. Res. 27, 209-219.

Stemler, A. and Radner, R. (1975) Science, 190, 457-458

Steppuhn, J., Hermans, J., Nechushtai, R., Ljungsberg, U., Thummler, G., Lottspeich, F. and Herrmann, R.G. (1988) FEBS Lett. 237, 218-224.

Steppuhn, J., Hermans, J., Nechushtai, R., Herrmann, G.S. and Herrmann, R.G. (1988) Curr. Genet. 16, 99-108.

Tagawa, K. and Arnon, D.I. (1962) Nature, 195, 537-543

Takahashi, Y., Koike, H. and Katoh, S. (1982) Arch. Biochem. Biophys. 219, 209-218.

Thornber, J.P., Morishige, D.T., Anandan, S. and Peter, G.F. (1991) in The Chloroplast (H. Scheer Ed.) CRC Press.

Thurnauer, M.C. and Gast, P. (1985) Photobiochem Photobiophys. 9, 29-38.

Towbin, H., Staehelin, T. and Gordon, J. (1979) Proc. Natl. Acad. Sci. USA, 76 4350-4354.

van Neil, C.B. (1931) Arch.Mikrobiol.Z., 3, 1

Vos, M.H. and van Gorkom, H.J. (1988). Biochim. Biophys. Acta, 934, 293-302.

Warren, P.V., Parrett, K.G., Warden, J.T. and Golbeck, J.H. (1990) Biochem. 29, 6547-6550.

Wasielewski, M.R., Fenton, J.M. and Govindjee, (1987) Photosyn. Res. 12, 181-190.

Wasielewski, M.R., Norris, J.R., Crespi, H.L. and Harper, J. (1981) Am. Chem. Soc. 103, 7664-7665.

Watanabe, T., Nakazato, M., Mazaki, H., Hongu, A., Konno, M., Saitoh, S. and Honda, K. (1985) Biochim. Biophys. Acta, 807, 110-117.

Whitmarsh, J. and Ort, D.R. (1984) Arch Biochem. Biophys. 213, 378-389.

Woese, C.R. (1987) Microbiol. Rev. 51, 221-271.

Warburg, O. and Negelein, E. (1922) Z.phys.Chem., 102, 235-266

Webber, A.N., Bingham, S.E., Gibbs, P.B., Misra, L.M. and Ward, J.B. (1992) in Current Research in Photosynthesis, (Murata, N. ed.) Vol. 1 561-564. Kluwer, Dortrecht.

Wynn, R.M. and Malkin, R. (1988_a) FEBS Lett. 229, 293-297.

Wynn, R.M. and Malkin, R. (1988_b) Biochem. 27, 5863-5863.

Wynn, R.M., Omaha, J. and Malkin, R. (1989) Biochem. 28, 5554-5560.

Zanetti, G. and Merati, G. (1987) Eur J Biochem. 169, 143-146.

Zhao, J.D., Li, N., Warren, P.V., Golbeck, J.H. and Bryant, D.A. (1992) Biochem. 31, 5093-5099.

Ziegler, K., Lockau, W. and Nitschke, W. (1987) FEBS Lett. 217, 16-20.

Zilber, A.I. and Malkin, R. (1988) Plant physiol. 88, 810-814.

Zilber, A.L. and Malkin, R. (1992) Plant Physiol. 99, 901-911.